SINGLE WALLED CARBON NANOTUBE NETWORKS AS SUBSTRATES FOR BONE CELLS

by

WOJTEK TUTAK

A Dissertation submitted to the

Graduate School-New Brunswick

Rutgers, The State University of New Jersey

in partial fulfillment of the requirements

for the degree of

Doctor of Philosophy

Graduate Program in Materials Science and Engineering

written under the direction of

Prof. Manish Chhowalla

and approved by

_____

_____

_____

_____

_____

New Brunswick, New Jersey

October 2010

ABSTRACT OF DISSERTATION

Title: Single Walled Carbon Nanotube Networks as Substrates for Bone Cells

By WOJTEK TUTAK

Dissertation Director: Prof. Manish Chhowalla

A central effort in biomedical research concerns the development of materials for sustaining and controlling cell growth. Carbon nanotube based substrates have been shown to support the growth of different kinds of cells. However the underlying molecular mechanisms remain poorly defined. To address the fundamental question of mechanisms by which nanotubes promote bone mitosis and histogenesis, primary calvariae osteoblastic cells were grown on single walled carbon nanotube (SWNT) network substrates. Using a combination of biochemical and optical techniques, we demonstrate here that SWNT networks promote cell development through two distinct steps. Initially, SWNTs are absorbed in a process that resembles endocytosis, inducing acute toxicity. Nanotube mediated cell destruction, however, induces a release of endogenous factors that act to boost the activity of the surviving cells by stimulating the synthesis of extracellular matrix.

In the second part of the research, minimally invasive SWNT matrices were used to further investigate network properties for biomedical applications without extensive presence of cytotoxicity. In the literature, carbon nanotube based substrates have been shown to support the growth of different cell types and, as such, have raised considerable interest in their possible use in biomedical applications. Nanotube matrices that are embedded in polymers cause inherent changes in nanotube chemical and physical film properties. Thus, it is critical to understand how the physical properties of the pristine networks affect the biology of the host tissue. Here, we investigated how the physical and chemical properties of SWNT networks impact the response of MC3T3-E1 bone osteoblasts. We found that two fundamental steps in cell growth: initial attachment to the substrate and proliferation, are strongly dependent on the energy and roughness of the surface, respectively. Thus, fine-tuning the properties of the film may represent a strategy to optimize the response of the biological host.

Above results guided the next set of experiments in which in-situ, real time cell interactions with SWNT films were investigated. Direct electrical measurements on SWNT films during osteoblastic cell growth were conducted. The experiments indicated that the nanotube networks may provide some interesting insight into the initial cell/material interactions.

Acknowledgments

I would like to express my great appreciation to my advisor Prof. Manish Chhowalla for providing ever important financial support and guidance. I also greatly appreciate help of my co-adviser, Prof. Federico Sesti for his continuous mentoring and providing access to biological laboratory throughout my study. Past year was also remarkably influenced by my co-advisers, specifically Prof. Mann and Prof. Klein.
I want thank them for their assistance and thoughtful advice.
Being a part of a collaborative research project between two institutions gave me the opportunity to interact with Dr. Kiho , Prof. Jitianu, Prof. Partridge, and Dr. Vasilov and many others who have influenced my life and shaped my research experience. All of whom I thank for being supportive and helpful in my research.
During these challenging times, my wife Andzelika, provided me with comfort and constant motivation to overcome obstacles. A wonderful person with whom I rejoice moments of happiness.
My words of appreciation also go to my brothers in law. Jerzy Okol for his time and patience in editing my thesis and Robert Myszka for helping me with my personal projects over the past few years.
I also acknowledge help of my parents, parents in law and friends who provided happy and comforting environment that helped me to successfully conclude my Ph.D .
I express my great appreciation to Prof. Partridge (Dept. Physiology and Biophysics, UMDNJ) for providing access to her laboratory and PCR equipment and Prof. Ulrich for authorizing use of contact angle analyzer (Dept. Chemistry and Chemical Biology, Rutgers University)

Finally, I want to acknowledge support of Corning Fellowship and Rutgers University for providing financial support for the past 4 years.

Table of Contents

List of Tables

List of Figures

Chapter 1

Chapter 2

Chapter 3

Chapter 4

Chapter 5

Chapter 1 Research Background

1.1 Motivation

Carbon is one of most widely present elements in the universe. Furthermore, it is a basic building block of all living organisms. Lipids, proteins and other biomolecules all contain carbon which is necessary to form proteins, cells, tissues and organs. From that perspective, carbon based nanomaterials provide an interesting prospect for incorporating functional devices within living organisms. In particular, single walled carbon nanotubes have unique chemical, structural, mechanical and electronic properties. The combination of these characteristics present exceptional opportunity to design and fabricate minaturalized multifunctional devices. Biomimetic single walled carbon nanotube (SWNT) characteristics include length to diameter ratio, Young's modulus and resilience which are similar to microtubules that constitute major parts of the cytoskeleton in all living cells [1]. When bundled, these nanotubes have a diameter and length which is similar to collagen fibers found in connective tissue [2].

Due to their unique chemistry related to their small diameter along with extraordinary physical properties SWNTs exhibit interesting bio-activity but also pose formidable challenges when applied to biological systems. This is exemplified by research reports that show significant differences in reported cell response when exposed to SWNTs in various forms. The nanotubes are characterized by high material cell activity that may be of benefit or cause toxicity [3,4].

Nanotechnology in biological systems is one of most interesting and intensively researched subjects because it has the potential to revolutionize the way we diagnose, treat and even possibly cure diseases. This treatment arises from the fact that nanomaterials and nanotechnology can address interactions at the nanoscale which in principle can be very potent since active biological sites can be specifically and locally targeted so that the entire biological system is not exposed to nondiscriminatory and potentially adverse effects of drugs.

Understanding these interactions in complex biological environments has only recently begun to emerge as a new interdisciplinary subject. Issues regarding controlling the behavior and assembly of nano-materials in biological environments are underreported and poorly understood. Further advances in understanding the kinetic, dynamic and chemical interactions between nanomaterials and the biological environments may eventually lead to ordered and controllable implementation of nanotechnology in biological applications including tissue regeneration, the subject of this thesis. The ability to understand how the nanomaterials interact in *in-vitro* settings, particularly in most basic and simplified systems, provide a pathway for investigating important interactions between nanomaterials and biological components. The evaluation and impact of nanomaterials and carbon nanotubes in particular can be affected by several different factors that can occur simultaneously by or at widely different time-scales (see Table 1). Therefore, the evaluation of cyto-toxicity or some other biological response of carbon nanomaterials requires a well defined and highly controllable testing procedure.

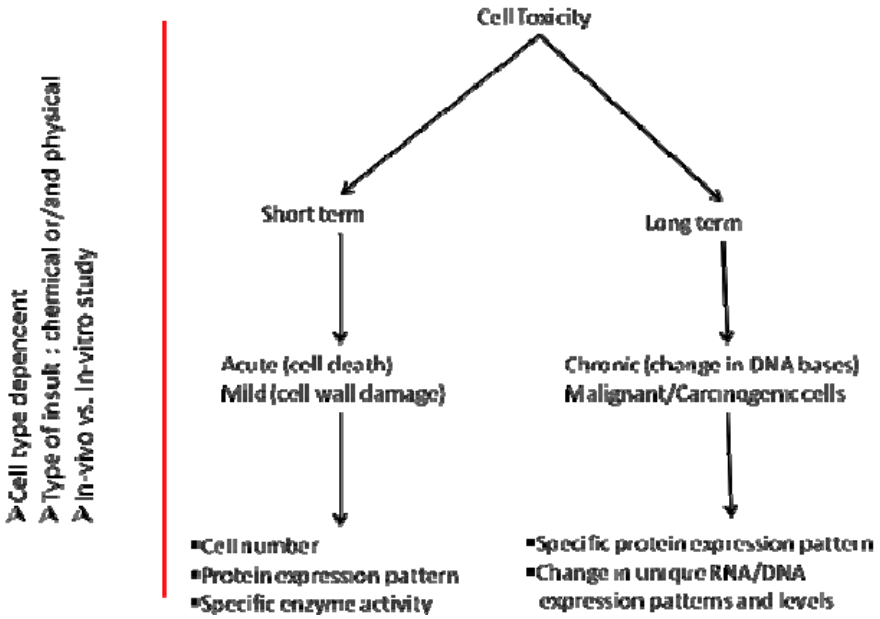

Table 1 Nanomaterials in biological systems. The multiple factors that effect the response of the cell culture system are shown.

Carbon nanotubes are the most prominent example of the difficulties encountered in studying the biological properties of nanomaterials. There have been numerous studies that have reported contradictory results on seemingly similar experiments. However a close examination in the literature reveals that subtle changes in experiments/procedures can lead to dramatically different results. For example, existing studies suggest that the SWNTs may help stimulate cell bioactivity (possibly similar to prebiotic effect) but when present in loose form and at high doses, SWNT may have adverse effect on cell cultures [5,3]. Nanotubes that act on cell walls only (no phagocytosis present), are capable of stimulating ion channels leading to changes in cell development [6]. Upon penetrating the cell wall, internalized SWNTs behave similar to oxidative species causing cell malfunction [7-9].

Complexity of interactions existing between the SWNTs and biological cells is multileveled, dynamic and predominantly related to SWNT toxicity. It is apparent that the cell toxicity masks other potentially stimulative mechanisms.

Therefore, assembled SWNTs in the form of networks may provide better testing platform for in-vitro biocompatibility tests. Iintertubular van der Wall (vdW) forces prevent SWNTs from spontaneously disassembling and in process limit number of loose tubes in the medium. Thus, the SWNT based matrices provide the opportunity to test material properties without directly endangering cell integrity and function.

Matrix/network coating would also be essential for assembling nanodevices, providing an active surface for biomolecules and cell interactions.

Scaffolds provide unique features capable of stimulating cell response. Specifically, surface roughness, chemistry and porosity (all summarized in form of total surface energy) can drive cell development. Equally important is a biological environment. The local biology actively shapes the matrix properties. For example, cell biochemistry and its physical presence may induce local changes in the pH, release biomolecules as well as introduce mechanical stress on the substrate. Therefore, the nanomaterials/biological system is dynamic in nature. Cell development rate, which itself is directed by matrix characteristics, actively shapes the matrix surface properties.

In this thesis, the experiments were carried out to further enhance the understanding of SWNTs behavior in biological systems. Specifically, the research is aimed as evaluation of the potential usage of SWNT networks as multifunctional scaffolds for bone regeneration. Three major research goals were targeted:

1. To understand the role of loose SWNTs on osteoblastic cell response.

a) Effect of SWNT matrix processing and preparation on the cellular response.

2. Control, test and validation of SWNT network surface and carbon chemistry on cell/materials interactions.

a) Define the factors affecting the cellular response

3. Utilize SWNT networks to sense cell number and initial cell-material interactions.

1.2 Materials: Introduction to Carbon Nanotubes

Carbon can be found in multiple allotropes and structures with carbon nanotubes being an interesting one dimensional form. Other well known carbon based structures include diamond, graphite, graphene and fullerenes. The structures of these allotropes are depicted in Figure 1.1

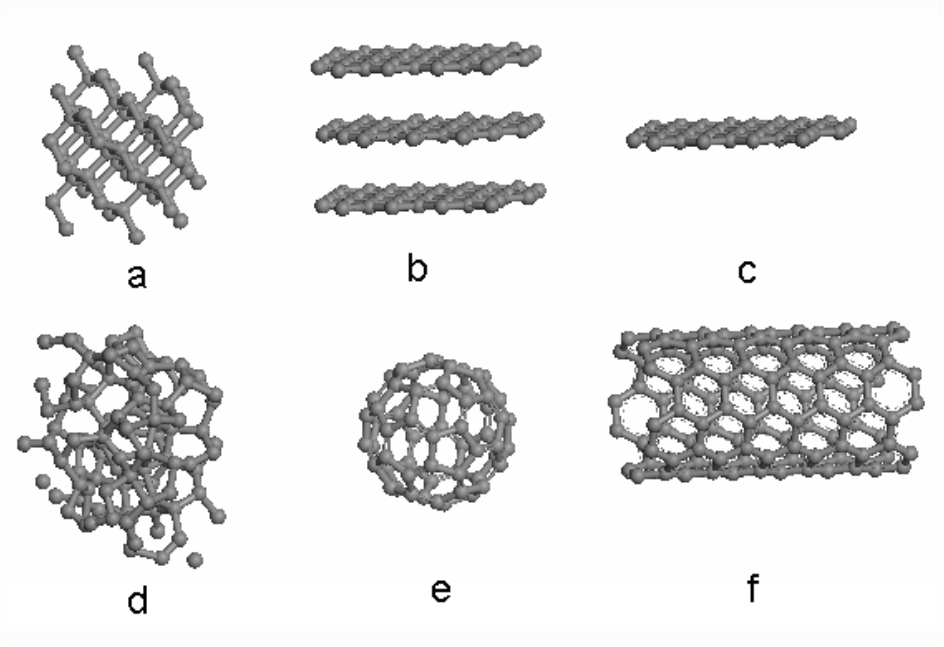

Figure 1.1 Various carbon allotropes are shown. Figures a,b correspond to 3-dimentional diamond and graphite structures. The 2-dimentional graphene and 1-dimensional SWNT are shown in Figures c and f. Amorphous carbon and zero dimensional fullerene molecule are shown in Figures d and e [10].

Over the last decade, carbon nanotubes have received considerable attention due to their interesting mechanical, chemical, electrical and structural properties. The SWNTs are formed by seamlessly rolling up single graphene sheets. SWNTs are characterized by high aspect ratios because they are microns in length (1-5 μm) with diameters raging from 0.7-1.5 nm. SWNTs have Young's modulus approaching 1 TPa and tensile strength of up to 30 GPa. Additionally, electrical properties show that SWNTs have relatively low resistance and capability of carrying very high current densities [11-13].

Over the last few years, intense research and scientific effort have led to better control over chemical and structural properties of SWNTs. Currently, SWNTs are being considered for wide range of applications including electrical and photovoltaic devices [14-16]. Another interesting aspect of SWNTs is their morphology and biocompatibility

that are of interest for biomedical applications. Interestingly, SWNT properties such as length to diameter ratio, Young's modulus and resilience are similar to microtubules constituting major parts of the cytoskeleton in living cells [1]. When bundled, these nanotubes have a diameter and length similar to collagen fibers found in connective tissue [2].

1.2.1 Single Walled Carbon Nanotubes Physical and Chemical Properties

1.2.1.1 Bonding and Carbon allotropes

Theoretical and experimental data suggest that fullerenes and carbon nanotubes contain higher curvature and different anisotropy than bulk graphite and diamond, which results in increased chemical reactivity. Because of its unique electronic configuration, carbon can form several allotropes with a range of chemical properties. The difference in allotropes arises from the different bonds that can be present (σ and π) which are convergence of hybridization of valence electrons. There are three possible hybridization levels in carbon, defined as sp^n where n is hybridization level related to the number of *2p* orbitals mixed with the *2s* orbital. Carbon exist in three possible hybridizations and form following carbon geometries: sp^1 (single molecules, linear), sp^2 (planar structures, flat triangular), sp^3 (tetrahedral structures). Variation in possible mixing between the *s* and *p* orbitals gives rise to different covalent bond formation which can be used to classify the different carbon allotropes. In the case of diamond, a fully 3-D covalent sp^3 network is formed. For the case of graphite, 3 σ bonds and one out of plane π bond is formed. The latter sp^2 hybridization is the basis of bounding in SWNTs [17], as depictured in Figure 1.2.

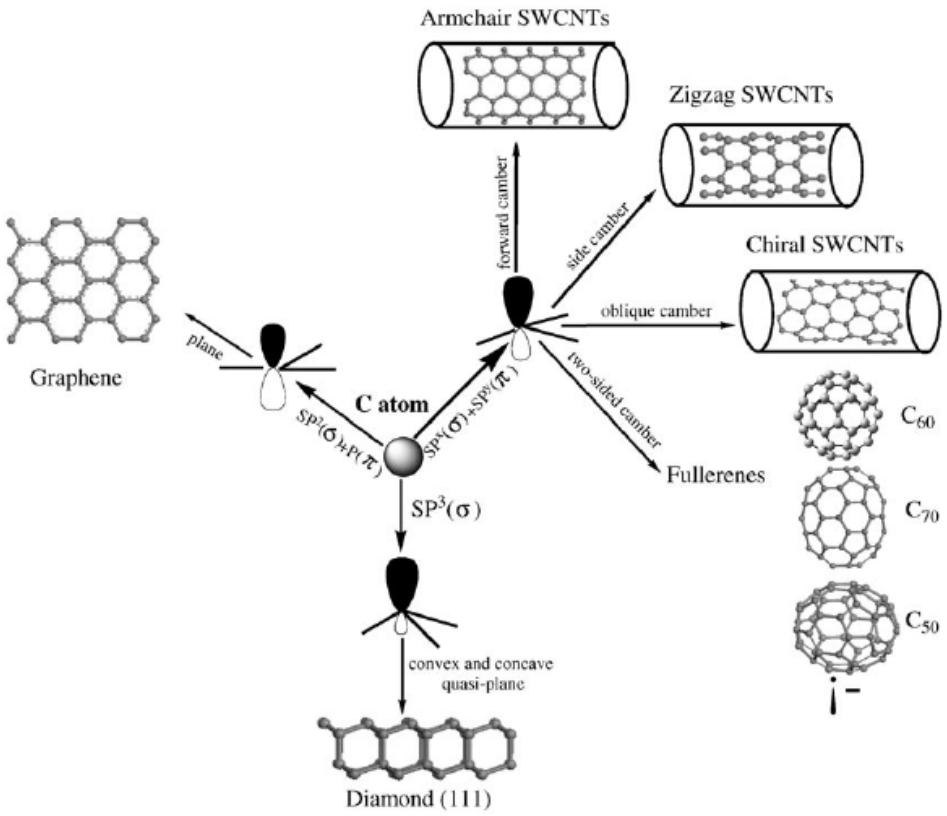

Figure 1.2 Variation in hybridization levels that define carbon bond type and their chemical and electronic characteristics. Carbon forms several different structures including graphene, diamond and carbon nanotubes [17].

The σ bond in sp^3 configuration is 0.15 nm long and has 315 kcal/mol energy whereas in sp^2 bond length is approximately 0.14 nm and binding energy is close to 420 kcal/mol. Carbon binding that is out of plane (π bond) causes SWNTs (and graphene) to efficiently conduct heat and electrons at higher rates. In addition, quantum confiment is calculated and experimentally confirmed to exist in SWNTs. This is directly related to the SWNT curvature as a result of σ- π rehybridization (bond mixing) [18]. Specifically, three σ bonds are slightly out of plane causing the π bond to be more delocalized, as outlined in Figure 1.3. The σ bond misalignment for (5,5) SWNTs is approximately 21.3^0 off from regular sp^2 binding [19].

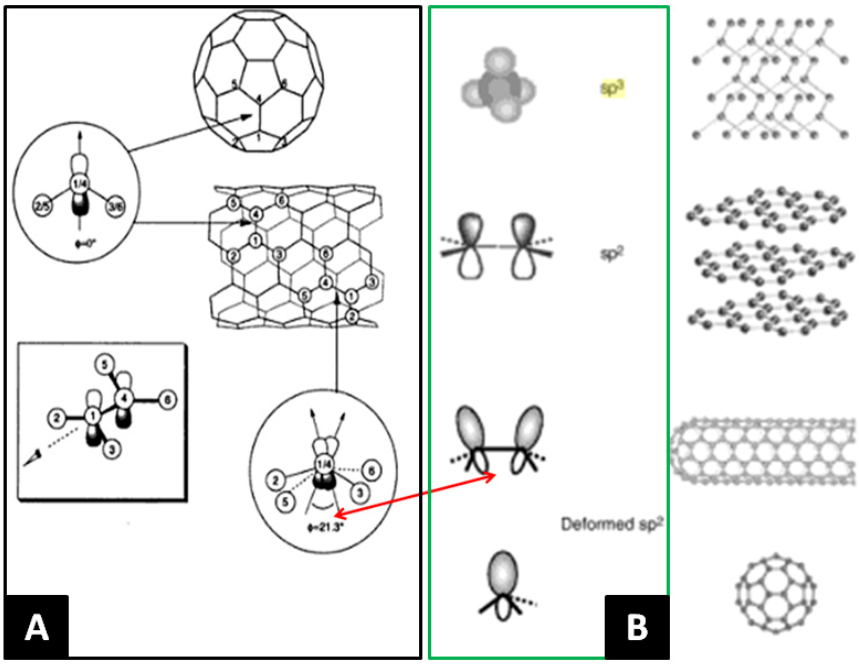

Figure 1.3 Carbon bonds associated with specific structures. (a) Specific configuration of σ- π bond in (5,5) SWNTs with delocalization angle of 21.3^0 is shown. (b) sp^2 and sp^3 carbon configurations found in graphene and diamond allotropes [19,20].

Carbon based materials also do not always form well defined structures. For example, metastable sp^3 bonds (dimond like carbon, DLC) , amorphous carbon (a-C) or hydrogenated amorphous carbon (a-C:H) consist of random networks of C-C (sp^3), C=C (sp^2) and C-H bonds, respectively. It has been found that sp^3 bonds degrade to the more stable sp^2 conformation over time unless stabilized by C-H bonds. Higher fraction of sp^3 bonds contribute to larger Young's modulus, hardness and chemical reactivity [20].

1.2.1.2 Structure of Single Walled Carbon Nanotubes

Nanotubes are made up from a single atomic layer of crystalline graphite, referred to as graphene, that is rolled up to form a tube. The nanotube structure can be described by a chiral vector (C_h) and translational lattice (T) vector as shown in Figure 1.4.

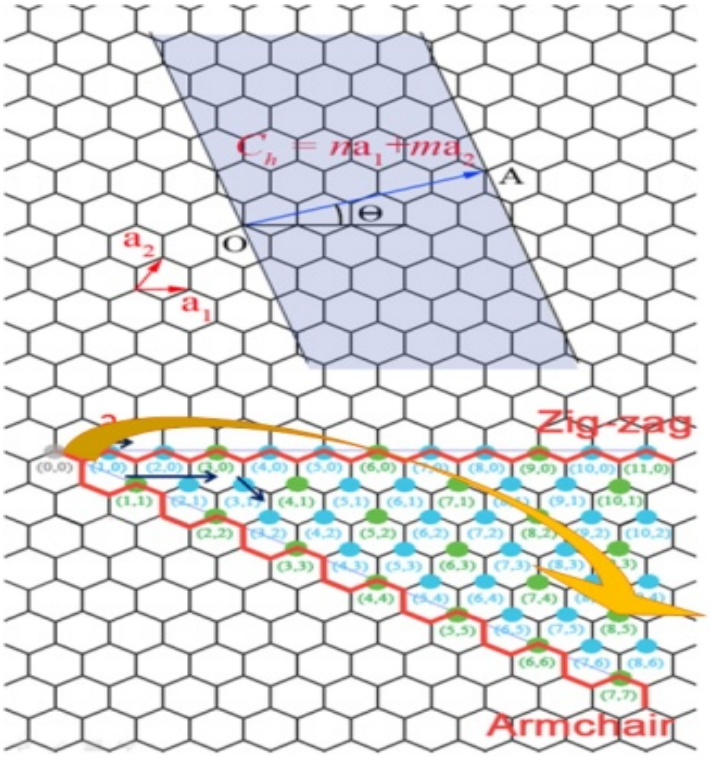

Figure 1.4 Chiral vector that defines single walled carbon nanotube structural characteristics. Upper diagram; Unit vectors a_1 and a_2 and an example of a chiral vector (C_h). Lower diagram represents possible vectors specified by the pairs of integers (n, m). In general, carbon nanotubes can have zigzag, armchair or chiral form (located between zigzag and armchair vectors). Blue arrows show how a nanotube with chiral vectors (3,2) may be formed. Orange arrow signifies direction of graphene sheet rolling to form a (8,5) armchair carbon nanotube. Blue dots correspond to semiconducting nanotube and green to metallic nanotubes [21].

Corresponding n and m chiral vectors define the SWNT circumference by equation:

$$C_h = na_1 + ma_2 \quad \text{(where n, m are integers)} \qquad \text{Eq. 1.1}$$

Theory showed that SWNT diameter d_t to be a function of vector C_h , length of C-C carbon bonds ($a_{C\text{-}C}$ = 1.44 Å) , and chiral angle θ. Where chiral angle θ is defined as the angle between the vectors C_h and a_1, according to equation 1.2 [15].

$$dt=\sqrt{3}a_{c\text{-}c}(m^2+mn+n^2)^{1/2}/\pi \qquad \text{Eq. 1.2}$$

Variations in chiral vectors produce nanotubes with well defined, and distinctive structures at the nano scale. Armchair, chiral and zigzag patterns carry either nanotube metallic, semi-metallic or non-metallic characteristics. Chirality is the most essential single parameter since it defines the diameter and corresponding electronic properties and reactivity (tube curvature) of SWNTs.

1.2.2 Interactions Between Nanosized Materials in Suspensions

The level of interactions of organic, inorganic or biological components with the surrounding environment is strongly correlated to its chemical, physical and structural properties. One key aspect of nanomaterials in general, and is also valid for SWNTs, is that for many biological applications they must be processed in solvents for either forming the scaffolds or for integrating into applications. In the case of SWNT networks, the carbon nanotubes are initially complementarily purified (see below) and placed in suspension. However, the creation of stable suspension is important because large van der Walls (vdW) interactions between the SWNTs lead to formation of bundles. Bundle sizes depend on dispersion properties including SWNT concentration and their size. The bundles have dramatically different physical and chemical properties which can significantly alter the chemical response to biological components. Therefore the nature of the bundling in suspension and that present in the network (assembled from SWNTs)

must be closely monitored to ensure reproducibility amongst biological assays. Typical SWNT bundle diameters have been experimentally measured to range from 10-20 nm in diameter, as shown in Figure 1.5 [19].

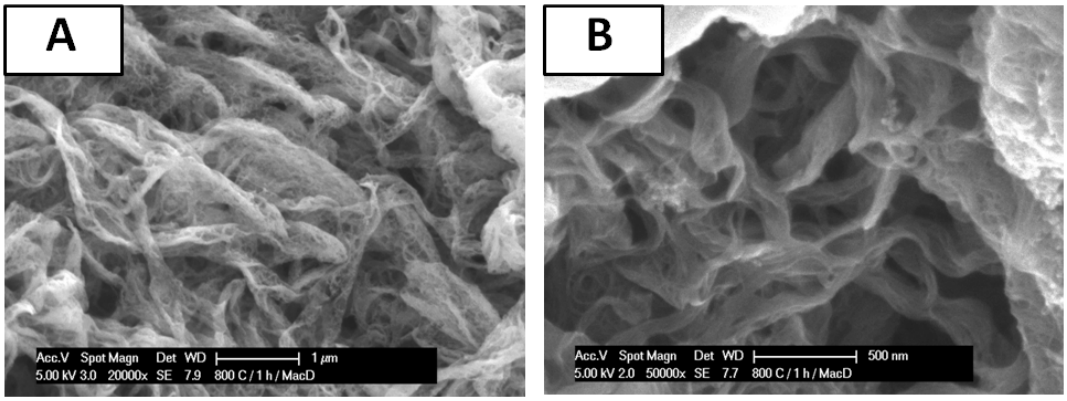

Figure 1.5 (a) Unpurified SWNTs tend to charge (bright image) when *Fe* particles are excited by electron beam. (b) Upon *Fe* removal charging effect diminishes indicating lower amount of iron catalyst.

Details of the purification procedure for as-synthesized SWNTs are provided in subsequent chapters of the thesis. However, it involves harsh acids necessary to remove metal catalysts used during nanotube synthesis [21]. The purification process leaves the SWNTs highly damaged, with ends open and defect sites present on the walls. The ends of the SWNTs are typically functionalized by carboxylic groups as indicated in Figure 1.6. It can be clearly viewed that the structure and chemical activity of purified SWNTs is dramatically different from ideal SWNTs. One of our aims was to study how this initially altered chemistry of SWNTs induced by the purification, impacts the bio-interaction rates in osteoblastic cells. Research experiments point out to purification process as one of major factors affecting carbon characteristics, that is reactivity and

nanotube bundling [19,22,23] . Harsh purification processes may cause nanotube side wall damage as seen in Figure 1.6.

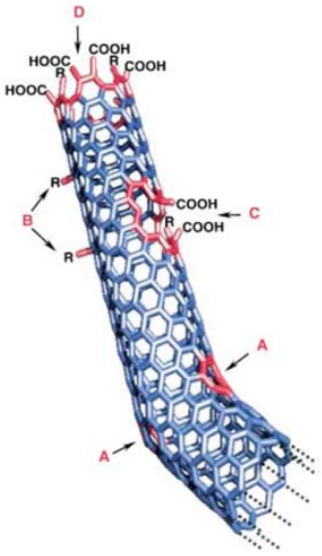

Figure 1.6 Defects present on a single-walled carbon nanotube. A and C correspond to pentagon and heptagon defect sites. B is double bond hybridization. Formation of active sites by removing end-cap is designated by D [22].

For uniform deposition of SWNT networks, stable dispersions of purified SWNTs are required. Such stable dispersions can be achieved with aid of surfactant. Sodium dedocyl sulfate (SDS) is the most commonly used dispersant for SWNTs which typically interact with defect sites on the SWNTs to create a charge cloud, as shown in Figure 1.7. Resulting double layer and steric repulsion forces create stable SWNT suspensions in SDS/water solutions. Similar forces are also expected to play major role in interactions between most biological components.

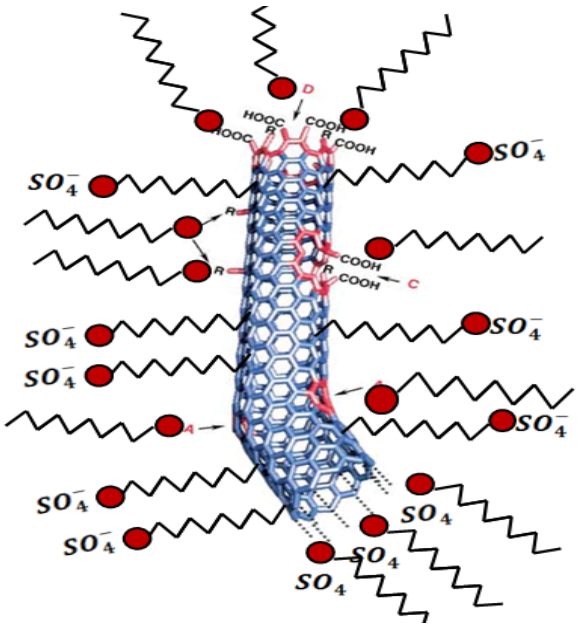

Figure 1.7 More realistic representation of SWNTs with defect sites and end caps being the most reactive sites on SWNTs. SDS surfactant cover most of the tube, but proteins may displace SDS and attach to active binding sites [22].

Like in many suspensions, micro and nano-particles interact and are subject to numerous forces. A colloidal system is defined as stable when existing attractive and dispersive forces acting between two particles in electrolyte solution are balanced. Van der Waal (vdW), Columbic and steric interactions are among the most likely ones to contribute in forming stable colloidal suspension [23,22], Figure 1.8.

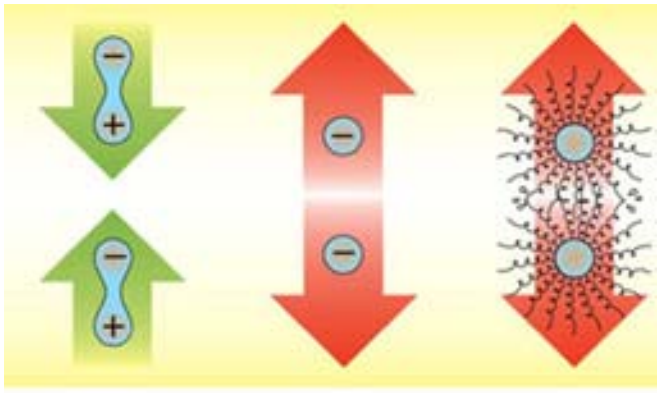

Figure 1.8 Attractive and dispersive forces existing in colloidal solutions. Listed in order from left to right: Van Der Waals, Coulombic and Steric forces [24].

In particular, colloidal particles are known to effect neighboring particles by inducing mutual repulsion based on columbic charge-charge interactions. At the same time, colloids are mutually attracted by fluctuating dipole-dipole (vdW) forces which arise due to fluctuations in the electron cloud around atoms in molecules [19]. These fluctuations will cause attractive interactions with neighboring molecules and their permanent dipoles (permanent dipole is defined as London dispersion force).

1.2.3 Forces Contributing to Nanotube Bundling and Matrix Formation

The unique structural properties of carbon materials contribute to formation of short and long dispersive forces (outlined in section 1.2.2). These electro-dynamic couplings originate from electron density charge distribution, a quantum –physics concept, and significantly contribute to van der Waals force formation [19]. SWNT stability in dispersion (coagulation rates) are governed by weak long and short vdW forces responsible for particles agglomeration. Specifically, density function (DF) theory is often applied to dense electron structures (bulk materials) to calculate electron density distribution to find bare static and dynamic susceptibility. However, contrary to bulk materials, soft elements (like MWNT and SWNT) have sparse electron density regions. These localized electron density sites are electro-dynamic coupling sites forming electromagnetic fields between interacting nanotubes. Locally, existing very low electron density regions are the effect of carbon nanotube chiral characteristics. These weak, but numerous interactions form local electromagnetic repulsion fields and shape static susceptibility. In that respect, tubes may become stabilized when equilibrium between

short-range repulsion and long-range attractive/repulsive vdW forces is established. Based on this mathematical model, energy between two rod like colloids is formed by electron densities defining static susceptibility factor χ_0. The factor is defined by repulsion forces (electrodynamic coupling) short range vdW and nanotube geometry [19,25].

Parallel carbon nanotubes are expected to strongly interact along its length mainly because numerous coupling sites and unique dipole coupling constant of the carbon nanotube system (shifted sp^2/sp^3 bonds, section 1.2.1.1). First-principle DF with plasmon-pole model was demonstrated to be capable of describing microscopic electron interactions produced by local-field effects expressed by susceptibility factor χ_0 , equation 1.4.

$$\chi_0(n(r), u, u_0) = \frac{n(r)}{u^2 + u_0^2} \qquad \text{Eq. 1.4}$$

Where u is frequency, $n(\mathbf{r})$ nanotube electron density at position r with effective energetic frequency limit at u_0. The equation points to an important link between unique electron density states, nanotube radius and its length and coagulation energy source; the inter-tubular vdW forces.

Cylindrical coordinate system *(s,θ,z)* defines *z* as being a main axis along the tube length, azimuth angle (*θ)* and specifies vector *s* perpendicular to the z-axis. Local effective susceptibility (χ^{ij}_{eff}) can be calculated under assumptions that electron density is uniformly distributed along the SWNT radius and local electric filed ($\emptyset(s, u, u_0)$) and charge is conserved. Susceptibility that is based on strong electron-dynamic coupling will take effect when externally applied electric field (E_0) induces local bond

polarization. Corresponding carbon tube electrical potential under external electric filed can be defined by equation 1.6

$$\phi(s,u,u_0) = -E_0(u)W(s,u,u_0)\cos\theta \qquad \text{Eq. 1.6}$$

Furthermore, the model evaluates susceptibility factor along tube radius (R), assuming thin tube wall approximation.

$$\chi^{\gamma}_{eff}(s,u,u_0) \rightarrow \chi^{\gamma}(R,u,u_0)\ \delta(s-R) \qquad \text{Eq. 1.7}$$

Then, amalgamate of these two equations in terms of dipole-dipole interactions between two nanotubes separated by distance *d,* was used to calculate vdW energy *(*where θ_1, θ_2, corresponds to a one and two dimensional integral frequencies and $I_{\beta\gamma}$ = (s, *θ,z)* under geometrical terms).

$$E_{vdW} = I_{\beta\gamma}(\theta_1,\theta_2,s_1,s_2) = \int_{\infty}^{-\infty} dz_{21}\,(T_{12}^{\beta\gamma}(d))^2 \qquad \text{Eq. 1.8}$$

Reported dipole coupling energy interaction between two nanotubes can be summarized, in equation 1.9, by gradient differential vector field (∇) in electron charge distribution (T_{12}) along the tube radius.

$$T_{12} = -\nabla_1\nabla_2|r_2 - r_1|^{-1} \qquad \text{Eq. 1.9}$$

Further integration helps to define cutoff atomic frequencies $u_0^{(1)}$ and $u_0^{(2)}$ that are related to tube diameter, and chirality but have little effect on its susceptibility [25].
The DF-vdW based approach can accurately describe discrete interactions between nanotubes and proteins and shed light on SWNT toxicity in biological systems. In fact, it

is estimated that distance between nanotubes at which point tubes strongly interact (assuming same distance between tubes) is close to 3-3.5 Å [25] for larger diameter SWNTs.

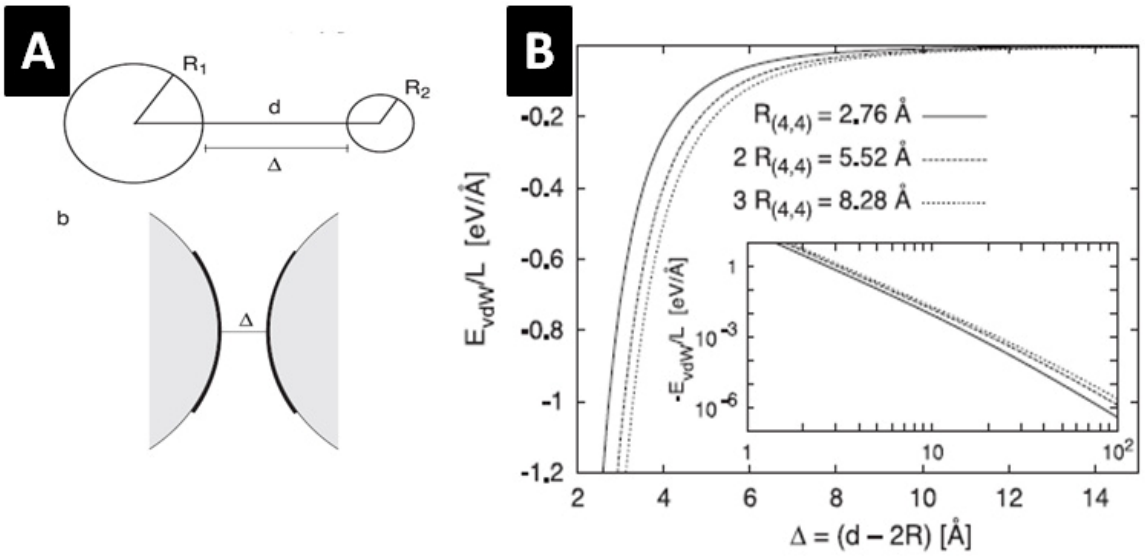

Figure 1.9 Van der Waals interaction between pair of nanotubes with same diameter as a function of separation distance Δd [25]. Larger nanotubes have less curvature and effectively larger charge per area ratio. At given distance *d* the relationship generates greater total energy interactions per tube length.

Reported electron density states and calculated vdW forces suggest that on nanoscale the attraction force between large nanotubes (diameter and length) will be greater than among small ones at given separation distance Δ*d*. The results suggest that agglomeration is nucleated by larger nanotubes. However, small nanotubes will have lower root mean square (R.M.S) displacement but higher Brownian motion and kinetic rates.

Heavier and larger bundled nanotubes (in simplified case, spheres of radius r) will settle quicker (u_t, terminal velocity) under gravitational pull (g), according to Stoke's equation 1.10

$$u_t = \frac{(\rho_s - \rho_l)gr^2}{18\eta} \qquad \text{Eq. 1.10}$$

Factors like fluid viscosity (η) , particle (ρ_s) and liquid density (ρ_l) will affect sedimentation rates up to microscopic scale.

However, small well dispersed unbundled nanotubes (loose) will not settle down but randomly move due to thermal diffusion process (D). This process is described by the Einstein equation. The Brownian motion depends on ambient temperature (T) , k (gas constant) and friction factor (B), see equation 1.11 [23].

$$D = \frac{kT}{B} = \frac{kT}{6\pi\eta r} \qquad \text{Eq. 1.11}$$

1.3 Biology: Introduction to Cell Biology

Basic cellular components include a nucleus, mitochondria and a cell membrane. The membrane is composed of a phospholipid bilayer that performs multiple functions. It encloses vital cell organelles but more importantly it hosts membrane sensors and channels allowing a cell for intra and extracellular communication. In cell growth and tissue generation experiments, the cell relies on external sensors mainly to seek out for the most suitable (appropriate roughness, bioactivity and surface energy) location for attachment. Process that is important during sequential bone healing.

1.3.1 Cell Biology

Upon seeding, each cell descends onto a substrate and surveys the matrix surface using peripheral filaments and membrane proteins, see Figure 1.10. The cell's membrane proteins probe the substrate and initiate contact points via chemical linkages involving ionic, Van der Walls and steric forces [26].

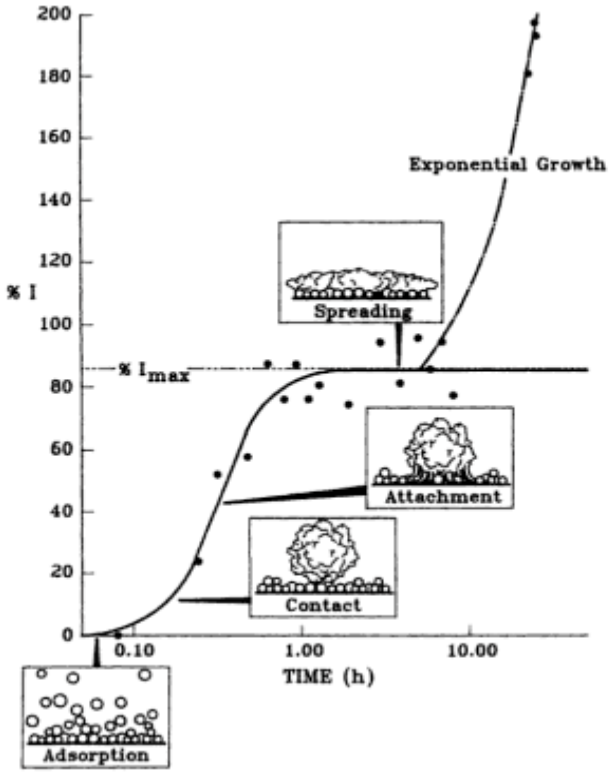

Figure 1.10 Initial cell-materials interactions are initiated only after a substrate is wetted by cell culturing media within first an hour [27].

During this time, the cell moves along the substrate. The movement itself consists of five steps that include cell extension, adhesion, contraction, and release and recycling (Figure 1.11). Once the cell finds a suitable location, it creates a vinculin based initial adhesion points, called focal points [28]. Cell adhesion is supported by contractile

meshwork (lamellar protrusion). This process is active until the cell begins interacting with other surrounding cells. At that point, inhabiting contractile proteins are released and cell retraction occurs. A settled cell is supported by cell membrane receptors (integrins) which are estimated to be 10-15 nm away from the substrate [29].

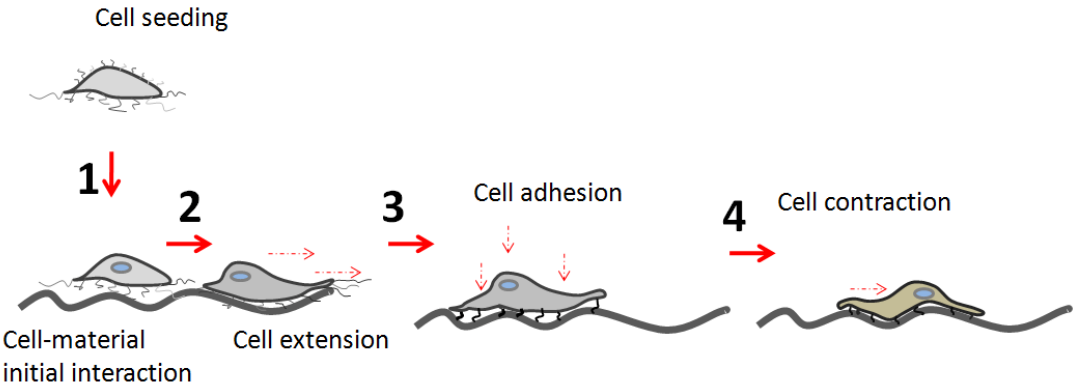

Figure 1.11 Initial interactions between a cell and the substrate. Following deposition on the substrate, cell moves around probing the surface [29].

A hypothesized cell-material mechanisms model points to integrins as the major entities responsible for initial and long term interactions. It is suspected that integrins receive the signal, either chemically or mechanically, and convey it via cytoskeleton proteins. Signal propagating pathway includes; Talin, paxillian, tensin, and actin filaments. Lastly, the actin filaments directly act on cell nucleus affecting gene expression and corresponding protein synthesis as seen in Figure 1.12.

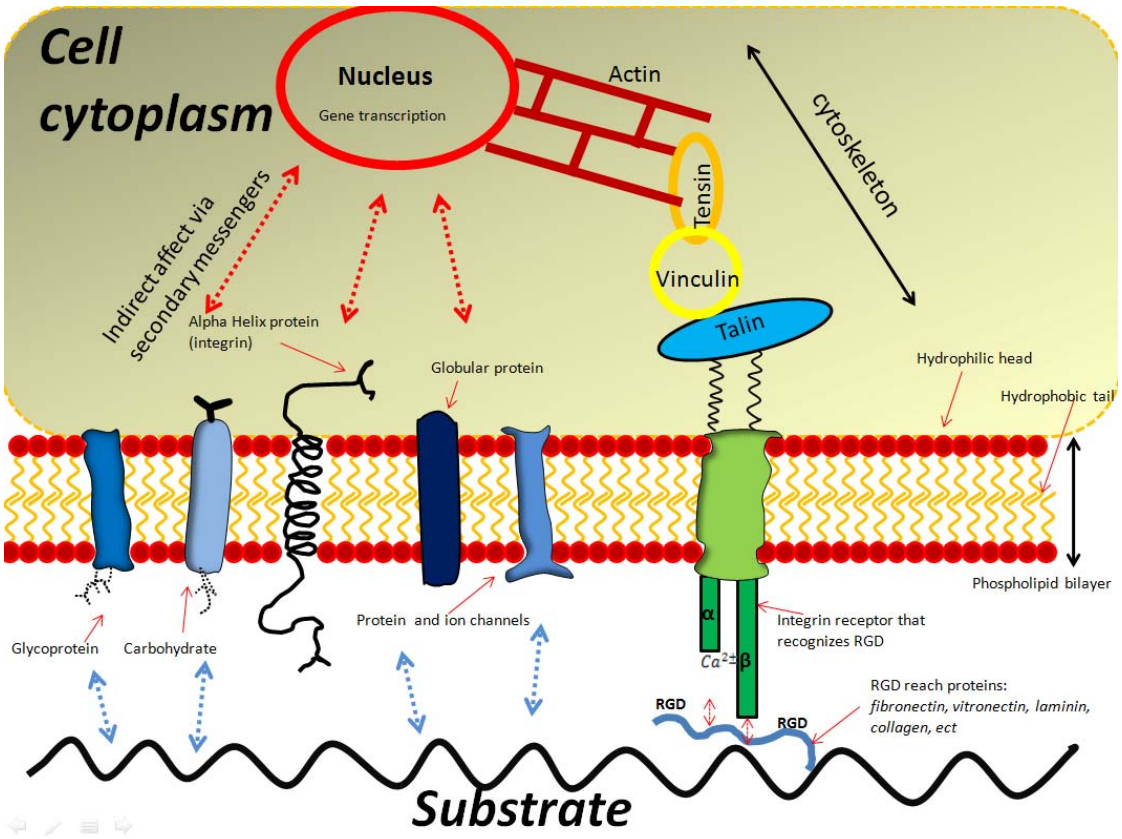

Figure 1.12 Schematic representation of simplified cell membrane-substrate interactions and signal transduction. These interactions affect cell nucleus and ultimately cell development [29].

.

It is known that actin fiber extensions support finger like protrusions from plasma membrane. These extensions are called filopodia or lamellipodia if protrusions form a mesh. Once the focal point is established, mature actin fibers are formed and over time reinforced by tubulin microtubules [29], as seen in Figure 1.13.

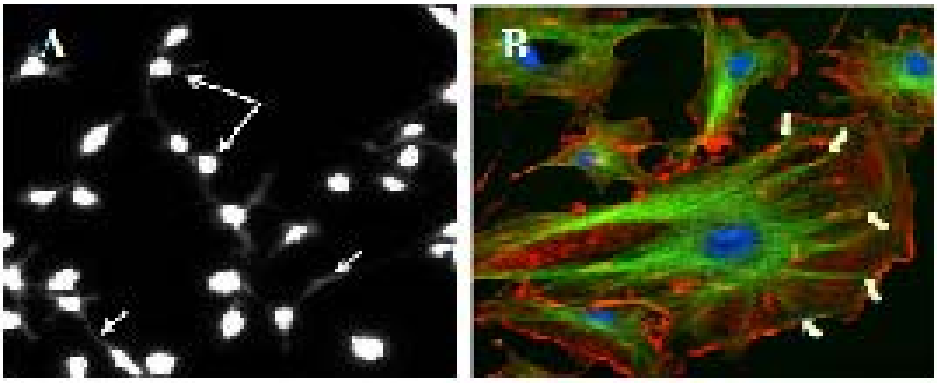

Figure 1.13 Cell attachment to a surface. (a) Arrows point to osteoblast cells attached on a nanotube substrate with visible filopodia extensions. (b) Actin filaments are shown in red, blue color correspond to cell nuclei and microtubules are designated green. Arrows point to cell adhesion focal points [29].

Once the cell is permanently attached, it experiences a physiological and morphological changes orchestrated by the nucleus. A cell nucleus is an organelle that stores and maintains genetic information such as deoxyribonucleic acid (*DNA*) as well as controls the function and development. Its genetic information is used as an internal clock directing and controlling cell life cycle. Similarly to human life, cells undergo growth, maturation, division and death stages. The cell life cycle is arbitrarily divided into four stages; ***S***, ***G2***, ***M*** and ***G1***, depicted in Figure 1.14. The cell cycle starts with DNA replication during ***S*** phase which is followed by a gap, ***G2*** phase, then mitosis and cytokinesis during ***M*** phase, to be finally followed by another gap, ***G1*** phase. ***M*** phase is cell division and growth phase. ***S*** phase is also associated with cell growth in addition to DNA replication. ***G1*** and **G2** are interphases in which cell cytoskeleton (*actin*, *tubulin*) is rearranged to give the cell a new shape or even accommodates cell division.

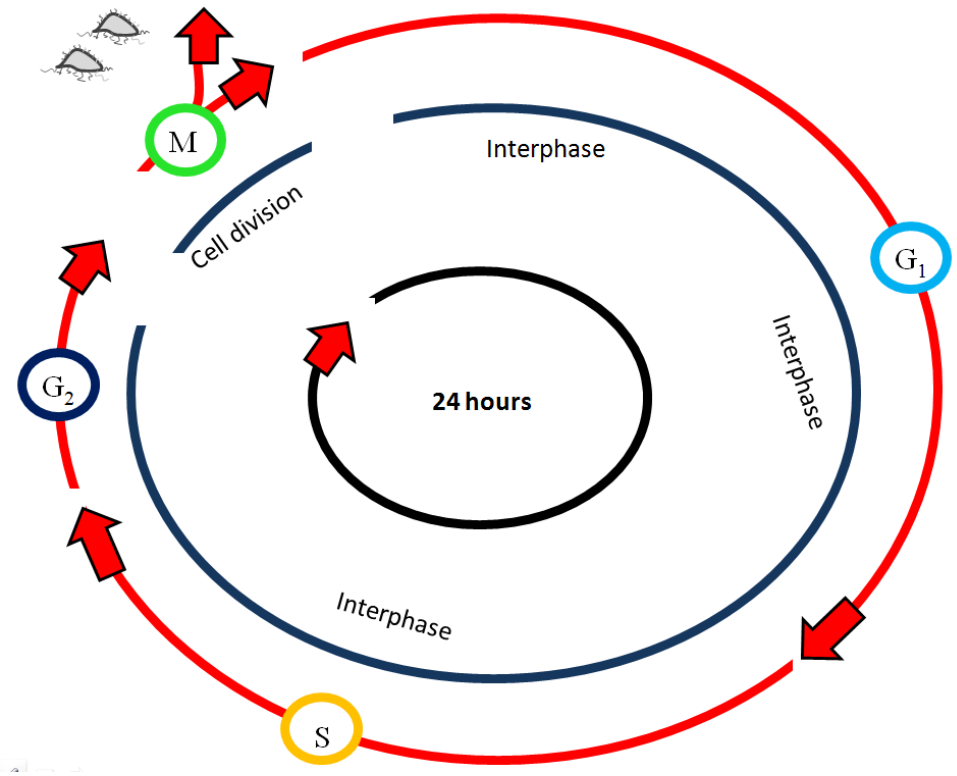

Figure 1.14 Schematic image representing a cell cycle. The cycle starts from cell division and takes 24 hours for completion [29].

It is important to understand that cell response is strongly affected by intercellular communications via small protein, glycoprotein or peptide based messengers [2]. For example, small 12-45 kDa in size complex proteins (growth factors, hormones, cytokines that are extracellular messengers) are secreted by cells as means to communicate and stimulate other cells. Cells within forming tissues rely upon an extracellular communication system which adjusts cell population levels.

An excellent example of cell to cell cross communication exists in primary osteoblastic cell cultures. The primary cells are known to include many different cell types such as macrophages, osteocytes, osteoblast or fibroblasts that form functional calvariea tissue. These cells form a functional unit that responds and impacts to surrounding tissue by

synthesizing and releasing as well as detecting and processing growth factors. One of most prominent aspect of the osteoblastic cell culture is their ability to synthesize cytokines. Cells forming bone tissue can express **t**ransforming **g**rowth **f**actors (*TGF),* **e**pidermal (*EGF)* or **f**ibroblast **g**rowth **f**actors (*FGF*). These factors could be released from macrophage or fibroblast cells either upon external stimuli or during stress-induced disruption of cell membrane [30]. For example, *TGF* is a polypeptide with α and β isoforms that is responsible for inducing cellular transformation, specifically tissue regeneration. The *TGF-*α growth factor is implicated in stimulating bone resorption in *in-vivo* systems and accelerating osteoblast differentiation processes. Concurrently, *EGF* was discovered to indirectly stimulate osteoclastogenesis by releasing osteoclast regulatory factors from osteoblast [31].

1.3.2 Characteristics of Osteoblastic Cells

Bone tissue serves as one of the most important parts of all living entities since it provides structural, biochemical and physiological framework for the entire body. Structurally, the bone acts as a physical frame for soft and muscle tissues placement, attachment and protection. Osteoblastic cells constitute major part of any skeleton including vertebral column, thoracic cage, skull or femoral bone. Bone tissue is actively engaged in maintaining mineral homeostasis of calcium phosphate, sodium and magnesium ions [32]. It is also the source of leukocytes and hemoglobin cells (hematopoietic) that serves as an important part of human immune and respiratory systems.

The bone tissue is being constantly remodeled throughout its lifespan. This varies in rate and extend, depending on species type, gender and age .The remodeling is a complex mechanism where depleted or damaged local bone tissue is removed (bone resorption) and replaced by newly produced bone matrix (bone formation).

Bone cells are derived from mesenchymal cells (found in mesoderm/ connective tissue) which can, upon proper physiological stimulation, differentiate into preosteoblast and then osteoblastic cells, Figure 1.15.

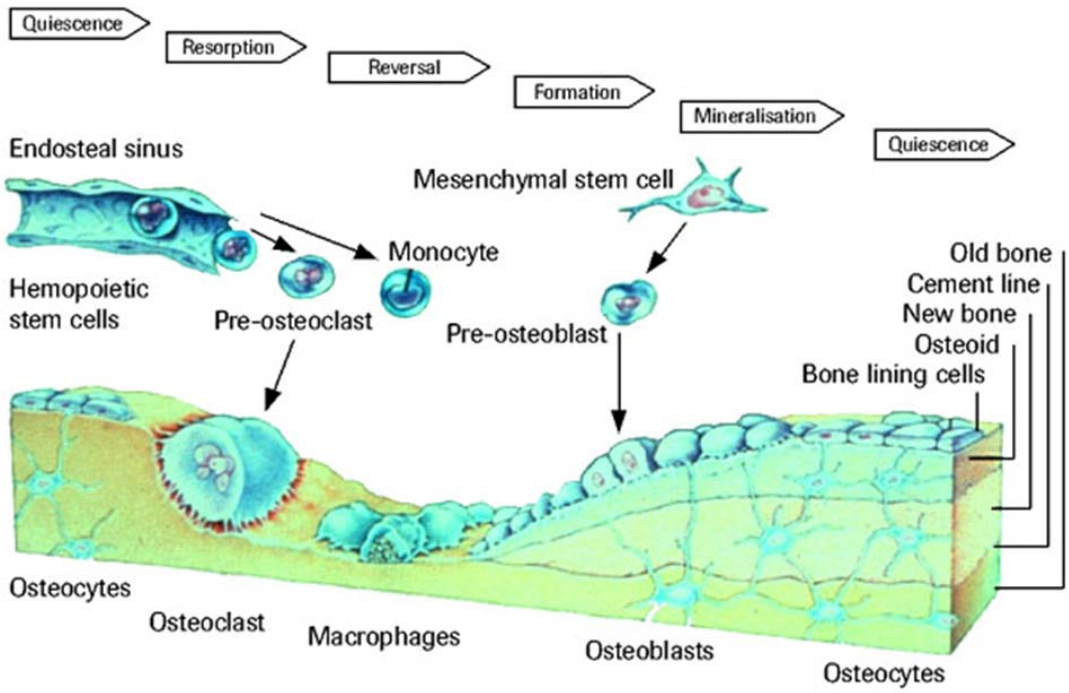

Figure 1.15 Bone tissue consist of three cell type; osteoblasts, osteocytes, osteoclasts that combine to form bone lining cells. Bone hosts numerous other cells including mesenchymal, chondrocytes and leukocytes. Arrows on top outline steps involved in bone formation [33].

Bone and blood cells originate from common precursor hematopoietic cells called stem cells. Stem cells may be either pluripotent/ mesenchymal (can renew itself for long time and differentiate into many type of cells) or unipotent, also known as progenitor cells

(committed to forming only one type of cells). Osteoblastic cells can be derived from stem cells originating from many tissues including adipocyte, muscle or marrow stromal fibroblast, with last one being most often the stem cell source.

The cells grown either in-vitro or in-vivo environment undergo series of specific metamorphoses including cell proliferation, differentiation, mineralization and finally calcification. It is a long and complex process summarized in Figure 1.15. The tissue will mineralize and form bone when the cells synergistically express bone phenotype markers, for example: extracellular matrix (*ECM*), tissue non specific alkaline phosphatase (*TNAP*) and *collagen I* . Fibril *collagen I* is a part of *ECM* and one of the major elements required for bone synthesis. Intercellular communication and synergetic cooperation between bone resorption (osteoclasts) and bone forming (osteoblasts and its mature form; osteocytes) cells assure healthy bone structure throughout the lifespan of any individual.

1.3.3 Cell Toxicity

Toxicity on cell, tissue or organ level can be defined as functional impairment or death of normally healthy subject. In case of cell cultures, this broad description includes direct (cell necrosis and apoptosis) but also indirect effects manifested by changes in cell DNA. Short term acute toxicity on cellular level (cell damage or death) can be quantified by counting cells or monitoring enzyme specific markers. Five initial days are usually sufficient to assess the material impact on biological systems, but long term effects are more challenging to detect. Most basic toxicity measurements rely on colorimetric and fluorescent methods which indirectly indicate cell viability. The

methods encompass cellular metabolic and viability rate tests , including alamur blue (*AB*) a neutral red dye (*NR*),(lysosomal activity) or tetrazolim salt based (*MTT*) assays. Additional information can be obtained by applying lactate dyhydroganase (*LDH*, cell membrane integrity), adenalate kinase (*AK*, specific enzymatic activity) or *TUNEL* test detecting fragmented *DNA* at 3'-hydroxyl ends [34] . Other toxicity verification methods may include quantification of cytokines, for example interlukins (*IL*). However, extent and amount released will depend on cell line type. Total protein expressed in cell cultures can also be used to indirectly monitor cell response (coomassie staining ,Briliant blue), but a careful data interpretation is required.

Long term toxicity effects are characterized by slow changes in cell genome (DNA bases) by changing DNA sequence and RNA expression levels. Literature indicates that particles like carbon nanotubes, act in biological systems in similar way to oxidizing species and affect cell cycle. Specifically, multiple and single walled nanotubes oxidative activity was linked to onset in formation of reactive oxygen species (ROS) ,overexpression of sp53 protein –master guardian of cell cycle (DNA reaper and cell apoptosis) and increase in 8-oxoguanine-DNA glycosylase 1 (OGG1,enzyme responsible for DNA repair) [35,36].

1.3.4 Mechanisms involved in Carbon Nanotube Cellular Internalization Process

Mechanism by which nanotubes affect cells is not entirely understood but some clues point to at least three possible possibilities. These include ion channel blocking, endocytosis mediated cell apoptosis and internalized DNA-SWNTs interactions leading to change in cell functioning [37] .

SWNTs have ability to reversibly block potassium (K+) channels without permanent chemical interaction between the channel and CNT molecules [38]. Controlled by channel potassium content, on molecular level, indirectly regulates cell differentiation and growth. In simplified model, K+ channels control membrane potential and as so directly regulate Ca influx. Change in Ca ion content is expected to directly regulate cell proliferation levels. Additionally, it was discovered that loose nanotubes are able to penetrate cell membrane and were found inside living cells. Nanotube may traverse cell membrane via endocytotic pathways including phygocytosis, pinocytosis and clathrin dependent/ independent endocytosis but also energy independent nonendocytotic mechanism [37,39,40]. High concentrations of internalized nanotubes have been reported to cause cell apoptosis and possibly necrosis [41].

1.4 Cell - Materials Interactions: Introduction

Environment is one of the strongest stimuli in actively shaping living organisms. Similar complex interactive processes can be observed on a much smaller cellular level. Cell cultures are responsive and adaptive to the surrounding environment. Factors which include substrate chemistry, morphology or reactivity affect some of the multiple membrane sensors that trigger signal transduction.

Cell membranes are dotted with multiple types of ion channels, predominantly Ca^{+}, Na^{+}, K^{+}. However, other membrane sensors include stretch activated ion channels, and mechano-transduction receptors are also present [42]. Cell membranes have ample other glycoprotein based sensing probes that involve integrins, cadherins or selectins which are utilized by cells to sense surface structural and chemical clues and

biomolecules. Upon proper stimulation, each cell is able to send information to the nucleus that indirectly affects the cell development. Stimulated cell will adjust its cycle accordingly to expressed genes and proteins that will eventually impact tissue development [2].

When cells are deposited on a matrix, they will immediately start to interact with it. This is because cells are equipped with biological sensors capable of detecting surface properties. Specifically, osteoblastic cells are known to be highly responsive to the physical properties of the substrate including mechanical stress, surface roughness and chemistry [43,44]. These material surface properties impact cell response, but the extent and type of response will depend on the type of stimulus and its duration.

Because sensitivity of osteoblastic cells to material properties is well documented, this particular cell line represents a good model to investigate the effect of SWNT networks and their properties on cell development.

1.4.1 Cell Exposure to Apically Deposited Nanotubes

Nanotubes in physiological environment are expected to behave similarly to nanotubes in water/surfactant dispersions, as outlined at the beginning of the chapter. In fact, small in size unbundled SWNTs (more kinetically active) are less susceptible to chemical and physical interactions that may lead to higher toxicity rates observed in biological systems (outlined in earlier sections). Experimental results reported by Zhang et.al., or Manna et.al., support the notion of loose SWNT toxicity and their ability for easy cell membrane penetration [39,41,43]. Carbon nanotube dispersions with

concentrations 100 μg/mL are often cited to cause decrease in cell viability, or necrosis [45].

Several examples of the studies reporting the influence of the cell response can be found in literature. The toxicity tests have been reported for single (diameter 0.9-1.7 nm) and multiple (diameter, 10-80 nm) walled carbon nanotubes. The studies utilize well purified and dispersed nanotube suspensions mixed with culturing medium. The nanotube concentrations are graduated to investigate cell toxicity response. For example, data reported by Zhang et al., suggest that SWNTs when present at low concentrations (up to 1 μg/mL), have no or minimum toxic effect on the osteoblastic cell cultures as shown in Figure 1.16 .

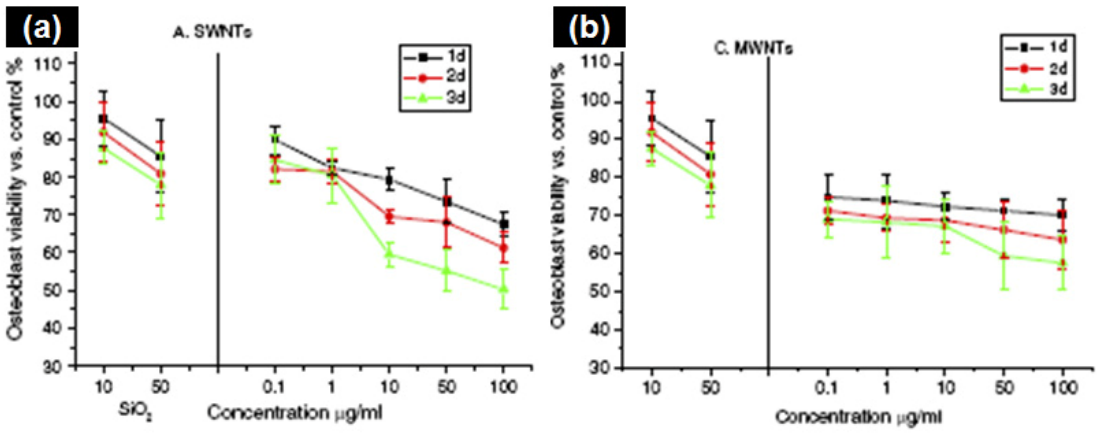

Figure 1.16 Exposing mouse primary osteoblastic cells to loose SWNTs and MWNTs at various concentrations. (a) Small amounts of SWNTs seem to cause limited toxicity. (b) Larger in size MWNTs appear to constantly damage cells [45].

The study indicates that cell exposure to high concentration of large or small diameter nanotubes leads to cell damage. It is interesting to notice that cell cultures do not exhibit linear toxicity response to SWNT stimuli. Two phasic behaviors can be observed. On the

other hand, osteoblastic cell cultures exposed to MWNTs showed weak but concentration depended response, Figure 1.16 (b).

It can be concluded that the amount, size and its availability within given system are important factors affecting cell toxicity.

1.4.2 Cell Exposure to Basally Deposited Nanotubes

Interestingly, literature review on single and multiple walled nanotubes deposited to form networks suggests that confined nanotubes cause less toxicity. For example, polymer/SWNT composites [9], SWNT based free standing papers [46] or sprayed on substrate and dried samples [46] are reported to evoke mild or no side effects, as seen in Figure 1.17 .

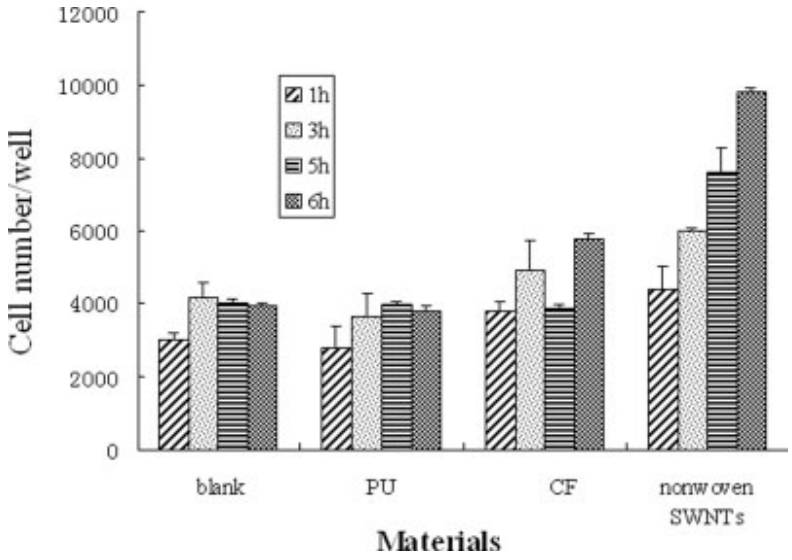

Figure 1.17 Biological experiments on SWNTs deposited in form of films indicate that confined nanotubes are minimally or non toxic and can be potentially used in biomedical application [47].

Although these results seem to be surprising in the light of earlier mentioned SWNT toxicity tests, they also corroborate existence of strong intertubular vdW forces. Calculated energy between two carbon nanotubes is approximately 1.1 eV/ Å (at minimum allowable distance of 0.3 nm) and increases with tube length and diameter. This could suggest that attraction between nanotubes (bundling) will likely originate between longer and larger SWNTs and slowly attract surrounding tubes forming aggregates. Free standing SWNT networks or their sprayed or drop-casted types are strongly held together by vdW forces. Nanotube confinement to substrate and between nanotube interactions effectively limit number of available loose nanotubes, eliminating or reducing cell toxicity.

1.5 References

[1] Pampaloni F, Florin EL. Microtubule architecture: inspiration for novel carbon nanotube-based biomimetic materials. Trends Biotechnol. 2008 Jun;26(6):302-310

[2] Alberts B, Bray D, Johnson A, Lewis J, Raff M, Roberts K, et al. Cytoskeleton. In: Robertson M, editor. Essential Cell Biology. 1st ed. New York & London: Garland Publishing, Inc; 1998.

[3] Hussain MA, Kabir MA, Sood AK. On the cytotoxicity of carbon nanotubes. Current Science 2009;96(5):664.

[4] Usui Y, Aoki K, Narita N, Murakami N, Nakamura I, Nakamura K, et al. Carbon nanotubes with high bone-tissue compatibility and bone-formation acceleration effects. Small 2008 Feb;4(2):240-246.

[5] Henning T, Salama F. Carbon in the Universe. Science 1998;282:2204-2210.

[6] Park KH, Chhowalla M, Iqbal Z, Sesti F. Single-walled carbon nanotubes are a new class of ion channel blockers. J.Biol.Chem. 2003 Dec 12;278(50):50212-50216.

[7] Shvedova AA, Kisin ER, Mercer R, Murray AR, Johnson VJ, Potapovich AI, et al. Unusual inflammatory and fibrogenic pulmonary responses to single-walled carbon nanotubes in mice. Am.J.Physiol.Lung Cell.Mol.Physiol. 2005 Nov;289(5):L698-708.

[8] Shvedova AA, Kisin ER, Murray AR, Gorelik O, Arepalli S, Castranova V, et al. Vitamin E deficiency enhances pulmonary inflammatory response and oxidative stress induced by single-walled carbon nanotubes in C57BL/6 mice. Toxicol.Appl.Pharmacol. 2007 Jun 15;221(3):339-348.

[9] Kagan VE, Tyurina YY, Tyurin VA, Konduru NV, Potapovich AI, Osipov AN, et al. Direct and indirect effects of single walled carbon nanotubes on RAW 264.7 macrophages: role of iron. Toxicol.Lett. 2006 Aug 1;165(1):88-100.

[10] http://cnx.org/content/m22963/latest/ Carbon allotropes.

[11] Thess A, Lee R, Nikolaev P, Dai H, Petit P, Robert J, et al. Crystalline Ropes of Metallic Carbon Nanotubes. Science 1996 Jul 26;273(5274):483-487.

[12] Yu MF, Files BS, Arepalli S, Ruoff RS. Tensile loading of ropes of single wall carbon nanotubes and their mechanical properties. Phys.Rev.Lett. 2000 Jun 12;84(24):5552-5555.

[13] Hone J, Whitney M, Piskoti C, Zettl A. Thermal Conductivity of Single-walled Nanotubes. Physical Review B 1999;59(4).

[14] Dresselhaus MS, Dresselhaus G, Avouris P. Carbon nanotubes, synthesis, structure, properties and applications. 1st ed. Berlin, Heidelberg,: Springer-Verlag; 2001.

[15] Fanchini G, Unalan EH, Chhowalla M. Optoelectronic properties of transparent and conducting single-wall carbon nanotube thin films. Applied Physics Letters 2006;88(19):191919-191919-3

[16] Cao C, Rogers JA. Ultrathin Films of Single-Walled Carbon Nanotubes for Electronics and Sensors: A Review of Fundamental and Applied Aspects. Adv. Mater. 2008, 20, 1–25 2008;20(4):1-25.

[17] Li J, Jia G, Zhang Y. Chemical anisotropies of carbon nanotubes and fullerenes caused by the curvature directivity. Chemistry 2007;13(22):6430-6436.

[18] Meyyappan M. Carbon nanotubes: science and applications. 1st ed. New York & London.; CRC Press; 2005.[19] Schwarz JA, Contescu CI, Putyeraitle K. Dekker Encyclopedia of Nanoscience and Nanotechnology , Volume . 1st ed. New York, N.; CRC Press; 2004.

[19] Shvartzman-Cohen R, Nativ-Roth E, Baskaran E, Levi-Kalisman Y, Szleifer I, Yerushalmi-Rozen R. Selective dispersion of single-walled carbon nanotubes in the presence of polymers: the role of molecular and colloidal length scales. J.Am.Chem.Soc. 2004 Nov 17;126(45):14850-14857.

[20] Donnet C, Erdemir A. Tribology of Dimond-like Carbon Films. Fundamentals and Applications. 1st ed. New York, NY: Springer; 2007

[21] H. E. Unalan. Single Walled Carbon Nanotube thin films: properties and applicationsRutgers, The State University; 2006.

[22] Dalton AB, Collins S, Muñoz E, Razal JM, Ebron VH, Ferraris JP, et al. Super-tough carbon-nanotube fibers. Nature 2003;423(703).

[23] Hunter RJ. Introduction to colloidal science. 1st ed. New York: Oxford Science Publications; 2003.

[24] http://www.iupac.org/didac/Didac%20Eng/Didac01/Content/C02.htm. Repulsion forces.

[25] Mylvaganam K, Zhang LC. Deformation-promoted reactivity of single-walled carbon nanotubes. Nanotechnology 2006;17:410-414.

[26] Bongrand P, Capo C, Depieds R. Physics of cell adhesion. Progress in Surface Science 1982;12(3):217-285.

[27] Berg J. Wettability. 1st ed. New York & London: CRC Press, 1993.p. 228.

[28] Li CY, Gao SY, Terashita T, Shimokawa T, Kawahara H, Matsuda S, et al. In vitro assays for adhesion and migration of osteoblastic cells (Saos-2) on titanium surfaces. Cell Tissue Res. 2006 Jun;324(3):369-375.

[29] Alberts B, Bray D, Johnson A, Lewis J, Raff M, Roberts K, et al. Cytoskeleton. In: Robertson M, editor. Essential Cell Biology. 1st ed. New York & London: Garland Publishing, Inc; 1998. p. 513-546.

[30] Clarke MS, Feeback DL. Mechanical load induces sarcoplasmic wounding and FGF release in differentiated human skeletal muscle cultures. FASEB J. 1996 Mar;10(4):502-509.

[31] Kwok S, Qin L, Partridge NC, Selvamurugan N. Parathyroid hormone stimulation and PKA signaling of latent transforming growth factor-beta binding protein-1 (LTBP-1) mRNA expression in osteoblastic cells. J.Cell.Biochem. 2005 Aug 1;95(5):1002-1011.

[32] Gideon AR. Bone homeostasis. Proc. Natl. Acad. Sci. 1998;95:13361-13362.

[33] www.roche.com/pages/facets/11/ostedefe.htm. Bone formation.

[34] Goping G, Wood KA, Sei Y, Pollard HB. Detection of fragmented DNA in apoptotic cells embedded in LR white: A combined histochemical (LM) and ultrastructural (EM) study. J.Histochem.Cytochem. 1999 Apr;47(4):561-568.

[35] Schranda AM, Daia L, Schlagerb JJ, . Hussain SM, Osawa E. Differential biocompatibility of carbon nanotubes and nanodiamonds. Diamond and Related Materials 2007;16(12):2118-2123.

[36] Zhu L, Chang DW, Dai L, Hong Y. DNA damage induced by multiwalled carbon nanotubes in mouse embryonic stem cells. Nano Lett. 2007 Dec;7(12):3592-3597.

[37] Kam NW, Liu Z, Dai H. Carbon nanotubes as intracellular transporters for proteins and DNA: an investigation of the uptake mechanism and pathway. Angew.Chem.Int.Ed Engl. 2006 Jan 16;45(4):577-581.

[38] Park KH, Chhowalla M, Iqbal Z, Sesti F. Single-walled carbon nanotubes are a new class of ion channel blockers. J.Biol.Chem. 2003 Dec 12;278(50):50212-50216.

[39] Shi Kam NW, Jessop TC, Wender PA, Dai H. Nanotube molecular transporters: internalization of carbon nanotube-protein conjugates into Mammalian cells. J.Am.Chem.Soc. 2004 Jun 9;126(22):6850-6851.

[40] Pantarotto D, Briand JP, Prato M, Bianco A. Translocation of bioactive peptides across cell membranes by carbon nanotubes. Chem.Commun.(Camb) 2004 Jan 7;(1)(1):16-17.

[41] Zhang D, Yi C, Zhang J, Chen J, Yao X, Yang M. The effects of carbon nanotubes on the proliferation and differentiation of primary osteoblasts. Nanotechnology 2007;18

[42] Martinac B. Mechanosensitive ion channels: molecules of mechanotransduction. J.Cell.Sci. 2004 May 15;117(Pt 12):2449-2460.

[43] Manna SK, Sarkar S, Barr J, Wise K, Barrera EV, Jejelowo O, et al. Single-Walled Carbon Nanotube Induces Oxidative Stress and Activates Nuclear Transcription Factor-KB in Human Keratinocytes. Nano Lett. 2005;5(9).

[44] Yehia HN, Draper RK, Mikoryak C, Walker EK, Bajaj P, Musselman IH, et al. Single-walled carbon nanotube interactions with HeLa cells. J.Nanobiotechnology 2007 Oct 23;5:8

[45] Zhang D, Yi C, Qi S, Yao X, Yang M. Effects of carbon nanotubes on the proliferation and differentiation of primary osteoblasts. Methods Mol.Biol. 2010;625:41-53

[46] Kalbacova M, Kalbac M, Dunsch L, Kataura H, Hempel U. The study of the interaction of human mesenchymal stem cells and monocytes/macrophages with single-walled carbon nanotube films. phys. stat. sol. (b) 2006;243(13):3514-3518.

[47] Meng J, Song L, Meng J, Kong H, Zhu G, Wang C, et al. Using single-walled carbon nanotubes nonwoven films as scaffolds to enhance long-term cell proliferation in vitro. J.Biomed.Mater.Res.A. 2006 Nov;79(2):298-306.

Chapter 2 Osteoblastic Cells Response to Single Walled Carbon Nanotube Films

Abstract

A central effort in biomedical research concerns the development of materials to sustain and control cell growth. Carbon nanotube based substrates have been shown to support the growth of different types of cells [1-3]; however the underlying molecular mechanisms remain poorly defined. To address the fundamental question of mechanisms by which nanotubes promote bone mitosis and histogenesis, primary calvariae osteoblastic cells were grown on single walled carbon nanotube thin film substrates. Using a combination of biochemical and optical techniques we demonstrate here that SWNT networks promote cell development through two distinct steps. Initially, SWNTs are absorbed in a process that resembles endocytosis, inducing acute toxicity. Nanotube-mediated cell destruction, however, induces release of endogenous factors that act to boost the activity of the surviving cells by stimulating the synthesis of extracellular matrix.

2.1 Materials

2.1.1 Preparation and Characterization of SWNT Substrates

Raw HiPCO nanotubes were purchased from “Carbon nanotechnologies INC”. Purification procedure involved a multi-step process adopted from both Chiang et al. and Xu et al. and optimized in our laboratory [4-6]. SWNTs were annealed in humid air at 230 °C for 24 hours. Subsequently, SWNTs were stirred in 6M HCl for 12 hours at 70 ºC followed by another humid annealing at 250 ºC . Acid treatment was repeated one

more time followed by an annealing step at 250 ºC temperature. This process is summarized in Table 2.1

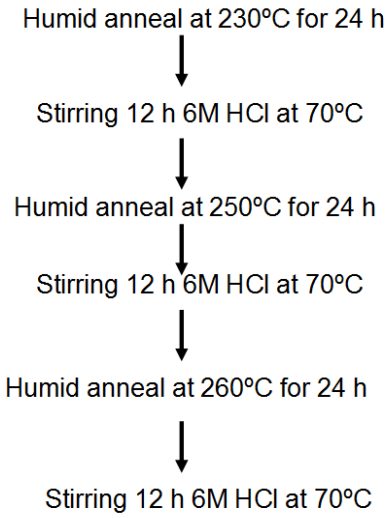

Table 2.1 Six step process used to purify SWNT samples.

To prepare nanotube films, SWNTs were dispersed in a 1 wt.% aqueous solution of sodium dodecylsulfate (SDS) and ultrasonicated for 3 hours. Typically, 8 mg of the purified nanotubes was dispersed in 1 L of 1 wt. % SDS (8 µg /ml) solution. A vacuum filtration apparatus was utilized to filter the dispersed SWNT solution and uniformly deposit them onto mixed cellulose ester (MCE) membrane with pore size of 220 nm (Millipore). The method utilized by our group was originally developed by Wu et al. and optimized in our laboratory [7-9]. Forty ml of the SWNT solution was deposited on each membrane (24.6 µg/sample).

Thin nanotube films deposited onto MCE membranes were cut into uniform circular samples with d=1.3 or d= 1.2 cm. Corresponding samples covered more than 75% and 65% of a corresponding well of a 24 well culture plate (d=1.5 cm) area. Smaller diameter

samples were placed in a series of acetone and methanol baths and deposited on glass slides (Fisher Scientific) [8]. The process is summarized in Figure 2.1.

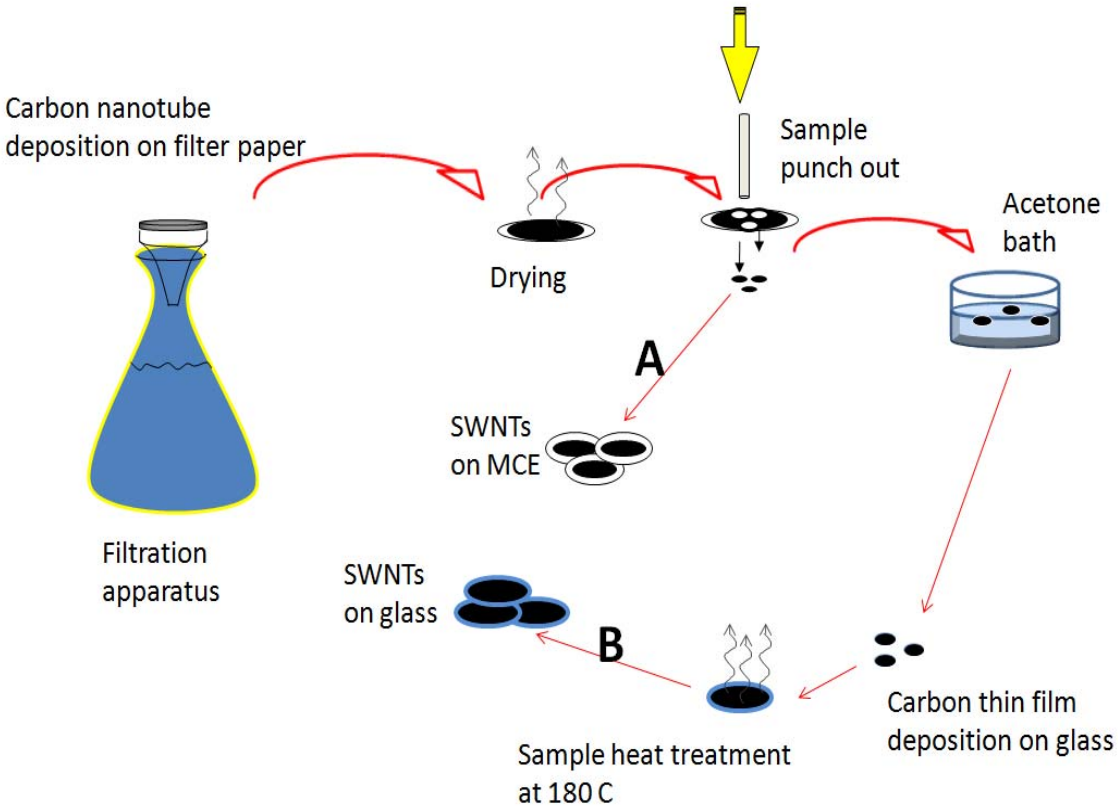

Figure 2.1 Schematics of SWNT thin film deposition process.

All samples were UV (254 nm) disinfected for 24 hours prior to seeding. Samples were soaked for 24 hours in phosphate buffer saline (PBS) solution prior to cell seeding.

2.1.2 Single Walled Nanotube Matrices

Carbon nanotubes deposited in form of thin films presented a unique opportunity to test SWNT's native properties for biomedical applications. Simple and controllable sample preparation allowed for designing samples for *in-vitro* tests with great

reproducibility. Deposition process included preparation of nanotube dispersions. To prevent nanotubes from aggregation, SDS surfactant was used. SWNTs coated with the surfactant monolayer created steric and double layer repulsion forces which formed relatively stable nanotube dispersion. Following nanotube dispersion and its stabilization (after 72-96 h) adequate amount of solution was withdrawn and deposited on a mixed cellulose membranes using filtration apparatus [6]. The process applied to form nanotube films is summarized in table 2.2.

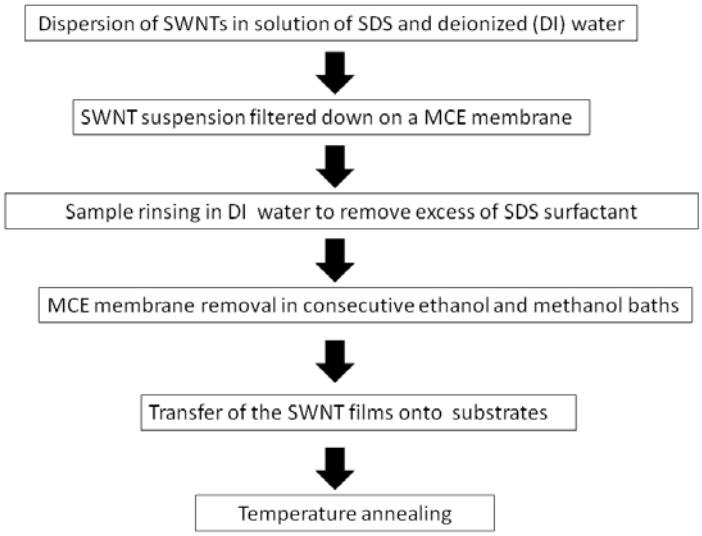

Table 2.2 Process used to assemble single walled carbon nanotube matrices.

Significant advantages of using the filtration deposition method include reproducibility and uniformity of deposited SWNTs films.

2.1.3 Cell Cultures

Primary osteoblastic rat cells and the mouse MC3T3-E1 osteoblast-like cell line used in this study were grown at 37 °C in a humidified atmosphere of 5% CO_2 in air. The

MC3T3-E1 cell line was supplemented with Eagle's minimal essential medium (α-MEM), 10% fetal bovine serum (FBS), 1% pen-strep bactericide (PS). MC3T3-E1 cells were seeded at 5000 cells/well. Primary calvariae cells were deposited at 16000 cells/well for up to 28 days in 24 well Falcon tissue culture plates (Falcon® Petri dish). If not stated otherwise, the medium in both cell cultures was changed every 2-3 days and each sample type was tested in triplicates. Primary osteoblast cells were obtained from newborn rats by sequential digestion of the calvariae in a solution of Collagenase A/Trypsin followed by cell centrifugation and counting [10,11]. The cells were then cultured in MEM containing 10% FBS, and 1% nonessential amino acids and 0.1 % PS. The medium was changed every 2 or 3 days up to day 8. Thereafter, BG Jb medium supplemented with 50 μg/mL ascorbic acid and 3.06 mg/mL of β-glycerolphosphate, 10% of FBS and 1 % PS was used.

2.2 Methods

A major effort in bone bioengineering research is to design new materials to support, increase and/or replace bone tissue. In recent years, several materials [12-14], as well as distinct original processing techniques [15-17], have been proposed and tested. Among them, single walled carbon nanotubes (SWNTs) have raised considerable interest because these materials possess unique mechanical, thermal and electrical properties [18-20]. Despite an intense effort, however, the notion that carbon nanotubes can have practical biomedical applications remains controversial [21]. While several studies have reported that a variety of cell lines of different species can grow on carbon nanotube substrates [1,3,22], others have underscored a significant level of toxicity intrinsic to

these nanomaterials [23,24]. Moreover, many issues such as long-term effects, whether carbon nanotubes can support the growth of primary cells and, more importantly, what are the mechanisms by which they act to stimulate multiple cellular activities remain to be elucidated.

Here, we unveil a mechanism through which carbon nanotubes not only induce toxicity but also promote bone cell differentiation leading to formation of bone nodules. We show that SWNTs deposited onto multicellulose ester (MCE) membrane (Millipore) stimulate the production of extracellular matrix, a central step in bone tissue formation in primary rat calvariae osteoblastic cells and mouse pre-osteoblastic MC3T3-E1 cells. Intriguingly, this enhancement is related to an initial decline in cell number and increase in protein expression. This initial decrease in the cell number and increase in protein expression are further reinforced by transmission electron microscopy observations which reveal that SWNTs enter the cells within the first few hours after cell deposition. We observe that above some critical concentration and size of SWNT vacuoles within the cells (after 24 hours), a decrease in total cell numbers occurs. In the absence of SWNTs entering the cells, cell toxicity is not observed. Our study suggests cell activity is strongly modulated by loose SWNTs entering the osteoblast cytoplasm.

2.2.1 Bradford Total Protein Assays

Upon sample collection, pieces were first rinsed twice in PBS and transferred to 0.5 mL of deionized water. Cells grown directly on growth plates were removed using a standard rubber scraper. All samples were placed in a freezer for at least 24 hours. Pieces were homogenized in an ultrasonic processor (Cole Parmer 750 W, model CV33) on ice

for 15 sec at 30% power and centrifuged at 14000 rpm for 5 min. Assays were done according to the microprotein assay procedure [25], and normalized to a calibration curve obtained using bovine serum albumin dilutions. Twenty μL of sample solution was mixed with 1 mL Bradford reagent in test tubes; absorbance of dye-protein complexes was measured after 1 min at 595 nm. The optical density (OD) was determined using general purpose UV/Vis dual beam spectrophotometer (Beckman Coulter DU 520). Relative ratios between SWNTs on MCE or SWNTs on glass and polystyrene area were calculated and applied to normalize expressed protein values. (SWNTs on MCE/ polystyrene area 1.33/1.77 = 0.75; and SWNTs on glass/ polystyrene 1.13/1.77= 0.64). Experiment was repeated three times.

2.2.2 Osteoblastic Cell Viability Assays

Osteoblast viability and numbers were determined by testing the mitochondrial enzyme activity according to the colorimetric 3-(4,5-dimethylthiazol-2-yl)-2, 5-diphenyltetrazolium bromide (Sigma Aldrich, Tox-1) assay. Accordingly, primary osteoblast cells were seeded in 24-well tissue culture plates. One hour before sample collection, pieces were very gently rinsed twice in PBS and 0.5 mL of phenol free Eagle's minimal essential media was introduced to each sample well. Upon sample collection, 50μL of prepared MTT solution was added to each well and incubated for another 2.5 hours at 37 ^{o}C. Formed formazan crystals were subsequently dissolved by adding the solubilization solution. The absorbance at 570 nm was recorded on the spectrophotometer. The optical density values were then normalized to cell number using

the standard curve. The calibration curve was established using titrated cell solutions measured 24 hours after cell seeding. MTT based experiments were replicated twice.

2.2.3 Lactate Dehydrogenase (LDH) Toxicity Assay

Lactate dehydrogenase enzyme activity in cell supernatant was measured using the TOX-7 kit (Sigma-Aldrich). SWNT on glass, SWNT on MCE and polystyrene samples were prepared as described before. Primary osteoblastic cells were deposited at 16000/well in serum free media, in triplicates and the test was repeated twice. Cell supernatant was collected after 2 and 24 hours and processed following manufacturer procedure. Toxicity, (T) was quantified as:

$$T = \frac{A - A_U}{A_{Tx} - A_U} \qquad \text{Eq. 2.1}$$

where the absorbances (OD) of the test sample (A), untreated cells (A_U) and cells lysed with Triton X-100, (A_{Tx}) were determined with a FlexStation 3 microplate reader (Molecular Devises) at 490 nm wavelength.

2.2.4 Alkaline Phosphatase (ALP) Assays

ALP activity from the scaffolds/cell samples was quantified by the specific conversion of *p*-nitrophenyl phosphate (*p*NPP) (Sigma Aldrich, P 7998) into *p*-nitrophenol (*p*NP). Samples were first rinsed twice in PBS solution and then the enzyme reaction was started by adding 1mL of substrate buffer (*p*NPP) to samples. The solution was incubated at 37 °C for 5 min. Upon reaction completion, 200 µL of solution was

withdrawn and reaction was stopped by adding 50 µL of 3 N NaOH. The OD was determined at 405 nm using the spectrophotometer. Five µL of titrated *p*NP (Sigma Aldrich, N-7660) solutions were used to construct a standard curve and applied to convert data to absolute values (µmol/h/cell number). Data from cells grown on SWNTs on MCE were multiplied by relative area ratios as outlined before. The test was performed twice.

2.2.5 Biochemical Assays

Cells grown on SWNT thin films and controls were washed twice with cold PBS and collected according to the method outlined above. Next, cells were lysed in 50 mM Tris-HCl (pH 6.8), 10 mM EDTA, glycerol and 10% SDS. Equal amounts of sample lysate were separated by 13 % sodium dodecylsulfate polyacrylamide gel electrophoresis (SDS-PAGE) and electrophoretically transferred onto PVDF membrane (Millipore).The membrane was blocked for 2 hours in 5% of commercially available dry milk and TBST solution (10 mM Tris HCl pH 8.0, 150 mM NaCl, 0.05% Tween 20). Then, the blots were incubated with either anti-collagen I or anti-tubulin primary antibodies (Sigma Aldrich) in the TBST solution at a 1:1000 dilution for 2 hours at room temperature. Secondary anti-mouse antibodies conjugated with horseradish peroxidase at a 1:10000 dilution were introduced and incubated for 1.5 hours then visualized with an enhanced chemiluminescence (ECL) kit (*GE* Healthcare, US). Membranes were exposed to Blue Basic Autorad films (ISC Bioexpresse, US) for 5–10 min.

2.2.6 Cell Lysates

Cell lysates for the experiments in Fig. 7 were obtained as follows: 30,500/ mL primary cells were dispersed in 1 mL of PBS and lysed by a series of short sonications at 160 and 266 W . A small representative sample was withdrawn and stained with trypan blue (0.04%) to verify, under the microscope, for any remaining intact cells. The remaining lysate was thoroughly mixed with 1 mL of the proliferation medium. Before any solution was added, medium was replaced in all samples. The mixture was then dispensed at 30 μL/well (4500 lysed cells/dose) to each well containing cells after 3 and 24 hours. Experiment was replicated twice.

2.2.7 Transmission and Scanning Electron Microscopy

The internalization of SWNTs within MC3T3-E1 osteoblasts was investigated using a TEM (JEM 100 CXII) operating at 80 kV and SEM (AMRAY -18301) using 20 kV power source. For the TEM experiments, osteoblasts cells were incubated on same number of various samples (SWNTs on glass, SWNTs on MCE and polystyrene). Specimens were collected at various times and subsequently rinsed three times in PBS and trypsinized. The samples were centrifuged for 4 min at 10000 rpm. The resulting cell pellets were fixed in Karnovsky's Fixative for 3 hours. After being washed, cells were postfixed with 1% osmium tetroxide for 1 h followed by dehydration in graded water: ethanol series (50 - 70 - 80 - 90 - 95 -100%) for 10-15min and embedded in Epon-Araldite solution. Sections were prepared using ultramicrotome. Corresponding carbon content was measured using Image J software. Black foreign bodies within cells were

identified as SWNT inclusions. Average inclusion area was calculated based on 6 images taken for each treatment type and collection time. Samples designated for SEM analysis underwent postfixation and dehydration processes similar to that outlined for TEM. Specimens were critical point dry-processed and platinum/gold coated. This experiment was replicated two times.

2.2.8 Statistics

Statistical significance was assessed by the *Student t-test* and one-way ANOVA (for multiple comparisons) and corrected using post hoc ANOVA/Tukey. A 95% confidence level was considered statistically significant.

2.3 Results

In order to understand the cell number, differentiation and interactions of primary rat osteoblast cells on SWNT networks, we performed biochemical assays to obtain information about the total protein expression (specifically collagen I production), cell number and alkaline phosphatase activity . Complementary to the biological measurements, we also performed scanning and transmission electron microscopy to investigate the morphology of the cell cultures and SWNT uptake as a function of time, respectively.

The purified and well dispersed SWNT networks were deposited onto a multicellulose ester membrane using the vacuum filtration method. Experimental substrates consisted of SWNTs deposited on MCE membrane (SWNTs on MCE) or well rinsed nanotubes placed on glass slides (SWNTs on glass). The SWNTs on glass adhere well after rinsing while loose SWNTs remain on the MCE membrane even after

extensive washing. A negative MCE membrane and positive polystyrene control samples were incorporated into testing setup to assess and evaluate cellular response.

The total protein expression was measured by the Bradford protein assay. Results of the total protein expression comparing the controls and the SWNT networks for primary and MC3T3-E1 cell lines are shown in Figure 1 (a-b).

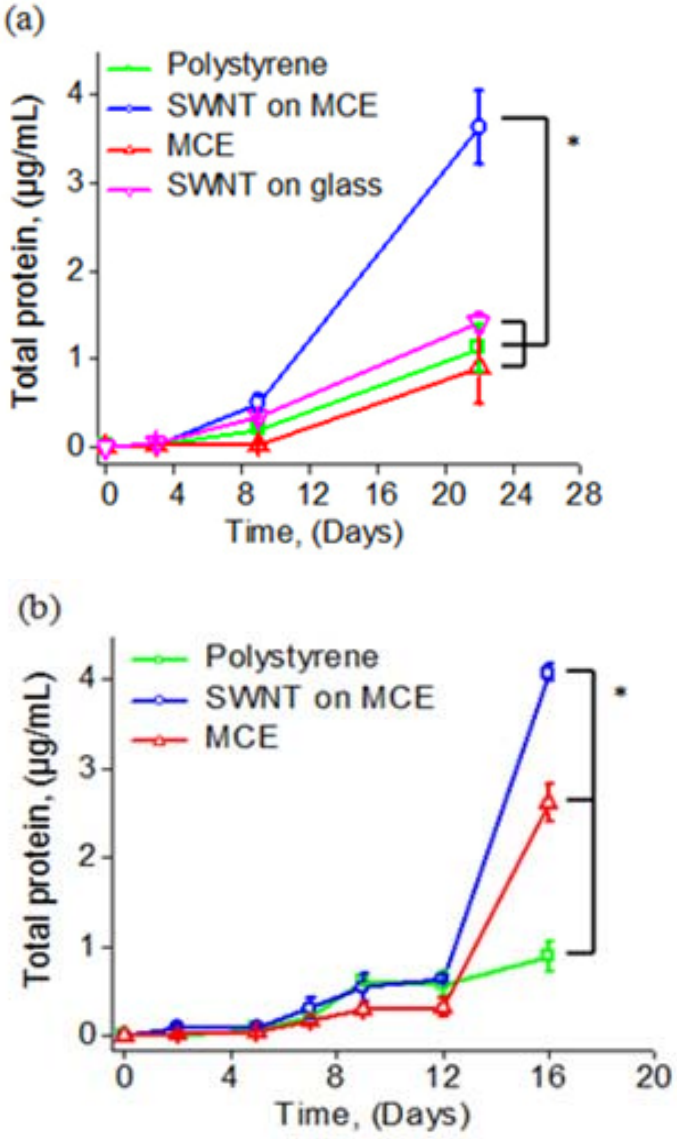

Figure 2.2 Total protein expression for cells grown on SWNT and control substrates. (a) Total protein content expressed in primary rat osteoblastic cells grown on SWNTs on MCE substrates (circles), rinsed SWNTs on glass samples (pointing down triangles), MCE alone (pointing up triangles) and polystyrene (squares). (b) Total protein content

expressed in mouse MC3T3-E1 osteoblastic cells grown on SWNTs on MCE, MCE alone and polystyrene. Values are mean ± SD of three individual cultures. Statistically significant differences from control are indicated with *; $p < 0.05$.

Both types of cells in long term study express proteins similarly, corroborating the notion that SWNTs impact cell response in very similar ways and validating the use of a cell line (the MC3T3) that is amenable to laboratory study. More importantly, it can be clearly observed that the total protein expression in both cell lines is significantly higher for the SWNTs on MCE substrate. In contrast, the protein expression for primary cells on SWNTs on glass substrates is comparable to control.

The effect of underlying MCE membrane on the protein expression was found to be negligible as shown in Figure 1 (a). Thus, these results suggest that cellular activity on SWNTs on MCE is different from SWNTs on glass. The main objective of this work is to elucidate the cause of this difference.

Bone histogenesis is characterized by several distinct phases: the tissue originates from mesenchymal cells, undergoes proliferation, synthesis of extracellular matrix, mineralization of the matrix, vascular invasion, and finally death. Hence, the fact that protein expression in cells grown on SWNTs on MCE substrate increased significantly after two weeks of culture suggests that the SWNT substrates acted primarily to alter post-differentiation processes. Therefore to confirm this notion we assessed Collagen I production, a hallmark of extracellular matrix production [26], in cells seeded on SWNTs on MCE and on polystyrene for control at different time points. As shown in Figure 2, Collagen I synthesis was significantly enhanced in SWNTs on MCE substrates in a time dependent fashion.

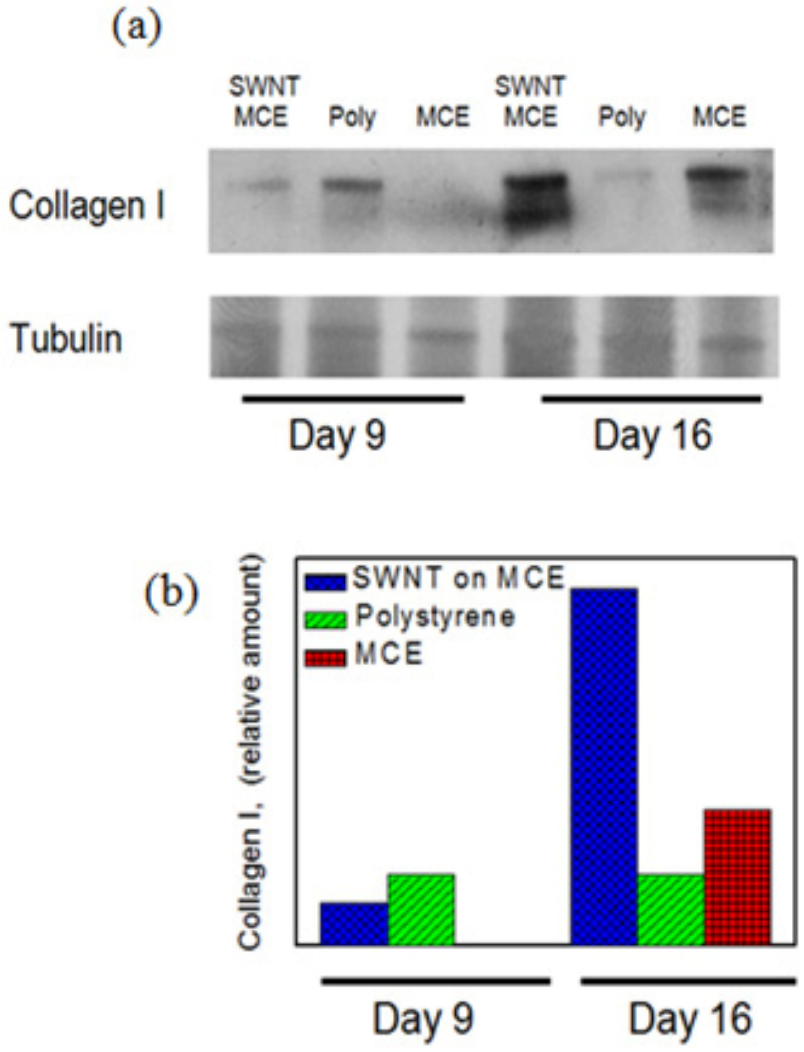

Figure 2.3 Increased collagen I synthesis in cells grown on SWNTs on MCE. (a) Western visualization of Collagen I in MC3T3-E1 cells grown on the indicated substrates. Bottom, Tubulin control. (b) Densitometry analysis of Collagen I protein expression in cells cultured on SWNTs on MCE (blue bar, fine mesh) and control (polystyrene and MCE alone) at two different time points.

The increased protein expression and collagen production for SWNTs on MCE substrates was correlated to the cell number using the standard colorimetric 3-(4,5-dimethylthiazol-

2-yl)-2,5-diphenyltetrazolium bromide assay. The cell number as a function of time for the control and SWNTs on MCE substrates is shown in Figure 3 (a). Significant difference between cells grown on the control and SWNTs on MCE substrate can be observed. Specifically, the number of cells increases monotonically in the control initially while it decreases (at 24 hours) and then increases for the SWNTs on MCE substrate. Cell number in polystyrene samples did not substantially vary after 3 weeks at which point cells reached confluence. However, the number of cells grown on SWNTs on MCE matrix does not fully recover to control values. The initial decrease in cell number is likely related to SWNT entry into the cells, as corroborated by our TEM investigation (see below).

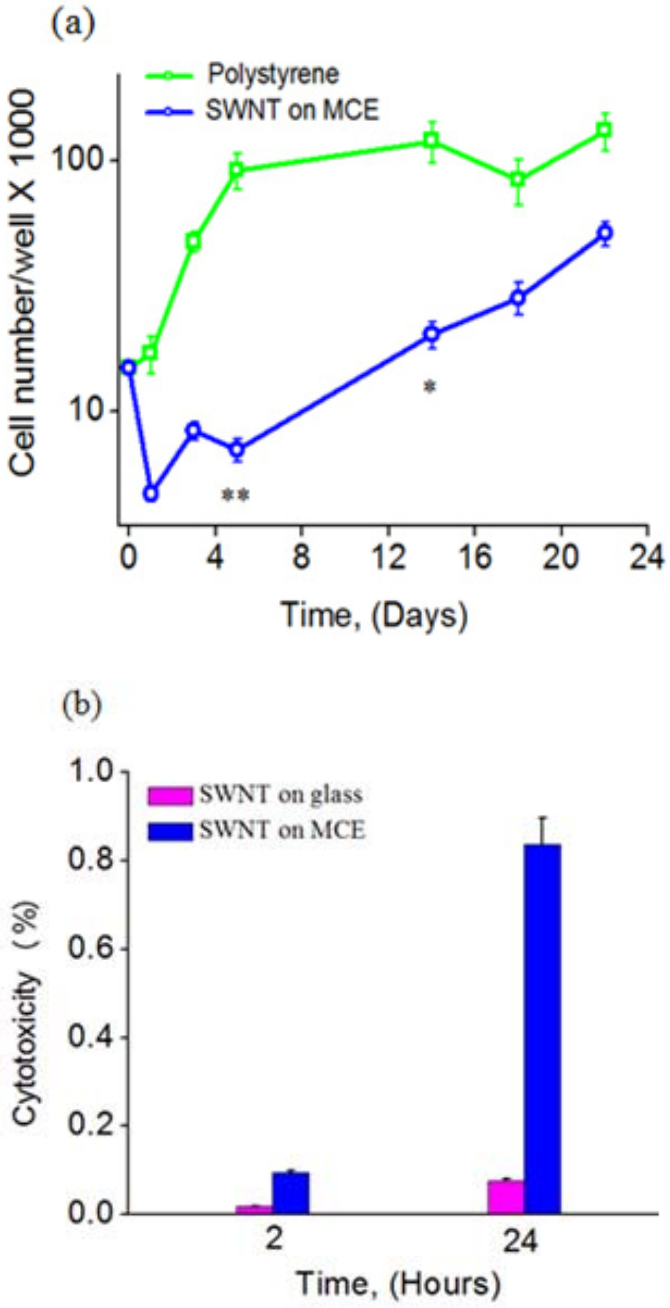

Figure 2.4 Primary cell viability (MTT) and lactate dehydrogenase (LDH) assays. (a) MTT colorimetric assay was applied to monitor primary osteoblastic cell viability on SWNTs on MCE and on polystyrene for control. Cell number noticeably drops within first 24 hours in cell cultures grown on SWNT matrix (ovals). Values are means ± SD of three independent cell cultures. Statistically significant differences from control are indicated with *; $p < 0.05$ and **; $p < 0.01$. (b) LDH levels in calvariae cells 2 and 24 hours after seeding on SWNT on MCE substrate.

Nanotube toxicity was further validated using a lactase dehydrogenase (LDH) assay, Figure 3 (b). As expected these experiments independently confirmed the presence of ruptured cells within first 24 hours after seeding.

We next measured alkaline phosphatase activity in order to obtain additional insight into the results presented in Figure 1 (a) and Figure 3. These results indicate that ALP activity on SWNT films on MCE is generally enhanced in comparison to the control (Figure 4). This is expected since the ALP activity reflects post-proliferation processes that are related to an increase in osteoblastic differentiation [27,28].

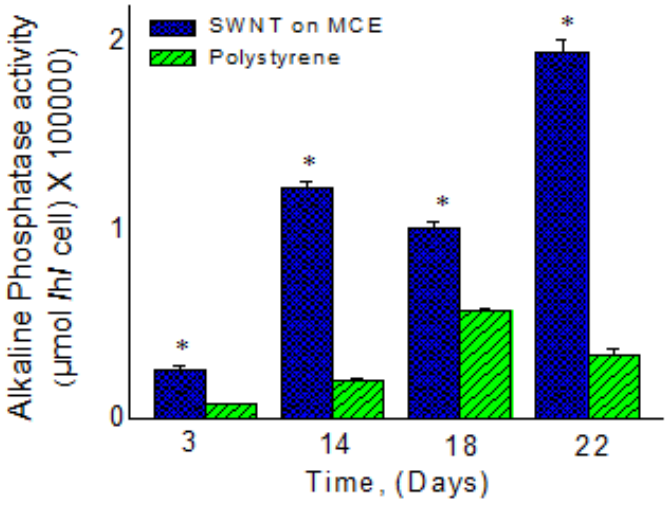

Figure 2.5 Alkaline phosphatase activity in primary calvariae cells cultured on the indicated substrates. Values are means ± SD of six independent cell cultures. Statistically significant differences from control are indicated with *; $p < 0.05$.

The morphological characteristics of the cells were monitored by SEM as a function of time. Images taken at days 3, 17 and 23 are shown in Figure 5. In contrast to the growth on control substrates, better adhesion of the primary cells was observed for SWNT networks on MCE substrates. Specifically, filopodia appendages can be seen after day 3 in Figure 5 (a), as indicated by the arrows. The morphology

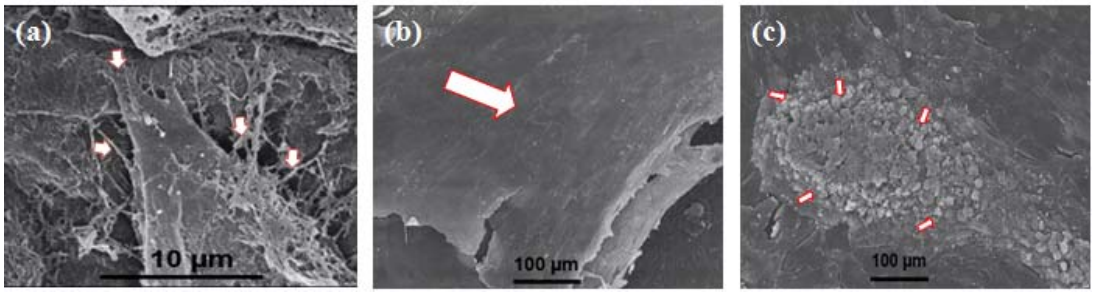

Figure 2.6. Primary rat cell morphology on SWNT matrix. (a) Representative SEM micrograph taken at day 3 showing cell attachment onto SWNTs on MCE substrate. Arrows indicate microfilaments. (b) Representative SEM micrograph taken at day 17 showing a confluent and differentiated cell layer during mid-stage formation of bone tissue (large arrow). (c) Representative SEM micrograph taken at day 23 showing characteristic late-stage calcification process (bone nodule-like formations, arrows).

of the cells on the SWNTs on MCE substrate did not change dramatically until day 23 when nodules representing calcified tissue were clearly visible, as indicated in Figure 5 (c).

Based on the analysis presented above, the results appear to suggest that SWNT thin films on MCE facilitate the differentiation of osteoblastic cells, leading to an increase in alkaline phosphatase activity, collagen I production and calcification of tissue. However, our data also suggest a cytotoxic effect. In order to better understand why protein expression increases while the cell number decreases initially, detailed observation of the interactions between SWNT substrates and cells as a function of time was conducted. TEM images of the cells cultured on SWNTs on MCE for 6 and 12 hours are shown in Figure 6 (a-b). Black carbonaceous inclusions of ~ 0.5 µm in diameter distributed in the cell cytoplasm are clearly visible.

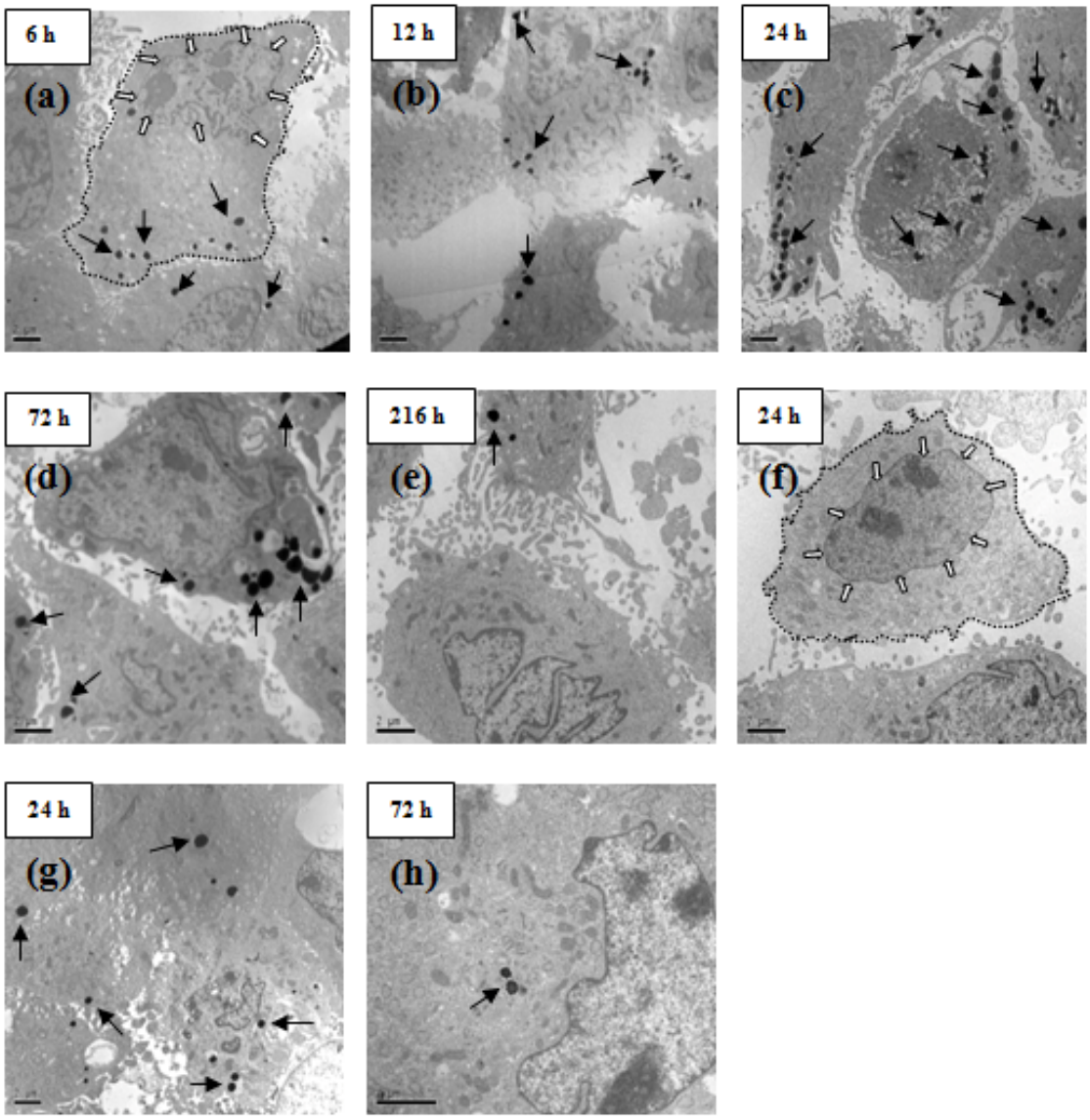

Figure 2.7 TEM images of sectioned cells with carbon nanotube inclusions. (a-e) MC3T3-E1 cells grown on SWNTs on MCE substrate were collected at various time points to monitor carbon nanotube uptake. In (a) the plasma membrane is underlined by a dotted line. The white arrows indicate the nucleus. Black arrows indicate carbon content within the cell cytoplasm. (f) Control on polystyrene at 24 hours. Black arrows, dotted line and white arrows as in (a). (g-h) SWNTs on glass at 24 and 72 hours. Scale bars are 2 μm.

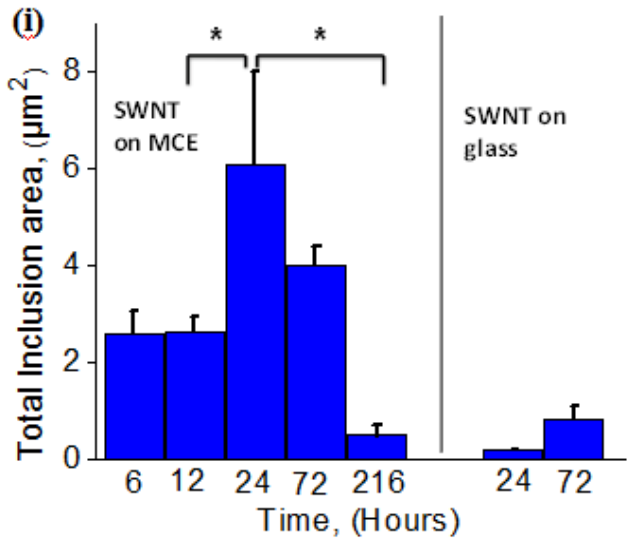

Figure 2.8 (i) Total carbonaceous areas of SWNT inclusions at the indicated time points on the indicated substrates. Values are the mean ± SEM of six micrographs. Statistical differences are indicated with *; $p < 0.05$.

These dark regions increase in size and number up to 24 hours, as seen in Figure 6 (c). At 72 hours, internalized SWNTs reach a diameter of ~ 1 µm and appear to aggregate to form larger inclusions. TEM analysis of longer growth times (9 days, Figure 6 (e)) shows that the black carbon regions diminish in size, number and total area. The TEM image observations are quantified in the bar graph shown in Figure 6 (i). It clearly indicates that the amount of carbon nanotubes within the cells peaks at 24 hours, correlating with the lowest cell count in Figure 2.

This appears to suggest that critical concentration and size of SWNT clusters within the cells leads to a decrease in viable cell number. It is not surprising to observe SWNTs within the cells as recent studies have shown that biological cells can absorb carbon nanotubes via endocytosis [29]. In our case it is likely that the uptake of SWNTs occurs via release of loosely bonded nanotubes within the SWNT network deposited on

top of MCE membrane. Once cells are seeded onto SWNTs on MCE substrate, they interact with nanotubes and likely enter the cells via phagocytosis [30]. It should be mentioned that no such exogenous clusters were observed within cells grown on polystyrene substrates as depicted in Figure 6 (f).

In order to confirm that the increase in protein expression and the decrease in viable cell count at 24 hours was due to cytotoxicity effects from loose nanotubes and not from well adhered nanotubes, we performed TEM analysis on cells grown on SWNTs on glass substrates because Van der Waals interactions prevent the release of the latter. As mentioned previously, the SWNTs adhere very well to this substrate. This has been confirmed by TEM images shown in Figure 6 (g-h) corresponding to cell growth times of 24 and 72 hours. The TEM images show that the number and concentration of inclusions in the cells grown on SWNTs on glass substrates are substantially lower.

Together, these data indicate that the uptake of nanotubes by the bone cells during the initial 24 hour period on SWNTs on MCE substrates is responsible for the toxicity which leads to the decrease in cell count and final increase in ECM levels. While a detailed elucidation of the mechanisms of carbon nanotube uptake will require further investigation, our results are consistent with the work of Yehia and co-workers which showed carbon nanotube uptake in HeLa cells [31]. However, the increase in protein expression on SWNT substrate is difficult to reconcile with toxicity results. We suggest the following: cells contain several growth factors in their cytoplasm. Nanotube uptake would cause cellular damage and subsequent release of growth factors such as FGF or TGF that may act to stimulate either the growth or differentiation of the surviving cells

[32,33]. In fact, Cui *at al* have shown that nanotube-mediated cytotoxicity is associated with increase in amount of proteins detected in the culture media [34].

Therefore to test the idea that the release of growth factors from the dying cells acts to boost the function of the surviving cells, we supplemented primary cells seeded on control substrate with a small amount of cell lysate after 3 and 24 hours. This treatment was sufficient to boost the synthesis of protein so that at day 21 the levels were comparable to those on SWNTs on MCE substrates, as shown in Figure 7.

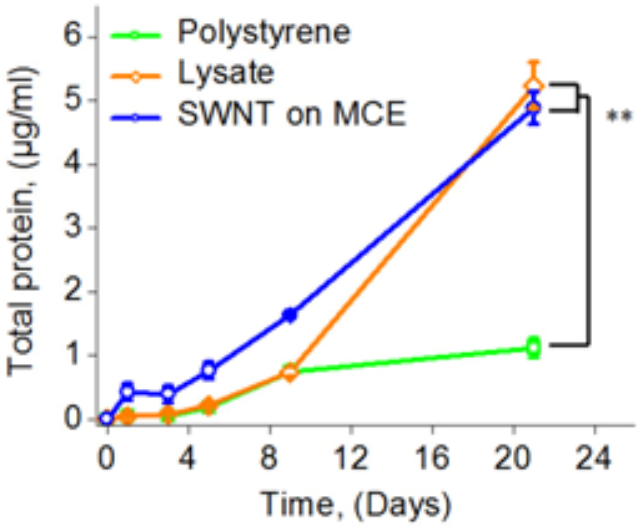

Figure 2.9 Release of cytosol improves cell growth. Total protein at different time points for cells grown on SWTNs on MCE (circles), polystyrene (squares) and on polystyrene supplemented with lysates of primary calvariae osteoblastic cells (diamonds). Values are mean ± SD of three independent cell cultures. Statistically significant differences from control are indicated with **; $p < 0.01$.

Although the total amount of protein expressed in lysed cultures is lower, the overall trend is increased protein production which is comparable between the SWNTs on MCE and polystyrene samples to which lysate was supplemented, as indicated in Figure 7. That

is, the rate of protein production steeply increased after the second week of culture, indicating that the release of endogenous growth factors during the first days of culture had profound and long-lasting effects on histogenesis of bone formation.

2.4 Analysis and Summary

Our results offer some intriguing insight into biological applications of nanomaterials. For example, CNTs have been reported to be toxic to mammalian cells through increasing oxidative damage via activation of the nuclear transcription factor NF-κB and cause G1 phase arrest, apoptosis and impairment of cellular adhesion [24,34]. In clinical trials with rodents, Lam *et al* found that CNTs induced inflammation, epithelioid granulomas, fibrosis, and biochemical/toxicological changes in the lungs [35]. On the other hand, a number of investigations have shown that CNTs can sustain cell growth (3T3-L1 mouse fibroblasts) and, in the case of bone cells (osteosarcoma ROS 17/2.8), support histogenesis [36,2]. Clinical studies using mice reported that multi-walled CNTs adjoining bone accelerate bone formation and when anodized titanium, one of the most commonly used materials for bone implant was mixed with CNTs, osteoblast functions were significantly enhanced [37]. Our findings show that both views are essentially correct. In fact, carbon nanotubes are toxic to the cells, when adsorbed by a process resembling phagocytosis. However when uptake of CNTs, and thus the number of killed cells, remains limited, it promotes the release of growth factors (by the dead cells) that act to stimulate in the long-range, post-mitosis processes such as synthesis of extracellular matrix, thereby enhancing bone tissue histogenesis.

Osteoblast primary cell cultures are known to include not only osteoblast cells, which are predominant, but also some residual number of macrophages and fibroblasts. Chang and collaborators studied the effect of resident macrophages on osteoblast cell function and found that the cells played an important role in bone homeostasis [38]. Future tests should carefully investigate effect of SWNTs on specific cell lines to determine which cell type predominantly internalize nanotubes, undergo apoptosis and contribute to bone histogenesis.

A crucial difference between our work and other reports in the literature is a fact that we observed a toxicity induced cell response that is controlled by loose nanotubes in cell cultures. However, in order to observe toxicity-mediated cell growth, a minimum number of cells is required. We found that if the primary cell number is very low (~ 5500/cm^2) then the SWNT uptake leads to the death of the entire cell population. A typical number of primary cells used to observe toxic effect and subsequent cell recovery was at 9000/ cm^2. This effect cannot be observed when using a high initial number of cells [37]. Thus, our results suggest that the effect of SWNT/cellular interactions are not only influenced by the biological environment but can also influence the biochemistry of the local environment.

2.5 Conclusions

In summary, we have demonstrated that osteoblast cells grown onto SWNTs on multicellulose ester (MCE) substrates experienced some toxicity from uptake of loose SWNTs. At sufficient dosage of SWNTs after 24 hours, cell death was observed. Cell destruction leads to release of proteins and other factors that stimulate remaining cells

causing them to produce higher levels of the osteoblast phenotype markers such as collagen I and alkaline phosphatase activity. We also performed control experiments with SWNTs on glass substrates where little or no uptake of SWNTs by cells occurred due to the absence of loose nanotubes. The cell activity on SWNTs on glass substrates was comparable to reference substrates. Finally, to test whether the enhanced protein expression for SWNTs on MCE was due to growth factors released by burst cells, we performed another control experiment in which lysed cells were added to cell cultures on reference substrates. This was done to mimic the introduction of growth factors by cell death on SWNTs on MCE substrates. The results showed that the introduction of lysed cells has the same impact on extracellular matrix expression. Thus, our observations can reconcile the apparent toxicity and benefits of SWNT substrates for osteoblast cell proliferation and differentiation.

2.6 References

[1] Kalbacova M, Kalbac M, Dunsch L, Kataura H, Hempel U. The study of the interaction of human mesenchymal stem cells and monocytes/macrophages with single-walled carbon nanotube films. phys. stat. sol. (b) 2006;243(13):3514-3518

[2] Zanello LP, Zhao B, Hu H, Haddon RC. Bone cell proliferation on carbon nanotubes. Nano Lett. 2006 Mar;6(3):562-567.

[3] Hu H, Ni Y, Mandal SK, Montana V, Zhao B, Haddon RC, et al. Polyethyleneimine functionalized single-walled carbon nanotubes as a substrate for neuronal growth. J Phys Chem B 2005 Mar 17;109(10):4285-4289.

[4] Chiang IW, Brinson BE, Smalley RE, Margrave JL, Hauge RH. Purification and Characterization of Single-Wall Carbon Nanotubes. J. Phys. Chem. B 2001;105:1157-1161.

[5] Xu YQ, Peng H, Hauge RH, Smalley RE. Controlled multistep purification of single-walled carbon nanotubes. Nano Lett. 2005 Jan;5(1):163-168.

[6] H. E. Unalan. Single Walled Carbon Nanotube thin films: properties and applications. Rutgers, The State University; 2006

[7] Wu Z, Chen Z, Du X, Logan JM, Sippel J, Nikolou M, et al. Transparent, conductive carbon nanotube films. Science 2004 Aug 27;305(5688):1273-1276.

[8] Fanchini G, Unalan EH, Chhowalla M. Optoelectronic properties of transparent and conducting single-wall carbon nanotube thin films. Applied Physics Letters 2006;88.

[9] H. E. Unalan. Single Walled Carbon Nanotube thin films: properties and applications. Rutgers, The State University; 2006.

[10] Shalhoub V, Conlon D, Tassinari M, Quinn C, Partridge N, Stein GS, et al. Glucocorticoids promote development of the osteoblast phenotype by selectively modulating expression of cell growth and differentiation associated genes. J.Cell.Biochem. 1992 Dec;50(4):425-440.

[11] Kwok S, Qin L, Partridge NC, Selvamurugan N. Parathyroid hormone stimulation and PKA signaling of latent transforming growth factor-beta binding protein-1 (LTBP-1) mRNA expression in osteoblastic cells. J.Cell.Biochem. 2005 Aug 1;95(5):1002-1011.

[12] Rinkevich B, Ben-Yakir S, Ben-Yakir R. Regeneration of Amputated Avian Bone by a Coral Skeletal Implant. The Biological Bulletin 1999;197(1):11-13

[13] Schroeder A, Francz G, Bruinink A, Hauert R, Mayer J, Wintermantel E. Titanium containing amorphous hydrogenated carbon films (a-C: H/Ti): surface analysis and evaluation of cellular reactions using bone marrow cell cultures in vitro. Biomaterials 2000 Mar;21(5):449-456.

[14] Ignjatovic N, Uskokovic D. Synthesis and application of hydroxyapatite/polylactide composite biomaterial. Applied Surface Science 2004;238(1-4):314-319

[15] Correa-Duarte MA, Wagner N, Rojas-Chapana J, Morsczeck C, Thie M, Giersig M. Fabrication and Biocompatibility of Carbon Nanotube-Based 3D Networks as Scaffolds for Cell Seeding and Growth. Nano Letters 2004;4(11):2233-2236.

[16] Schwarz JA, Contescu CI, Putyera K. Dekker encyclopedia of nanoscience and nanotechnology. 1st ed. New York: CRC Press; 2004

[17] Nishimura I, Huang Y, Butz F, Ogawa T, Lin A, Wang CJ. Discrete deposition of hydoroxyapatite nano-particles on titanium implant with predisposing substrate micro-topography accelerated osseointegration. Nanotechnology 2007;18(245101).

[18] Yu MF, Files BS, Arepalli S, Ruoff RS. Tensile loading of ropes of single wall carbon nanotubes and their mechanical properties. Phys.Rev.Lett. 2000 Jun 12;84(24):5552-5555.

[19] Dalton AB, Collins S, Muñoz E, Razal JM, Ebron VH, Ferraris JP, et al. Super-tough carbon-nanotube fibers. Nature 2003;423(703).

[20] Baughman RH, Cui C, Zakhidov AA, Iqbal Z, Barisci JN, Spinks GM, et al. Carbon Nanotube Actuators . Science 1999;284(5418):1340-1344.

[21] Kagan VE, Tyurina YY, Tyurin VA, Konduru NV, Potapovich AI, Osipov AN, et al. Direct and indirect effects of single walled carbon nanotubes on RAW 264.7 macrophages: role of iron. Toxicol.Lett. 2006 Aug 1;165(1):88-100.

[22] Usui Y, Aoki K, Narita N, Murakami N, Nakamura I, Nakamura K, et al. Carbon nanotubes with high bone-tissue compatibility and bone-formation acceleration effects. Small 2008 Feb;4(2):240-246.

[23] Zhang D, Yi C, Zhang J, Chen J, Yao X, Yang M. The effects of carbon nanotubes on the proliferation and differentiation of primary osteoblasts. Nanotechnology 2007;18.

[24] Manna SK, Sarkar S, Barr J, Wise K, Barrera EV, Jejelowo O, et al. Single-Walled Carbon Nanotube Induces Oxidative Stress and Activates Nuclear Transcription Factor-KB in Human Keratinocytes. Nano Lett. 2005;5(9)

[25] Bradford MM. A rapid and sensitive method for the quantitation of microgram quantities of protein utilizing the principle of protein-dye binding. Anal.Biochem. 1976 May 7;72:248-254.

[26] Bornstein MB. Reconstituted rattail collagen used as substrate for tissue cultures on coverslips in Maximow slides and roller tubes. Lab.Invest. 1958 Mar-Apr;7(2):134-137.

[27] Millan JL. Mammalian alkaline phosphatases: from biology to applications in medicine and biotechnology. 1st ed.: WILEY-VCH Verlag GmbH & C0; 2006

[28] Gerstenfeld LC, Chipman SD, Kelly CM, Hodgens KJ, Lee DD, Landis WJ. Collagen expression, ultrastructural assembly, and mineralization in cultures of chicken embryo osteoblasts. J.Cell Biol. 1988 Mar;106(3):979-989.

[29] Shi Kam NW, Jessop TC, Wender PA, Dai H. Nanotube molecular transporters: internalization of carbon nanotube-protein conjugates into Mammalian cells. J.Am.Chem.Soc. 2004 Jun 9;126(22):6850-6851.

[30] Porter AE, Gass M, Muller K, Skepper JN, Midgley PA, Welland M. Direct imaging of single-walled carbon nanotubes in cells. Nat.Nanotechnol 2007 Nov;2(11):713-717.

[31] Yehia HN, Draper RK, Mikoryak C, Walker EK, Bajaj P, Musselman IH, et al. Single-walled carbon nanotube interactions with HeLa cells. J.Nanobiotechnology 2007 Oct 23;5:8.

[32] Clarke MS, Feeback DL. Mechanical load induces sarcoplasmic wounding and FGF release in differentiated human skeletal muscle cultures. FASEB J. 1996 Mar;10(4):502-509.

[33] Roberts AB, Anzano MA, Meyers CA, Wideman J, Blacher R, Pan YC, et al. Purification and properties of a type beta transforming growth factor from bovine kidney. Biochemistry 1983 Dec 6;22(25):5692-5698.

[34] Cui D, Tian F, Ozkan CS, Wang M, Gao H. Effect of single wall carbon nanotubes on human HEK293 cells. Toxicol.Lett. 2005 Jan 15;155(1):73-85.

[35] Lam CW, James JT, McCluskey R, Arepalli S, Hunter RL. A review of carbon nanotube toxicity and assessment of potential occupational and environmental health risks. Crit.Rev.Toxicol. 2006 Mar;36(3):189-217.

[36] Meng J, Song L, Meng J, Kong H, Zhu G, Wang C, et al. Using single-walled carbon nanotubes nonwoven films as scaffolds to enhance long-term cell proliferation in vitro. J.Biomed.Mater.Res.A. 2006 Nov;79(2):298-306.

[37] Sirivisoot S, Yao C, Xiao X, Sheldon BW, Webster TJ. Greater osteoblast functions on multiwalled carbon nanotubes grown from anodized nanotubular titanium for orthopedic applications. Nanotechnology 2007;365102(36).

[38] Chang MK, Raggatt LJ, Alexander KA, Kuliwaba JS, Fazzalari NL, Schroder K, et al. Osteal tissue macrophages are intercalated throughout human and mouse bone lining tissues and regulate osteoblast function in vitro and in vivo. J.Immunol. 2008 Jul 15;181(2):1232-1244.

Chapter 3 Minimally Invasive Single Walled Carbon Nanotube Matrix Surface Modulation. Investigating Short Term Osteoblastic Cell Response to the Nanotube Substrates

Abstract

Carbon nanotube-based substrates have been shown to support the growth of many distinctive cell types [1-3]. Nanotube matrices are often embedded in polymers, which causes an inherent change in nanotube chemical and physical film properties. However, it is critical to elucidate how the physical properties of the film affect the biology of the host tissue. Here, we investigated how the physical and chemical properties of single-walled carbon nanotube films impact the response of MC3T3-E1 bone osteoblasts. We have found that the two fundamental steps in cell growth, initial attachment to the substrate and proliferation are strongly dependent on the energy and roughness of the surface. Consequently, fine-tuning the properties of the film may represent a valid strategy to optimize the response of the biological host.

3.1 Materials

Cell cultures, cell culturing technique and methods used to disperse and form SWNT films have been previously described. Please refer to chapter 2.1 for more details.

3.2 Methods

Numerous studies accentuate the potential application of single-walled carbon nanotubes in cell scaffolding, [4-6] cancer cell therapies, and drug delivery, [7-11]. In

an effort to develop SWNT-based substrates that are able to promote the growth of bone cells, we recently introduced chemical and morphological modifications to the substrates. Free standing nanotube networks were assembled by depositing SWNTs onto multicellulose ester membranes. These scaffolds promoted the development of primary rat calvariae osteoblastic cells and mouse preosteoblastic MC3T3-E1 cells by stimulating the production of the extracellular matrix; a central step in bone tissue formation [12]. SWNTs are remarkably attractive because they appear to be bio-inert and multifunctional in nature. This serves as a principle characteristic in view of their viable use for biomedical applications.

Imperative factors that concerns SWNTs-based substrates include physical, and chemical characteristics. The film properties will vary depending on the methods used to synthesize and purify the nanotubes [13,14]. In all cases, the nanotube require post synthesis processing necessary to remove impurities and provide means to assemble reproducible matrices. For example, purification performed in acids such as HCl, HNO_3 or H_2SO_4 may significantly alter the nanotube chemistry (side wall attachment of functional groups) and its size (tube cleavage) distribution [15-17]. These modifications amend the attributes of the substrate, ultimately affecting the response of the biological host. Therefore, it is crucial to comprehend how the physical and chemical characteristics of SWNT films affect cell growth.

Here we show that the two basic film parameters, namely surface energy density and roughness serves as source of modulating the growth of bone osteoblasts. Specifically, the surface energy density is important in promoting the initial attachment of cells to the substrate. Subsequent cell proliferation appears to be modulated by surface

morphology. Film surface energy and roughness properties may be controlled during material processing step. This implies, that by controlling these variables, it is possible to tailor SWNT films in order to optimize bone histogenesis.

3.2.1 Surface Properties

Carbon nanotubes are intrinsically hydrophobic. The carbon material poor wettability is inherently related to its low surface charge density. Other type of materials, specifically solid metals or solid metallic semiconductors contain more densely packed atomic structures with corresponding higher surface charge density. Surface chemistry will be defined by the present concentration of surface charge density [18]. Surface morphology is yet another imperative factor contributing to the total surface energy. Although, measuring surface energy directly is a challenging task at hand, some simplified models may be applied to extrapolate values. For example, the Kelvin equation (Eq. 3.1) provides description of surface microscopic properties including charge concentration and related chemical character. The resulting work of adhesion (W_A) delineates surface interactions, which are summarized in the equation below [18].

$$W_A = Ln\frac{P}{P_0} = \frac{2\gamma V_{mol}}{r\,RT} \qquad \text{Eq. 3.1}$$

The equation describes the relationship between two materials with interrelating surface tensions (2γ) and amount the chemical element present (molar volume, V_{mol}). The interacting surfaces cause a change in film curvature (r) with a corresponding change in

pressure ($\frac{P}{P_0}$). Respectively, constant R and T correspond to gas and temperature. Work of adhesion may also be expressed yet in another simplified form outlined below,

$$\delta W_A = F * dA * 2\gamma \qquad \text{Eq. 3.2}$$

where the change in work of adhesion W_A is a function of surface area change (dA), acting force (F) and existing surface energies (2γ).

The outlined above equations provide a general description of surface properties, including chemistry and surface morphology, equally important contributors to the general term of work of adhesion [19].

3.2.2 Surface Energy

Work of adhesion may also be expressed on a microspcopic level, alone by surface energy terms. The two ideal surfaces faced together, will cross interact by means of an adhesion force. The interactions are summarized by Equation 3.3.

$$W_A = \Gamma_x + \Gamma_y + \Gamma_{xy} \qquad \text{Eq. 3.3}$$

where Γ_x is free energy of surface *x*, *y* or *xy* and resulting work of adhesion (W_A) .

The corresponding work of adhesion formed between interacting surface tensions; (γ_A, γ_B and interface $\gamma_{A,B}$) may be approximated by :

$$\Delta W_A = -2\gamma_{AB} \qquad \text{Eq. 3.4}$$

A value of a unknown surface free energy may be extrapolated based on interactions between liquid and solid/liquid interface (unknown) [19]. Liquid placed on the surface

forms a sessile drop, depictured in Figure 3.1. (assuming vapor (gas) factor is neglected)

.

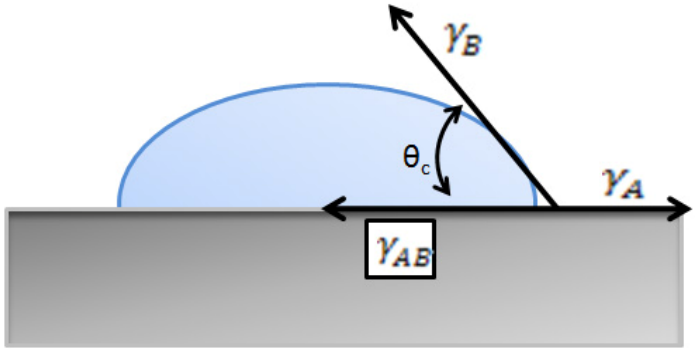

Figure 3.1 Measurement of a contact angle (θ_c) formed between a sessile drop (B) and a substrate (A). γ_{AB} corresponds to surface energy of liquid/surface interface.

Formed $cos\theta$ between the sessile drop (liquid B) and surface (A) may be experimentally measured. The sessile drop angle is related to the interface surface energy (γ_{AB}), as outlined by Young's equation:

$$\gamma_A + \gamma_B \cos\theta = \gamma_{AB} \qquad \text{Eq. 3.5}$$

The angle is formed by the droplet corresponding to the material surface energy. The surface energy is function of work of adhesion per unit surface area [19]. The interaction is summarized by Young-Dupre equation 3.6.

$$\gamma_B (1 + \cos\theta) = \Delta W_A \qquad \text{Eq. 3.6}$$

The Young-Dupre equation may be further simplified to yield :

$$\gamma_{AB} = \gamma_A + \gamma_B - W_A \qquad \text{Eq. 3.7}$$

More importantly, in the study reported a few decades ago by D.K. Owens and R.C. Wendt presented a model with focus on an interface surface energy from a molecular

point of view. Surface tension (or energy) may be correspondingly divided into two terms; 1) polarity γ^p (electrostatic) and 2) dispersive γ^d (von der Waal) surface tension terms [19]. Summarized in equation 3.8.

$$\gamma = \gamma^d + \gamma^p \qquad \text{Eq. 3.8}$$

Surface tension (between solid (s) and liquid (l)) is expressed in polarity and dispersive terms:

$$\gamma_{sl} = \gamma_s + \gamma_l - 2\left(\sqrt{\gamma_s^d + \gamma_l^d} + \sqrt{\gamma_s^p + \gamma_l^p}\right) \qquad \text{Eq. 3.9}$$

The polar and dispersive terms for a large number of liquids and solids are tabulated [19,20].

Furthermore, solid surface energy may be calculated by substituting γ_{sl} to equation 3.9, to obtain the final equation 3.10.

$$1 + \gamma_l \cdot \cos\theta - \gamma_s + \gamma_l - 2\left(\sqrt{\gamma_s^d + \gamma_l^d} + \sqrt{\gamma_s^p + \gamma_l^p}\right) \qquad \text{Eq. 3.10}$$

3.2.3 Film Chemical Functionalization

In the outline above, the equations dealing with surface properties indicated that the chemistry of materials significantly contributes to the total surface energy. Unique carbon nanotube chemistry is known to be hydrophobic with low surface energy. However, in order to verify our ability to control surface energy, nanotube film's chemistry was reversed by attaching COOH groups. The chemical treatment was performed according to a procedure outlined by Parekh et. al., [21]. Exclusively, the carbon films were treated for 3 hours in an azetropic nitric acid bath (69.7% HNO_3)

which were then gently blown with nitrogen gas and vacuum dried. Prior to surface measurements, the films were rinsed in deionized water (DI) and dried.

3.2.4 Surface Roughness

Surface roughness and surface area were assessed using an atomic force microscope (AFM; Nanoscope IIIa, Veeco, CA) in tapping mode on 10 x 10 micron area. The surface roughness coefficient, R_q , was calculated as the root mean squared of the height (h):

$$R_q = \sqrt{\frac{\sum_{j=1}^{N} (h_j)^2}{N}} \qquad \text{Eq. 3.11}$$

where <h> is the average height and N sampling size .

3.2.5 Goniometer Measurements

A goniometer (Ramehart, model 200) was applied to measure surface-liquid contact angles. Tests were repeated in triplicate. Surface energy density (φ) was calculated as the unitary surface tension (for liquid these two quantities are identical):

$$\varphi = \gamma_s^d + \gamma_s^p \qquad \text{Eq. 3.12}$$

where the solid dispersion and polar coefficients, γ^d_s and γ^p_s were calculated by the outlined earlier Owens–Wendt function. For these measurements the surface tension coefficient γ^d_l and γ^p_l for PBS and ethylene glycol are respectively, 0.22 and 35.2 and 0.29 and 19.0 mN/m.

3.2.6 Visualization and Direct Cell density Count

Cells were stained using Calcein AM fluorescent dye (Invitrogen), 1 hour prior to rinsing with PBS. The cells were visualized under a 10 X objective (Olympus) with 2.4 mm^2 field of view, on the areas located on opposite sides of each sample. Corresponding cell density at day 1, 3 and 5 was calculated using Image J software.

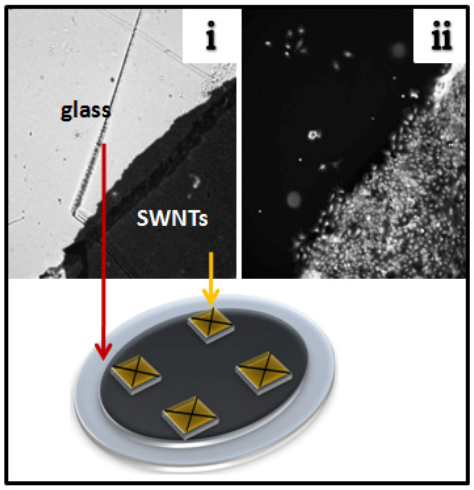

Figure 3.2 Typical sample setup used in the experiments. The yellow crossed boxes correspond to carbon films viewed under a microscope (not to scale). Insets: bright light (i) and fluorescent light (ii) of the same areas.

3.2.7 Statistical Analysis

Origin Pro 8 software with ANOVA extension was used to perform a statistical analysis. Post hoc pairwise comparisons on the data sets with Tukey's expansion with average +/- standard error of the mean (SEM) are reported unless specified otherwise. Statistical significance levels were set at $P < 0.05$

3.3 Results

3.3.1 Surface Morphology Control

The carbon nanotube suspension was filtered using a vacuum filtration apparatus at a stable suction power , as described earlier.

Specifically, 20, 35 and 50 mL of nanotube suspension had been deposited onto 20, 220 and 800 nm pore size filter membranes. The amount of SWNT suspension deposited onto MCE membranes was experimentally optimized to form freestanding SWNT films using the minimum amount, as depictured in Figure 3.3.

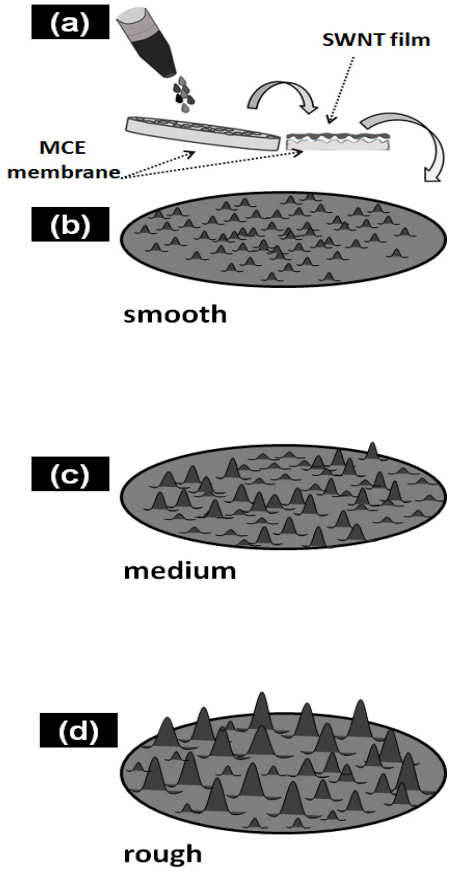

Figure 3.3 (a) Graphical representation of deposition method used to form SWNT substrates. (b-d) Larger filter membrane pore size causes nanotube suspension to penetrate deeper into membrane and form more diverse SWNT films. The process allows for controlling SWNT matrix surface roughness. From top to bottom: Formation of smooth, medium and rough films is shown.

Carbon nanotube membranes were cut into circular shape and then the MCE backing dissolved in a series of acetone baths. Free floating SWNT films were then detached and placed on glass slides (Fisher Scientific), dried in an oven and maintained under UV light (254 nm) prior to their utilization. Representative scanning electron microscopy images of the formed films are depictured in Figure 3.4.

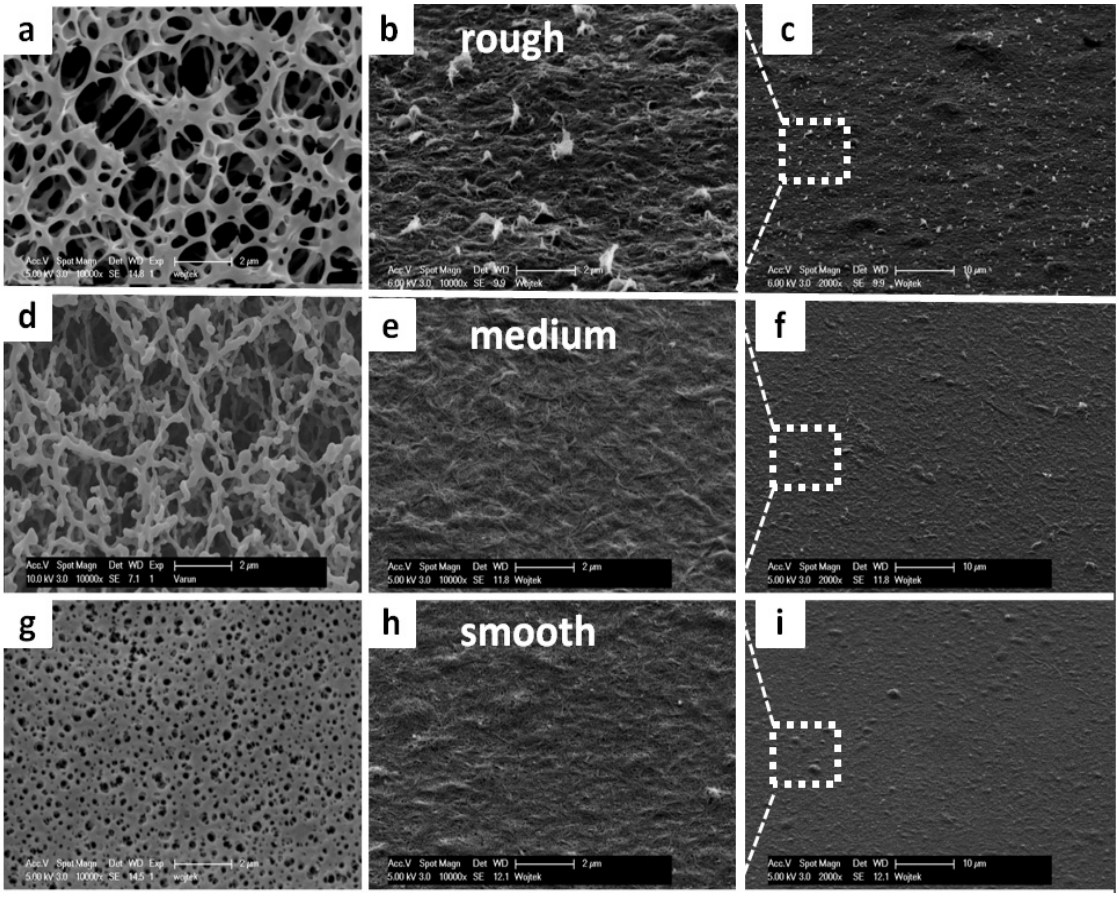

Figure 3.4 Series of carbon nanotube matrices with gradient surface morphology. (a,d,g) Underlying filter membranes (MCE) with various pores sizes (a) 0.8 , (d) 0.22 and (g) 0.025 nm are used during SWNT matrix formation. SWNTs penetrate deeper within MCE with larger pore size. (b,c) Rough SWNT films formed on largest pore size MCE, (X 10 K and X 2 K images shown respectivly). (e,f) Carbon nanotube matrices are less rough (smooth) when deposited on smaller pore size MCE. (h,i) Uniform and least rough matrices are formed when deposited on the smallest size MCE.

3.3.2 Surface Roughness

Formed films were further analyzed in order to quantify surface area and corresponding roughness values. Surface morphology was directly characterized using an atomic force microscope (AFM). Results reported in Figure 3.5.

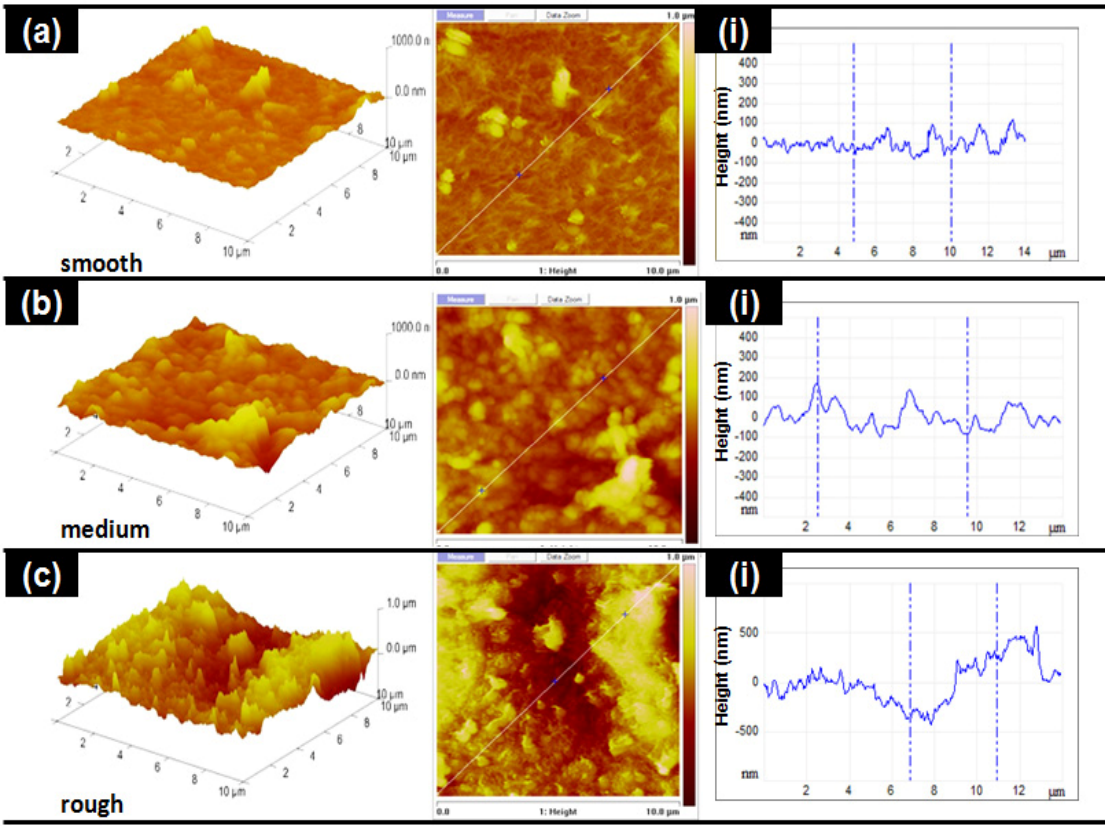

Figure 3.5 (a-c) Representative AFM digital images of the SWNT networks. The a(i)-c(i) inserts illustrate typical cross-section areas for tested films showing variation in height, peak size and peak distribution.

Qualitative analysis on created nanotube films indicated that the increase in surface roughness may be correlated with an increase of pore size, of underlying the MCE . Example of roughness values detected for tested films are summarized in Table 3.1.

	Roughness values Rq (nm)		
	smooth	**medium**	**rough**
1	60.8	91.1	181
2	53	71.7	318
3	57.9	109	287
4	62.9	94.6	117
5	57.9	71.9	366
6	71.5	103	250

Table 3.1 Representative roughness data collected for 100 μm^2 SWNT substrates

Detecting surface features, particularly its morphology, may be influenced by the AFM' s probe initial setting and device performance. To mitigate the possibility of erroneous data, multiple SWNT films ($n \geq 3$) were measured. Moreover, we confirmed that the roughness measurements done on a large area may be recreated on a smaller one. This is imperative, since the number of scanned points per imaged area is limited to 512 X 512 points at any given scan rate (28 kHz on average). Scanned on 5 X 5 and 10 X 10 μm films showed similar trends in roughness, seen in Figure 3.6.

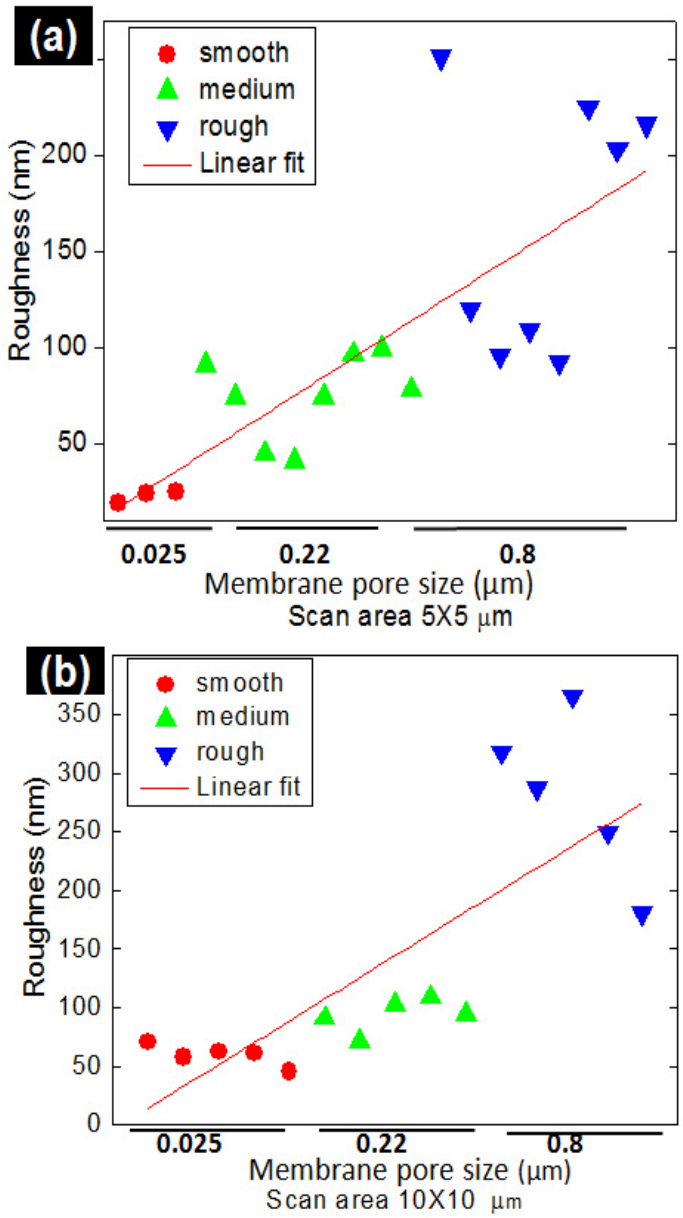

Figure 3.6 The relationship between surface roughness and underlying filter membrane (MCE) pore size used when depositing SWNT networks. Applied filtration technique allowed to control surface roughness. A linear trend is visible between SWNT substrates and underlying MCE films. (a,b) Detected root mean square of roughness values (R_q) appear to be in a good agreement between corresponding 25 and 100 μm^2 scan areas.

3.3.3 Surface Area

Additional data collected on surface area indicated its poor correlation with surface roughness. Weak treads may be seen on both small and large area scans with a large variation in detected values. The trend may be seen in the samples that were previously scanned for surface roughness, as seen in Figure 3.7.

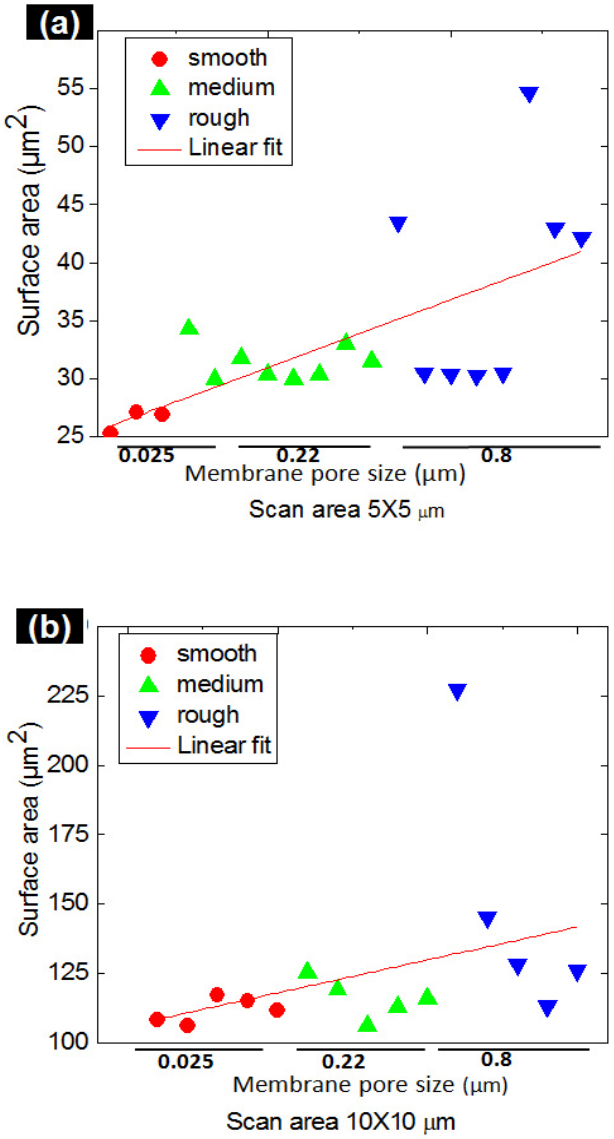

Figure 3.7 Variation in carbon nanotube matrix surface area. SWNT surface area measurements indicate poor correlation with pore size of MCE membranes used during network formation. (a,b) 25 and 100 μm^2 scans have resulted in similar results.

Detected surface roughness could arise either due to increase in surface area or presence of single sporadic features. A poor correlation between a measured surface roughness and surface area suggests that few but large in height spikes contributed to improved roughness values. This observation is in a respectable agreement with the electron microscope images, seen in Figure 3.4. If large and abundant features were present, the detected surface area would show a linear increase with roughness values.

3.3.4 Contact Angles

Surface properties of SWNT scaffolds were obtained by measuring a sessile drop angle formed between liquids and a matrix. Outlined earlier in the methods (section 3.2.4) Youngs' equation provides the means to relate the detected contact angle to Owens-Wendt equation.

In these measurements, two different liquids; phosphate buffer solution (PBS) and ethylene glycol were placed on smooth, medium, rough and control glass samples to obtain contact angles. Representative images for pristine SWNTs (hydrophobic) showed a large variation in drop shape, see Figure 3.9. Corresponding static contact angles varied from 30 to 130^{o} . Each drop was measured 30 seconds after a drop (~ 15 μL) of PBS or ethylene glycol was casted on a surface.

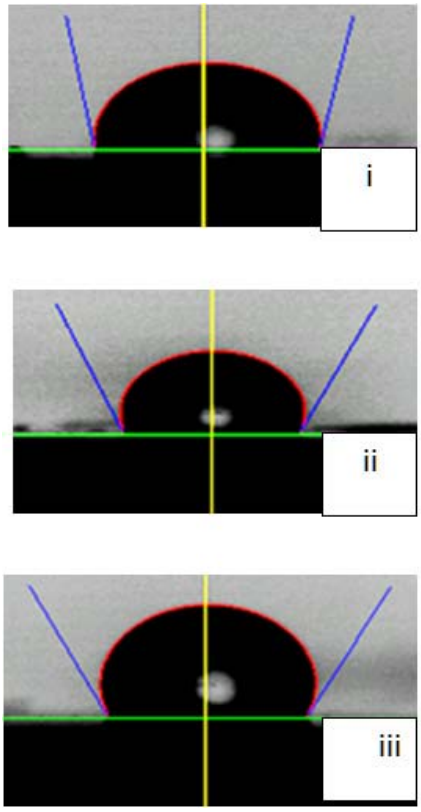

Figure 3.8 Contact angles of phosphate buffer solution drop formed on pristine SWNT films. (i) Smooth, (ii) medium and (iii) rough SWNT networks caused deformation of PBS drop to various extends.

Linear decrease in obtained contact angles with increase in hydrophilic film roughness is reported in Figure 3.10. The films tethered with COOH groups formed hydrophilic, high surface energy films.

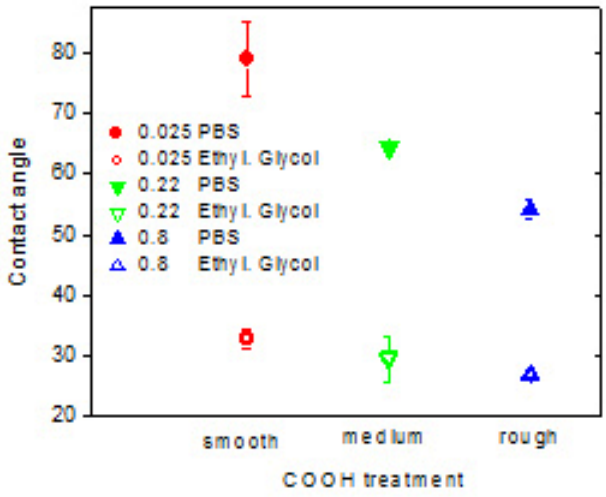

Figure 3.9 Representative contact angle values recorded on SWNT-COOH films. Decrease in detected sessile drop contact angle for PBS and ethylene glycol sessile drop can be seen.

3.3.5 Surface Morphology and Surface Energy

Morphology and surface chemistry contribute to the matrix surface properties. Film morphology is particularly essential, for it contributes to film's surface energy. Specifically, there are two factors that impact contact angle measurements:

a) surface capillaries

b) surface roughness

Visual assessment of the nanotube films performed using scanning electron microscope confirmed existence of meso-sized pores (~ 50 nm). However, their small size insinuates that the liquid will be unable to rapidly penetrate the small crevices. That is particularly true in the case of pristine SWNTs which are inherently hydrophobic, with a low γ_s. Particularly, exfoliated graphene has γ_s= 46.7 mJ/m^2 and γ_s= 62.1 mJ/m^2 is reported for

graphene oxide respectively [22]. Pristine SWNT substrates with lower interface surface energy than the difference between energy of the solid and liquid ($\gamma_{sl} < \gamma_l - \gamma_s$) will not readily allow to wet the capillaries [23].

Homogeneous films with a linear increase in surface roughness and corresponding surface area are expected to react with liquids in accordance to Wenzel equation (3.13).

$$cos\theta^* = r cos\theta \qquad \text{Eq. 3.13}$$

where *r* is the ratio of projected area to the actual one and $cos\theta$ is measured as a contact angle [24,25].

However, in cases where surface roughness and peak amplitude steady increases, air pockets may be formed [25]. In these cases, a heterogeneous surface is formed. The detected contact angle value will be then larger from the real one. Corresponding phenomena is described by Cassi-Boxter equation (3.14) .

$$cos\theta^* = r_f * f(cos\theta_y) + (f - 1) \qquad \text{Eq. 3.14}$$

where r_f corresponds to roughness ratio, f -fraction of solid surface and $cos\theta_y$ is a solid surface angle.

Accordingly, our observations indicated that the surface roughness strongly influence surface energy, presented in Figure 3.11 . It is seen that pristine SWNT films become increasingly more hydrophobic with the increase in surface roughness. Similar but reversed behavior may be observed in hydrophilic (COOH) films, trend seen in Figure 3.10.

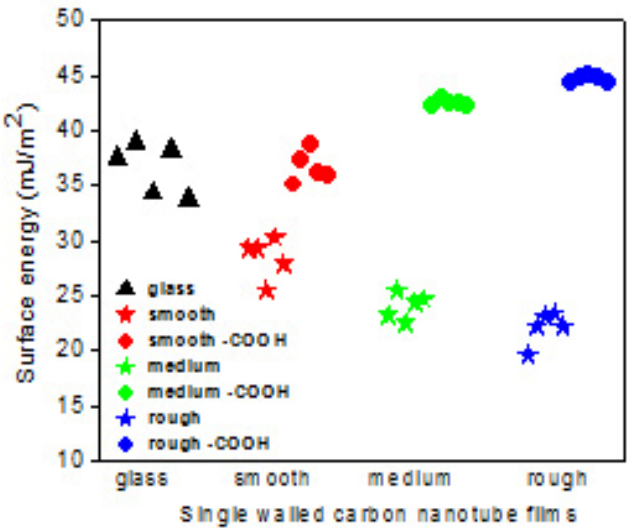

Figure 3.10 Correlation between SWNT network surface energy and corresponding surface morphology**.**

3.4 Analysis

In this study, we have utilized highly purified SWNT suspensions to deposit uniform carbon nanotubes networks using a vacuum filtration method [26,27]. The protocol allows for the control substrate roughness and thickness. The resulting films have similar physical and chemical properties. Therefore, the direct comparison between networks with a varying roughness and/or surface energy density (φ) is able to be distinguished.

To control the morphology of the substrate, we maintained the supporting membrane (MCE) under constant vacuum pressure while allowing the insertion of the nanotubes into the pores of the membrane. Figures 1(a-c) show scanning electron images of the SWNT films and the corresponding MCE membranes (insets) with three different pore sizes (25, 220 and 800 nm, left to right). It appears that the larger pores permits a

rise to rougher surfaces. This qualitative impression was confirmed by measuring the roughness coefficient (R_q, Eqn. 3.15) of the various films by the means of the atomic force microscopy (AMF) in tapping mode. Typical digitalized AFM scans of the films are shown in Figures 3.5 (a-c), along with a representative line scan showing the variation in height (Figures 3.5 a(i)-c(i)). The calculated R_q values of the SWNT networks were 60.64 ± 12.38, 90.22 ± 15.58 and 253.41 ± 91.47 nm (n = 6 experiments) on corresponding 25, 220 and 800 nm MCE membranes. These observations confirm the notion that there is a reasonable increase in network roughness with an increase in underlying membrane pore size (Figure 3.6 (b)).

To investigate the substance of the basic properties of the SWNT networks even further, we measured their surface energy density, (φ, Eqn. 3.16), using the contact angle formed between PBS and ethylene glycol (EG) sessile drops deposited on top of the films. Representative images of the drops on the various surfaces are illustrated in Figures 3.8 (a-c). Our results, presented in Figure 3.11, show that for films constructed with pristine nanotubes, φ decreases with roughness.

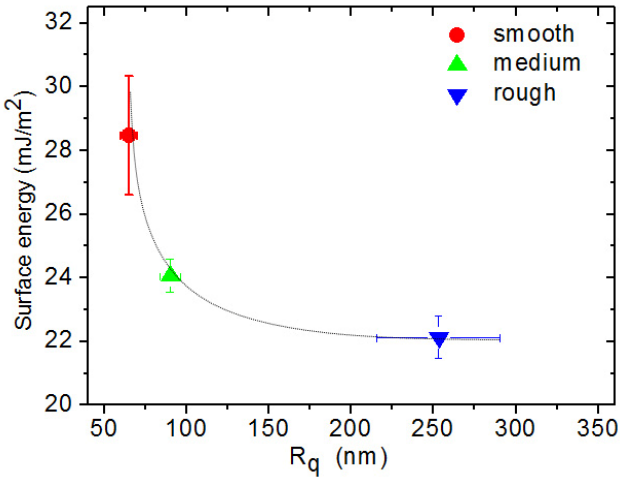

Figure 3.11 Relationship between surface energy density and surface roughness in pristine nanotube films. The line highlands trend in film hydrophobicity (n=6 experiments).

However, pristine SWNTs may be turned hydrophilic by a mild treatment with nitric acid (see methods section) [21]. For carbon films functionalized with carboxyl groups (SWNT-COOH) φ increased with roughness (Figure 3.12).

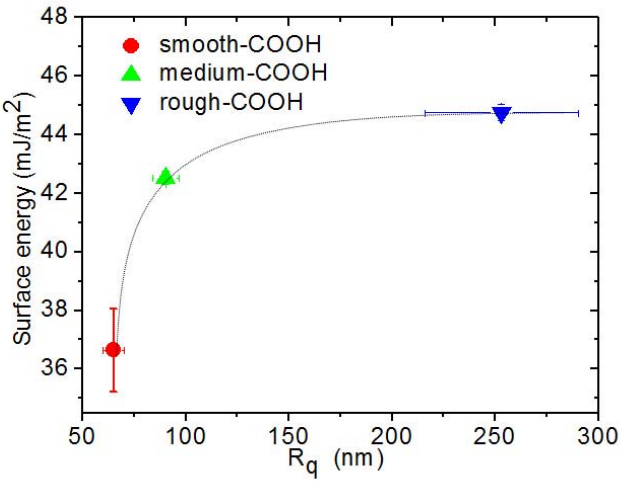

Figure 3.12 Relationship between surface energy density and surface roughness in SWNT-COOH films (n=6 experiments).

Specifically, at a medium roughness (R_q~100 nm) the extrapolated φ roughly doubled in hydrophilic SWNT-COOH films. Thus, φ in SWNT films may be controlled by surface chemistry and roughness.

Having characterized the physical and chemical properties of the SWNT films, we focused on the influence of these parameters on biological cells. We used *MC3T3-E1 osteoblastic cells* in our experiments, which we previously showed to respond well to this type of substrates [28]. We initially investigated a cell attachment to the substrate as a function of φ and roughness. In order of compare SWNT films before and after adhesion tests, we developed the *ad hoc* sample design shown in Figure 3.2.Cells were stained with Calcein AM fluorescent dye and counted. After thorough rinsing, the remaining cells on the film were counted second time and compared to the initial cell number. The figure shows the regions investigated under an optical microscope, with the yellow squares corresponding to the SWNT networks. Bright light images are shown in the inset (*i*) whereas the same areas under fluorescent light are indicated in inset (*ii*). The results of cell attachment tests for the various film types are shown in Figure 3.13.

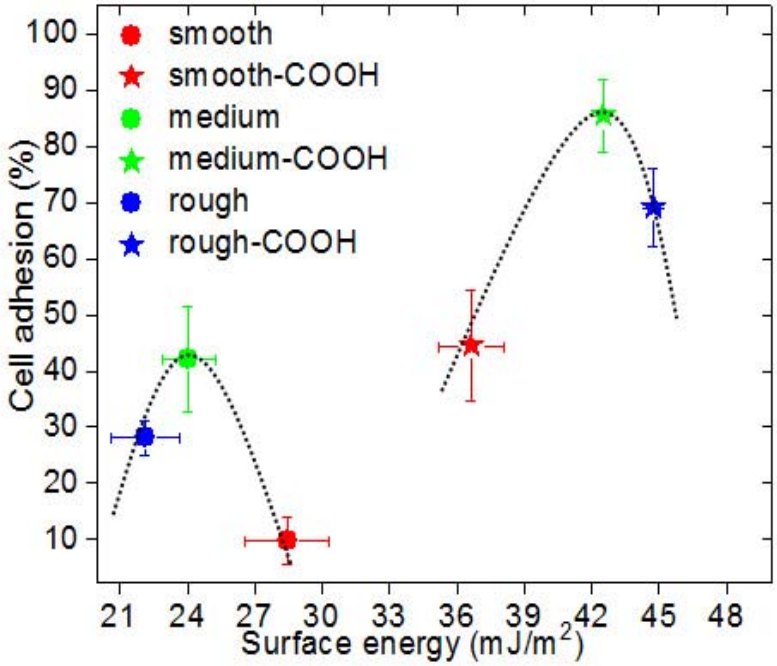

Figure 3.13 Osteoblastic cell attachment as function of the surface energy density of hydrophobic and hydrophilic films ($n \geq 6$).

An observed cell attachment was higher on hydrophilic than hydrophobic films, independent of their surface roughness. However, in both hydrophilic and hydrophobic films, cell adhesion was at its highest in medium roughness ($R_q \sim 100$ nm). Representative images of cells taken 72 hours after initial seeding are shown in Figures 3.14 (a-c). Cells showed robust spreading on medium roughness networks (Figure 3 (b)).

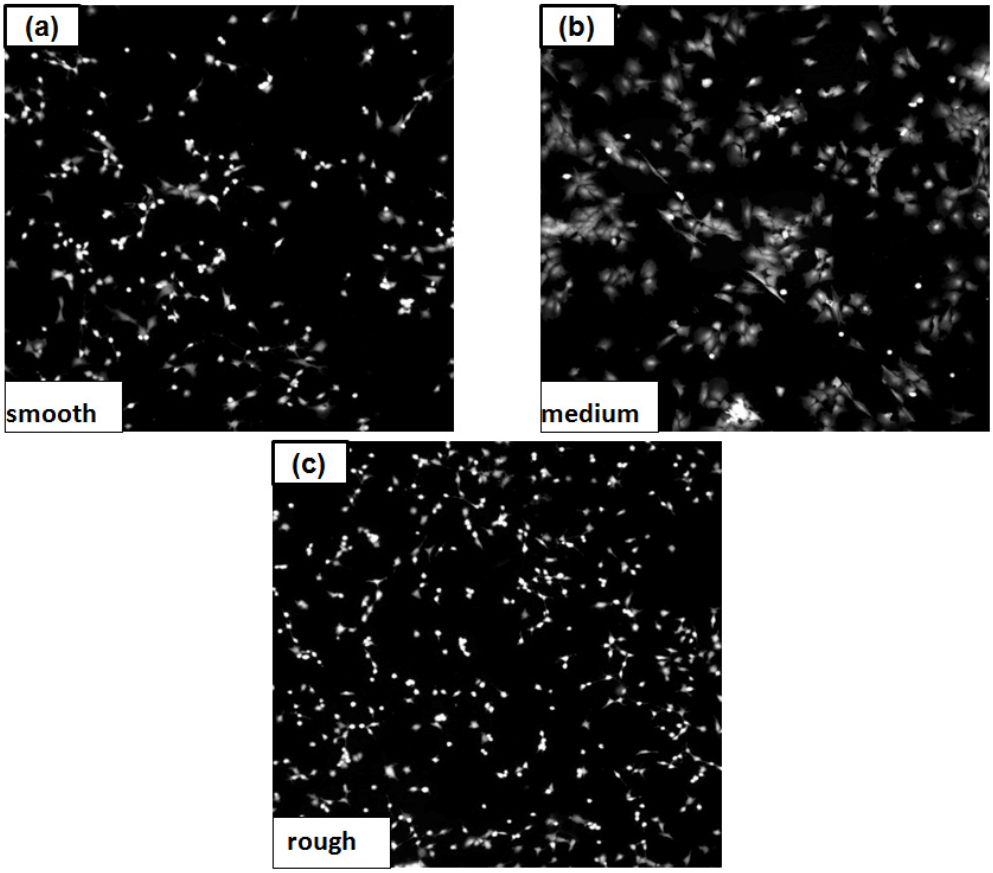

Figure 3.14 Representative images showing cell's cytoplasmic extensions on the hydrophobic surfaces. (b) Cell extensions are visibly larger on medium films indicating higher cell-materials interaction.

Filopodia and lamellipodia cytoplasmic digitations were noticeably present in these samples under a fluorescent light. On the other hand, cells grown on the smooth and rough substrates showed less cytoplasmic extensions, (Figures 3.14 (a,c)).

Collectively, this data indicates that φ and to a lesser extent, surface roughness, play a vital role in initial cell adhesion. Films constructed with hydrophilic nanotubes yield better attachment than hydrophobic films even though the roughness was the same in both film types. Our observations insinuate that the surface roughness may improve cell adhesion.

Cell interaction with materials was further investigated by measuring cell proliferation within the first five days. The results of these experiments, carried on both hydrophobic and hydrophilic films, are shown in Figure 3.15. Proliferation was moderately enhanced in hydrophilic films. Most notably, proliferation was at its highest on smooth surfaces. This suggests that the roughness of the surface is the most important parameter in determining cell proliferation whereas φ appears to play only a minor role.

In conclusion, an optimized surface morphology in which φ is high and roughness is low provides optimal conditions for this cell type.

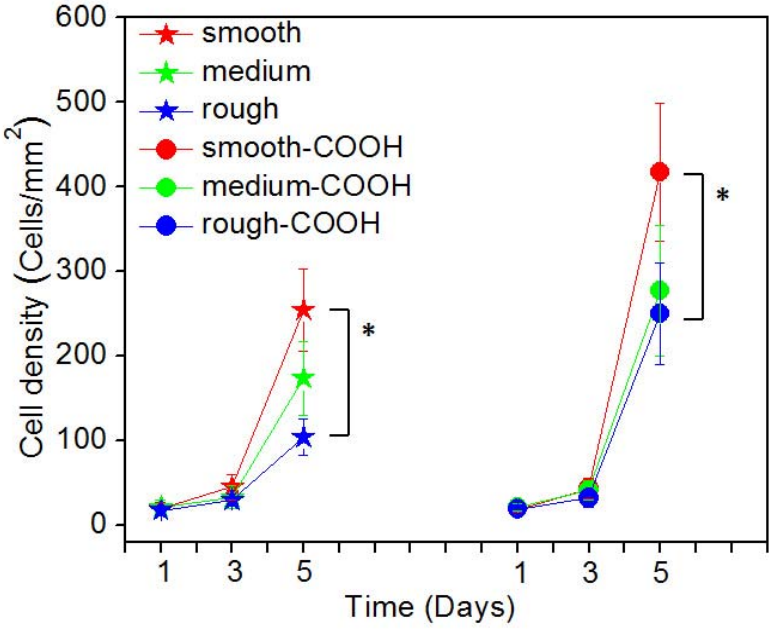

Figure 3.15 Surface energy density and roughness affect cell proliferation
Cell density for osteoblastic cells grown on morphologically similar SWNT films yield different results. Hydrophilic and smooth films stimulated highest cell proliferation. Values are mean ± SD of four individual cultures. Statistically significant differences between samples are indicated with *; $p < 0.05$.

3.5 Discussion

In this study, we have investigated how the physical and chemical characteristics of SWNT-based films support the growth of *MC3T3-E1* osteoblasts. We have found that both, the surface energy density and the roughness of the SWNT surface are key in determining the cell's response. Two fundamental cellular processes, adhesion and proliferation, were affected by these two quantities in a complementary fashion. Our study shows that φ was crucial in promoting cell attachment and played only a subsidiary role in subsequent proliferation. In contrast, surface roughness was the source in proliferation and only marginal in initial adhesion. The reported high proliferation rates on smooth nanotube films are expected, particularly when considering dynamics of cell mitosis. However, it is not completely understood why initial cell attachment peaks in medium roughness surfaces and future studies should address this issue.

Overall, wettable SWNT-COOH films exhibit the best growing conditions for *MC3T3-E1 osteoblasts*. It is most likely that the high φ of these films, by promoting attachment and the development of cytoplasmic extensions, provides a growing advantage to cells that enhances their later development. A unique feature of SWNT films is that they can be hydrophobic and support cell growth, despite the fact that majority of bioactive materials commonly used for cell culturing is wettable [29]. Even though cell adhesion was poorer in hydrophobic than wettable films, cell proliferation was comparable. The effect may be attributed to the hydrophobic nature of nanotubes and films' appropriate micro structure. Very likely, the nanotube films have the ability to self-hydrogenate and favorably adsorb proteins. It is generally acknowledged that the proper material-protein adsorption may subsequently support cell proliferation and

differentiation [24]. For example, osteoblastic cells response to fibronectin treated hydrophobic films lead to higher proliferation rates [30]. It is likely that the hydrophilic films yield better proliferation rates (despite initial poor cell adhesion) by capturing and later releasing growth factors present in the culture media.

The fact that specific physical and chemical attributes of SWNT films control singular aspects of cell growth underscore the tremendous degree of flexibility of these materials. This is an important asset due to the fact that they are bio-compatible. By affording the possibility of maximizing a specific cellular response, initial attachment for instance, they might become versatile tools for multiple biomedical applications.

3.6 Conclusions

In summary, we have demonstrated that SWNT film properties alone may affect the osteoblastic cell response. Our observations highlight a key role of φ and roughness in determining initial cell attachment and proliferation. Best growing conditions were provided by relatively smooth (R_q ~ 60.64 nm) and hydrophilic samples with φ ~ 36.5 mJ/m^2.

3.7 References

[1] Manna SK, Sarkar S, Barr J, Wise K, Barrera EV, Jejelowo O, et al. Single-Walled Carbon Nanotube Induces Oxidative Stress and Activates Nuclear Transcription Factor-KB in Human Keratinocytes. Nano Lett. 2005;5(9)

[2] Chang MK, Raggatt LJ, Alexander KA, Kuliwaba JS, Fazzalari NL, Schroder K, et al. Osteal tissue macrophages are intercalated throughout human and mouse bone lining tissues and regulate osteoblast function in vitro and in vivo. J.Immunol. 2008 Jul 15;181(2):1232-1244.

[3] Kalbacova M, Kalbac M, Dunsch L, Kataura H, Hempel U. The study of the interaction of human mesenchymal stem cells and monocytes/macrophages with single-walled carbon nanotube films. phys. stat. sol. (b) 2006;243(13):3514-3518.

[4] Meng J, Song L, Meng J, Kong H, Zhu G, Wang C, et al. Using single-walled carbon nanotubes nonwoven films as scaffolds to enhance long-term cell proliferation in vitro. J.Biomed.Mater.Res.A. 2006 Nov;79(2):298-306.

[5] Sirivisoot S, Yao C, Xiao X, Sheldon BW, Webster TJ. Greater osteoblast functions on multiwalled carbon nanotubes grown from anodized nanotubular titanium for orthopedic applications. Nanotechnology 2007;365102(36).

[6] Correa-Duarte MA, Wagner N, Rojas-Chapana J, Morsczeck C, Thie M, Giersig M. Fabrication and Biocompatibility of Carbon Nanotube-Based 3D Networks as Scaffolds for Cell Seeding and Growth. Nano Letters 2004;4(11):2233-2236.

[7] Palwai NR, Martyn DE, Neves LFF, Tan Y, Resasco DE, Harrison RG. Retention of biological activity and near-infrared absorbance upon adsorption of horseradish peroxidase on single-walled carbon nanotubes. Nanotechnology 2007;18(235601).

[8] Pantarotto D, Briand JP, Prato M, Bianco A. Translocation of bioactive peptides across cell membranes by carbon nanotubes. Chem.Commun.(Camb) 2004 Jan 7;(1)(1):16-17.

[9] Shi Kam NW, Jessop TC, Wender PA, Dai H. Nanotube molecular transporters: internalization of carbon nanotube-protein conjugates into Mammalian cells. J.Am.Chem.Soc. 2004 Jun 9;126(22):6850-6851.

[10] Kam NW, O'Connell M, Wisdom JA, Dai H. Carbon nanotubes as multifunctional biological transporters and near-infrared agents for selective cancer cell destruction. Proc.Natl.Acad.Sci.U.S.A. 2005 Aug 16;102(33):11600-11605.

[11] Singh R, Pantarotto D, McCarthy D, Chaloin O, Hoebeke J, Partidos CD, et al. Binding and condensation of plasmid DNA onto functionalized carbon nanotubes: toward the construction of nanotube-based gene delivery vectors. J.Am.Chem.Soc. 2005 Mar 30;127(12):4388-4396.

[12] Millan JL. Mammalian alkaline phosphatases: from biology to applications in medicine and biotechnology. 1st ed.: WILEY-VCH Verlag GmbH & C0; 2006.

[13] Yu MF, Files BS, Arepalli S, Ruoff RS. Tensile loading of ropes of single wall carbon nanotubes and their mechanical properties. Phys.Rev.Lett. 2000 Jun 12;84(24):5552-5555.

[14] Kukovecz A, Kramberger C, Holzinger M, Kuzmany H, Schalko J, Mannsberger M, et al. On the Stacking Behavior of Functionalized Single-Wall Carbon Nanotubes. J. Phys. Chem. B 2002;106(25):6374-6380.

[15] Hou P, Liu C, Cheng H. Purification of carbon nanotubes. Carbon 2008;46(1):2003-2025.

[16] Zheng L, Li Y, Liu J. CVD synthesis and purification of single-walled carbon nanotubes on aerogel-supported catalyst. Apllied Physics A 2002;74(1):345-348.

[17] Chen W, Li J, Liu L, Jia Z, Yu Y, Zhang Z. Purification of carbon nanotubes using anodic oxidation in a solid polymer electrolyte (SPE) cell. Journal of Applied Electrochemistry 2003;33(1):755-758

[18] Lee LH editor. Fundamentals of adhesion (New Horizons in Therapeutics). 1st ed. New York: Springer; 1991.

[19] Khang D. Adhesion protein adsorption and bone growth on carbon nanotubes composite materials. Doctoral Dissertation. Brown University; 2006.

[20] Khang D, Kim SY, Liu-Snyder P, Palmore GT, Durbin SM, Webster TJ. Enhanced fibronectin adsorption on carbon nanotube/poly(carbonate) urethane: independent role of surface nano-roughness and associated surface energy. Biomaterials 2007 Nov;28(32):4756-4768.

[21] Parekh BB, Fanchini F, Eda G, Chhowalla M. Improved conductivity of transparent single-wall carbon nanotube thin films via stable postdeposition functionalization. Applied Physics Letters 2007;90(121913).

[22] Wang S, Zhang Y, Abidi N, Cabrales L. Wettability and surface free energy of graphene films. Langmuir 2009;25(18):11078-11081.

[23] Sernelius BE. Surface Modes in Physics. 1st ed. Berlin: Wiley-Vch Verlag Berlin GmbH; 2001.

[24] Glasgow CK, Dhara D. Polymers for biomedical applications. 1st ed. Washington, DC: American Chmical Society; 2008.

[25] Wenzel RN. Resistance of Solid Surfaces to Wetting by Water. Ind. Eng. Chem 1936;28(8):988-994.

[26] Xu YQ, Peng H, Hauge RH, Smalley RE. Controlled multistep purification of single-walled carbon nanotubes. Nano Lett. 2005 Jan;5(1):163-168.

[27] Fanchini G, Unalan EH, Chhowalla M. Optoelectronic properties of transparent and conducting single-wall carbon nanotube thin films. Applied Physics Letters 2006;88.

[28] Tutak W, Park KH, Vasilov A, Starovoytov V, Fanchini G, Cai SQ, et al. Toxicity induced enhanced extracellular matrix production in osteoblastic cells cultured on single-walled carbon nanotube networks. Nanotechnology 2009 Jun 24;20(25):255101.

[29] Baier RE. Applied Chemistry at Protein Interfaces (Advances in Chemistry Series). 1st ed. New York: American Chemical Society; 1976.

[30] Kennedy SB, Washburn NR, Simon CG,Jr, Amis EJ. Combinatorial screen of the effect of surface energy on fibronectin-mediated osteoblast adhesion, spreading and proliferation. Biomaterials 2006 Jul;27(20):3817-3824

Chapter 4 Long Term Effect of Surface Roughness on Primary Osteoblastic Cells

Abstract

Carbon nanotube based matrices are appealing for biomedical applications due to their multifunctionality. However, there are only a few reported studies on single walled carbon nanotube films which suggest that the matrices can be bio-inert or capable promoting cell proliferation in osteoblastic cells [1-3]. Existing knowledge explaining how SWNT network properties influence the short and long term osteoblastic cell response is still limited. Here we show that the pristine SWNT film roughness alone can impact primary osteoblastic cell cultures. Optimized surface roughness is shown to enhance cell attachment, proliferation and late stage differentiation in primary osteoblastic cells.

4.1 Materials

4.1.1 SWNT films

Nanotube films deposition and variation in surface properties were carried out as previously described. Details contained in chapter 2 and 3.

4.1.2 Cell cultures

Primary cell cultures were retrieved and seeded according to methods outlined in chapter 2.

4.1.3 Long Term Primary Osteoblastic Cell Response to SWNT Films

Transcriptase-PCR

Messenger RNA (mRNA) levels for gene expression including alkaline phosphatase (ALP) and collagen I (Col I) were measured. Confluent cell cultures at day were rinsed once with 1 ml of cold PBS, pH 7.4, and collected. QIAGEN RNeasy Mini kit was applied to extract total RNA levels followed by applying TaqMan - reverse transcription reagents (Roche Applied Science, Indianapolis, IN) for reverse transcription (RT). PCRs were performed using a real time PCR DNA Opticon Engine (MJ Research, Inc., Watertown, MA) according to the manufacturer's instructions. Specifically, an increase in SYBR green fluorescence caused by binding of SYBR green to double-stranded DNA was used for real time quantitative detection and measurement of the PCR product. Each analysis was performed once on n=6 samples for each sample type. The data is represented as mean+/- SEM for n=6 . Statistical analysis was performed by Student's t-test. Primers for rat ALP, Col I and GDHAP (reference mRNA) were designed using Primer Express software (PerkinElmer Life Sciences) according to protocols outlined by Selvamurugan et al [4]. The sequences of the above primers for the gene expression were used as follow:

Alkaline phosphatase-567 Forward : ACAATGAGATGCGCCCAGAG

Alkaline phosphatase-680 Reversed: ACATGTACTTCCGGCCACCA

Ratmus col1a1-3689 Forward: AGATTGAGAACATCCGCAGCC

Ratmus col1a1-3793 Reversed: TCCAGTACTCTCCGCTCTTCCA

GDHAP Forward: AACCCATCACCATCTTCCAGG

GDHAP Reversed: GCCTTCTCCATGGTGGTGAA

Statistical analysis

For all statistical analysis the data was analyzed using Origin Pro 8, with Post hoc pairwise comparisons with Tukey's extension. Average +/- standard mean error (SEM) is reported unless specified otherwise. Statistical significance levels were set at $P < 0.05$.

4.2 Methods

Presently there exists a great deal of interest in utilizing single walled carbon nanotubes in biological applications. Potential applications include cell scaffolding [2,3] and biosensing [5,6]. However, long term cellular response to the SWNT bio-inert films was never reported in detail. Assembling carbon nanotubes to form films is especially attractive because the matrices are easy to deposit, process and characterize. Resulting matrix physical and chemical surface properties can be controlled and are known to affect electrical characteristics [7] but also biological cell response [8,9]. The challenge is to understand how microscopic SWNT film morphology and associated surface energy can potentially affect long term cell response. Applying minimally invasive SWNT films with only one varying parameter, the roughness factor, is a suitable platform to investigate the long term cell-SWNT film interactions. A filtration technique that was applied to assembled matrices provided uniform, controllable and reproducible films suitable for controlling the matrix roughness parameters.

4.3 Results

In this study, we have utilized purified SWNT suspensions to deposit carbon networks based on a vacuum filtration method [10]. The vacuum filtration method allowed for deposition of SWNT networks with controllable and reproducible thickness and roughness. The formed films had similar matrix chemical and physical properties and therefore allowed for direct comparison between networks with varying roughness values. Controlling matrix surface morphology was possible because during SWNT deposition nanotubes penetrated deeper into larger pore size MCE filter membranes. Schematic of the process was depictured in section 2.1.

Variation in carbon nanotube film morphology was controlled by adjusting underlying filter membrane pore size. Changing underlying MCE pore size (from diameter; 0.025 , 0.22 to 0.8 μm respectively) allowed to control nanotube film morphology. Corresponding smooth, medium and rough films are depictured in section 3.3.1.
Our results presented in that section, indicate that a systematic increase in the MCE membrane pore size was critical in controlling surface roughness.
To further investigate basic matrix properties, contact angle formed between sessile drops deposited on top of SWNT films and glass controls were measured and used to calculate surface energy. Phosphate buffer drops were placed on glass, smooth, medium and rough films, as seen in section 3.3.2, to formed wide range of contact angles (from ~70 to 120^{o}).

After thoroughly characterizing SWNT networks, they were subjected to biological tests. Primary osteoblastic cell cultures were cultured on the films to investigate the effect of pristine film surface on initial and late cell developmental stages.

The first biological experiments aimed at testing initial cell adhesion and proliferation rates, seen in figure 4.1 a,b.

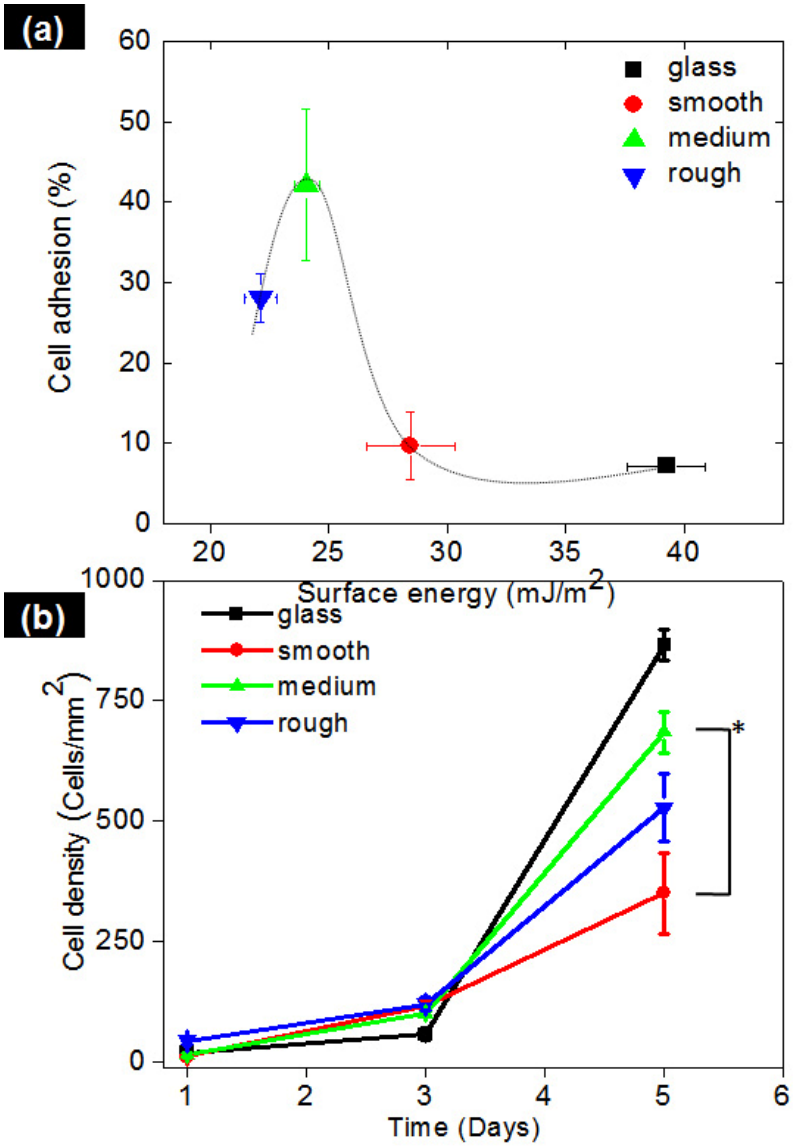

Figure 4.1 Trends in primary cell adhesion and proliferation on SWNT matrices. (a) Primary cells adhere significantly better on rougher but lower in surface energy films. Glass samples are included for comparison. (b) Cells seem to respond very well to SWNT films during the proliferation stage. There was no detectable change in cell number within the first three days, indicating bio-inert SWNT matrix properties. Highest cell proliferation rates appear to be induced by medium rough samples, (n=6).

These tests revealed the highest cell attachment ratio to rougher SWNT networks

(medium and rough), as indicated in figure 4.1 a. The results are unexpected since surfaces with energy values of ~ 25 mJ/m^2 do not wet very well and have limited surface-cell interactions [11]. However, results reported by Meng et. al., and colleagues support the notion that cells may adhere better to SWNT films than other commonly used control substrates including polystyrene Petri dish, possibly because of a roughness factor [2]. The results point to an optimized surface morphology as an important parameter capable of modulating cell response. It is apparent that cells which adhered well to medium rough films were stimulated and expressed higher proliferation rates.

Following the initial cell interaction study, we have monitored cell proliferation within the first five days. Among the SWNT samples, the medium films exhibited the highest cell proliferation levels. It is important to notice that there was no detectable toxicity present throughout initial proliferation stage, as indicated in figure 4.1 b. More importantly, initial cell-materials interactions directly influenced cell proliferation. These trends are being represented in figures 4.1 a and are highlighted in figure 4.2 a.

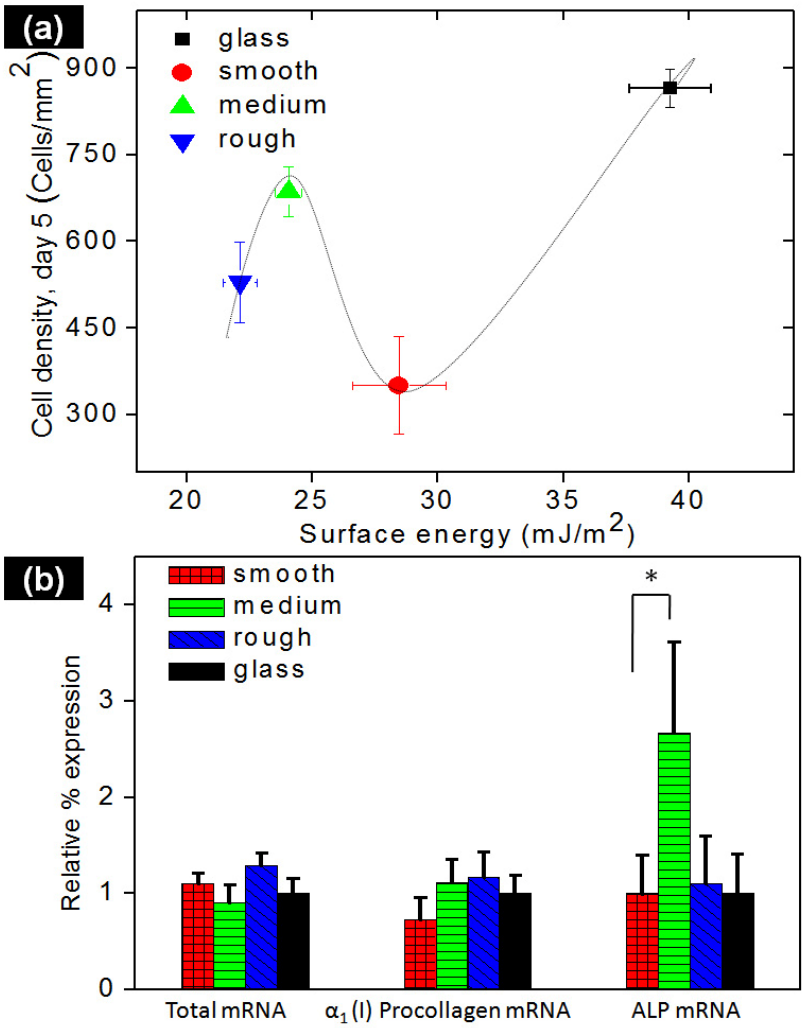

Figure 4.2 Later stage primary cell response to SWNT matrices. (a) Cell density and cell adhesion appear to follow similar trends. Highest values reported for medium rough matrices. It is apparent that initial cell adhesion may directly affect later proliferation and differentiation stages, as seen in above Figures (a and b). Significantly higher ALP mRNA levels are expressed by the cells grown on medium rough matrices. Samples collected at day 12 ($n = 6$, $p \leq 0.05$).

It is interesting to notice that the cell adhesion and proliferation patterns (at day 5) appear to be similar.

Cell-materials response was further investigated at late cell differentiation stage by measuring osteoblastic mRNAs gene marker expression levels. Typical differentiation

markers on molecular level included collagen I and alkaline phosphatase (ALP) mRNAs. Specifically, α_1 (I) procollagen, and ALP mRNA levels along with total mRNA were recorded

It can be seen that molecular expression levels for these primers is significantly increased with increase in surface roughness, notably for medium and to limited extend rough films (Figure 4.2 b), when compared to smooth SWNT networks. These observations further indicate that initial cell-surface interactions on SWNT films are indeed guiding cell biological response.

4.4 Discussion

Pristine SWNT films appear to have unique properties since the majority of bioactive materials that are considered suitable for cell adhesion are wettable (hydrophilic, 40-80 mJ/m^2) but not as hydrophobic as carbon materials [12]. On the other hand, hydrophobic materials with the appropriate micro structure and ability to self-hydrogenate are required for proper protein adsorption and preferential cell-material interactions. The protein adsorption is a desired material property necessary to direct cell development and to minimize immune system related response to foreign elements within host body. It is generally acknowledged that proper material-protein adsorption may subsequently lead to higher cell proliferation and differentiation rates [11].

The cell-materials interactions may be further influenced by modulating film morphology [13,14]. Our study suggest that relatively large changes in surface roughness (50%, increase between smooth and medium and 160 % between medium and rough samples) are primarily responsible for controlling cell response. Drop in surface energy due to

increase in roughness appears to have lesser effect on matrix properties, with 16 % decrease in energy between smooth and medium and 8 % between medium and rough samples. Although total increase in roughness contributes approximately only up to 22 % to the surface energy, it is the roughness factor that controls cell response on pristine SWNT matrices.

Likely, the SWNT films initially interact with cell culture medium proteins via weak physiosorbtion and/or chemiosorbtion rendering substrate bioactive. These proteins may poorly attach to hydrophobic smooth films due to low interaction energy and weak steric interactions. Although surface energy drops with increase in roughness, optimized surface morphology appears to play dominant role during cell adhesion and growth. Consequently, the cell adhesion is higher on rougher (that is, medium and rough) nanotube substrates. Reported 50 % increase in surface roughness with modest drop in surface energy apparently provides the optimum growth conditions for cell culturing. Rough samples with relatively large surface peak amplitude and lower surface energy seem to hinder cell development, likely by influencing protein attachment and cell movement.

4.5 Summary and Conclusions

In summary, we have demonstrated that SWNT film properties, specifically surface roughness, may alone affect short and long term primary osteoblastic cell response. Our observations suggest that higher cell proliferation and differentiation rates can be expected on films with higher roughness values. Specifically, osteoblastic cells interacted very well to medium rough SWNT films. The pristine SWNT matrix with $R_q \sim$

90 nm and $\gamma_s \sim 25$ mJ/m^2 appear to have optimum parameters for primary osteoblastic cell development. The cell initial adhesion and consequent proliferation and differentiation stages were highest when stimulated by the medium rough films samples.

4.6 References

[1] Correa-Duarte MA, Wagner N, Rojas-Chapana J, Morsczeck C, Thie M, Giersig M. Fabrication and Biocompatibility of Carbon Nanotube-Based 3D Networks as Scaffolds for Cell Seeding and Growth. Nano Letters 2004;4(11):2233-2236

[2] Meng J, Song L, Meng J, Kong H, Zhu G, Wang C, et al. Using single-walled carbon nanotubes nonwoven films as scaffolds to enhance long-term cell proliferation in vitro. J.Biomed.Mater.Res.A. 2006 Nov;79(2):298-306.

[3] Khang D, Kim SY, Liu-Snyder P, Palmore GT, Durbin SM, Webster TJ. Enhanced fibronectin adsorption on carbon nanotube/poly(carbonate) urethane: independent role of surface nano-roughness and associated surface energy. Biomaterials 2007 Nov;28(32):4756-4768

[4] Selvamurugan N, Jefcoat SC, Kwok S, Kowalewski R, Tamasi JA, Partridge NC. Overexpression of Runx2 directed by the matrix metalloproteinase-13 promoter containing the AP-1 and Runx/RD/Cbfa sites alters bone remodeling in vivo. J.Cell.Biochem. 2006 Oct 1;99(2):545-557.

[5] Haddad R, Cosnier S, Maaref A, Holzinger M. Non-covalent biofunctionalization of single-walled carbon nanotubes via biotin attachment by pi-stacking interactions and pyrrole polymerization. Analyst 2009 Dec;134(12):2412-2418.

[6] Wang L, Chen W, Xu D, Shim BS, Zhu Y, Sun F, et al. Simple, rapid, sensitive, and versatile SWNT-paper sensor for environmental toxin detection competitive with ELISA. Nano Lett. 2009 Dec;9(12):4147-4152.

[7] H. E. Unalan. Single Walled Carbon Nanotube thin films: properties and applications. Rutgers, The State University; 2006.

[8] Sinha N, Yeow JT. Carbon nanotubes for biomedical applications. IEEE Trans.Nanobioscience 2005 Jun;4(2):180-195.

[9] Saito N, Usui Y, Aoki K, Narita N, Shimizu M, Hara K, et al. Carbon nanotubes: biomaterial applications. Chem.Soc.Rev. 2009 Jul;38(7):1897-1903.

[10] Wu Z, Chen Z, Du X, Logan JM, Sippel J, Nikolou M, et al. Transparent, conductive carbon nanotube films. Science 2004 Aug 27;305(5688):1273-1276.

[11] Andrde JD, Smith LM, Gregonis DE. The Contact Angle and Interface Energetics. In: Ratner BD, Hoffman AS, Schoen FJ, Lemons JE, editors. Biomaterials Science . 2nd ed. California, USA: Elsevier Academic Press Inc.; 1996. p. 249-270.

[12] Baier RE. Applied Chemistry at Protein Interfaces (Advances in Chemistry Series). 1st ed. New York: American Chemical Society; 1976.

[13] Kennedy SB, Washburn NR, Simon CG,Jr, Amis EJ. Combinatorial screen of the effect of surface energy on fibronectin-mediated osteoblast adhesion, spreading and proliferation. Biomaterials 2006 Jul;27(20):3817-3824.

[14] Price RL, Ellison K, Haberstroh KM, Webster TJ. Nanometer surface roughness increases select osteoblast adhesion on carbon nanofiber compacts. J.Biomed.Mater.Res.A. 2004 Jul 1;70(1):129-138.

Chapter 5 Single Walled Carbon Nanotube Substrates for Real-time Probing of Initial Cell Interactions and Numbers.

5.1 Introduction

Previous chapters outlined basic physical interactions between cells and SWNT networks. These universal interactions are an integral part of any material behavior in a biological setting. In this chapter, we have carried out an initial study to investigate the electrical response of SWNT scaffolds during seeding and growth of cells. Our aim was to monitor the changes in SWNT network conductivity due to presence of biological medium and osteoblastic cells. These changes would in principle provide insights into the initial adhesion and electrical interactions between SWNT networks and the cells. The electrical properties of the SWNT networks should be appreciably altered by the presence of cells and medium.

Our initial results indicate that there is some influence of the electrical properties of SWNT networks as a function of exposure to biological medium. These results are preliminary but have provided the basis for lunching further studies. Specifically, interesting investigations related to cell interactions with SWNT scaffolds would be studied. More specifically, the electrical conductance is used to monitor the release of ions during the initial cell interactions. In future, these tests will require more sophisticated high frequency impedance measurements. Nevertheless, these initial results provided some interesting results.

Pristine SWNT networks with optimized surface morphology for cell active adhesion (medium rough films) were assembled and deposited on glass substrates. The deposition method was described in detail in chapter 2.

The selected measurements were performed by placing a (~500 nm thick) strip of SWNT network on glass or silicon SiO_2 chip. A polyvinyl chloride (PCV) cup was placed over the middle portion of the SWNT strip, as shown in Figure 5.1. The cell culturing medium was placed within the PCV cup. The walls of the raised cup also facilitated light microscope observations.

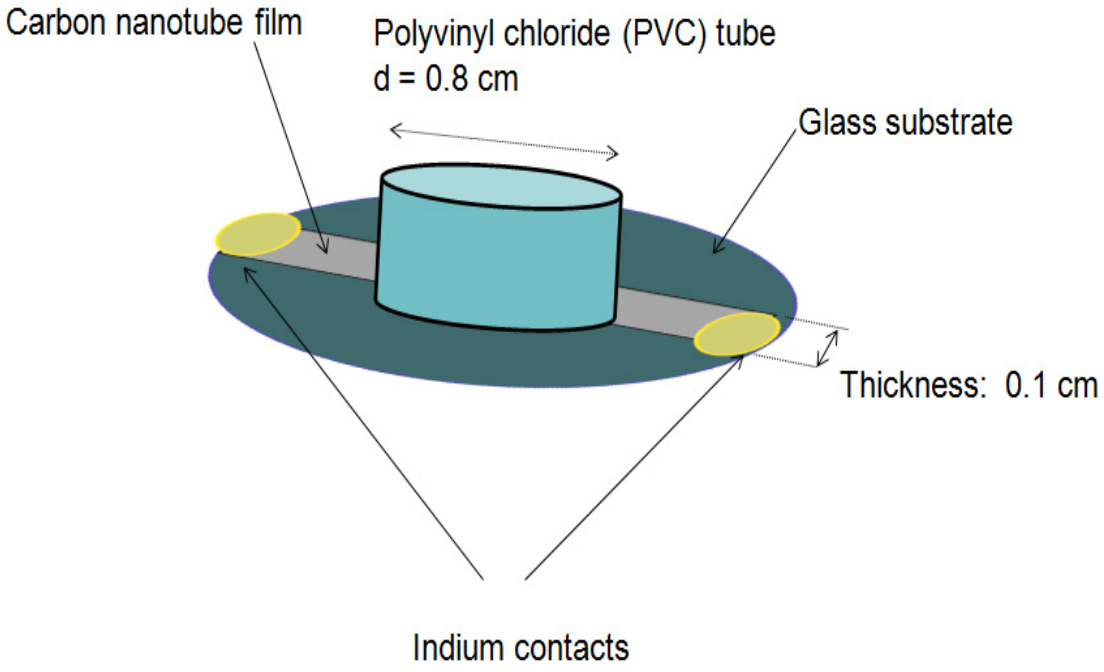

Figure 5.1 Outline of experimental setup used to monitor the changes in electrical properties of SWNTs with cell cultures.

5.2 Cell Cultures

Osteoblastic (MC3T3-E1) and Chinese hamster ovary (CHO) cell cultures were grown according to protocols outlined in chapter 2. Experiments were carried out for under 15 min in ambient conditions. Some experimental data is reported to have lasted in 3 hour long experiments.

5.3 Electrical Measurements

Carbon nanotube film conductivity was measured using a computerized system as well as portable Fluke 117 electric multimeter. A digital/analog signal acquisition system was used to monitor the SWNT network conductivity, "Lab View" software was employed to record signals from an interface card (GPIB) connected to a "Keithly" model 2400 series sourcemeter. The sourcemeter generated source bias from -100 to 100 mV , which was applied across the nanotube film. The difference in bias was then recorded and processed by the Lab View program.

5.4 Methods

Measuring changes in current density would provide some insights into is how SWNT networks interact with living cells. Time dependent variation in an electrical current may also potentially provide information about biochemical and mechanical changes; in association with cell attachment and threading. Variation in environmental biochemistry should depend on fluctuations in ionic current density. Film resistance is

expected to vary depending on the number and affinity of biomolecules and elements present in cell culturing medium. For example: Ca, P, Na, Cl, OH^-,H^+ and charged proteins will affect the electrical measurements [7-10]. Cell culturing medium is a source of ions in suspension. However, the ionic charge balance, specifically the amount of H^+, can also be regulated by cellular activity (Kreb cycle) [11]. This nonspecific biosorption to nanotubes would occur via weak vdW and columbic interactions [12,13]. These interactions are potentially capable of changing the number and type of available carriers in semiconducting nanotubes [14], leading to shifts in the Fermi energy level. Other major factors that may potentially cause changes in the electric current within the SWNT network include mechanical stress induced by cells during attachment onto the substrates. The pulling force exerted by cells on a matrix has been estimated to be 380 nN [15]. This mechanical force is substantial which would lead to dislodging or removal of loose SWNTs from the scaffold which would affect the electrical measurements. Understanding cell/materials interactions through electrical measurements would be an interesting frame work for future experiments. Initial tests provide information about how nanotube based electrodes sense cell behavior. Our experiments provide a basic outline for applying SWNT films to detect in-situ, real time cell interactions.

5.5 Results and Discussion

Synthesized and purified SWNTs are two thirds semiconducting while the remaining one third is metallic [16-18]. Typical electrical behavior of various SWNT types is summarized in Figure 5.2. Its synthesized SWNTs could be metallic and semiconducting and the latter types can be doped to become either ***p*** or ***n*** type.

The exact electrical characteristics of SWNT networks are complicated and have been characterized in fundamental detail within our group. This provides us with the point of analyzing the electrical properties of SWNT networks in the presence of physiological medium. For example; metallic, semiconducting p and n type and mixed type (ambipolar) SWNT are known to exist.

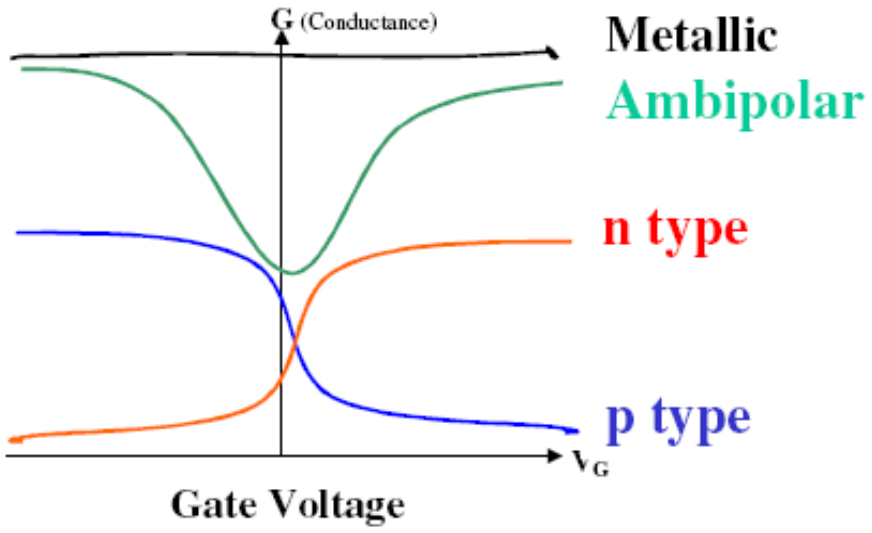

Figure 5.2 Unique SWNT charge transfer characteristics may be detected when single nanotubes are used to form transistors. Source-drain current versus gate voltage graph is shown. Figure adopted from [18].

In networks containing mixed SWNTs, the electrical properties are defined by the most conducting metallic SWNTs. Briefly, the transport in SWNT networks is mediated by the measuring junctions between the SWNTs forming the interconnected network. This type of electrical transport can be modeled by the percolation theory where a critical function of SWNTs is required to form an interconnected network that facilitates electrical transport.

The fraction of nanotubes required to form a percolation network is defined by:

$$\sigma \propto (N - Nc)^{\alpha} \qquad \text{Eq. 5.1}$$

where corresponding σ is the conductivity network, N density of conducting sticks, and Nc is the critical density analogous to the percolation threshold. The exponent α is the dimensionality variable of the network and usually is in the range of 1.33 and 1.94 for two- and three-dimensional systems, respectively [19-21]. Parameter Nc corresponds to a network of randomly dispersed conducting sticks, as defined in equation 5.2

$$l\sqrt{\pi N_c} = 4.236 \qquad \text{Eq. 5.2}$$

where l is the length of the conducting nanotube.

Initial experiments were designed to test in-situ cell/materials interactions.

The investigation focused on cell behavior on SWNT matrices within a confined area; effect of cell density on its agglomeration and cell movement. Our observations provide some interesting insights into how cells distribute themselves within confined area. Figure 5.3 (a,d) shows two devices with a black strip in the background (SWNT film) and just deposited cells (black small dots). Cells pictured on the images are well distributed, However, within 15-30 minutes, they quickly aggregate, as shown in Figure 5.3 (b,c and e,f). It can also be seen that cells move away from the PCV wall and are well distributed over nanotubes and glass substrates.

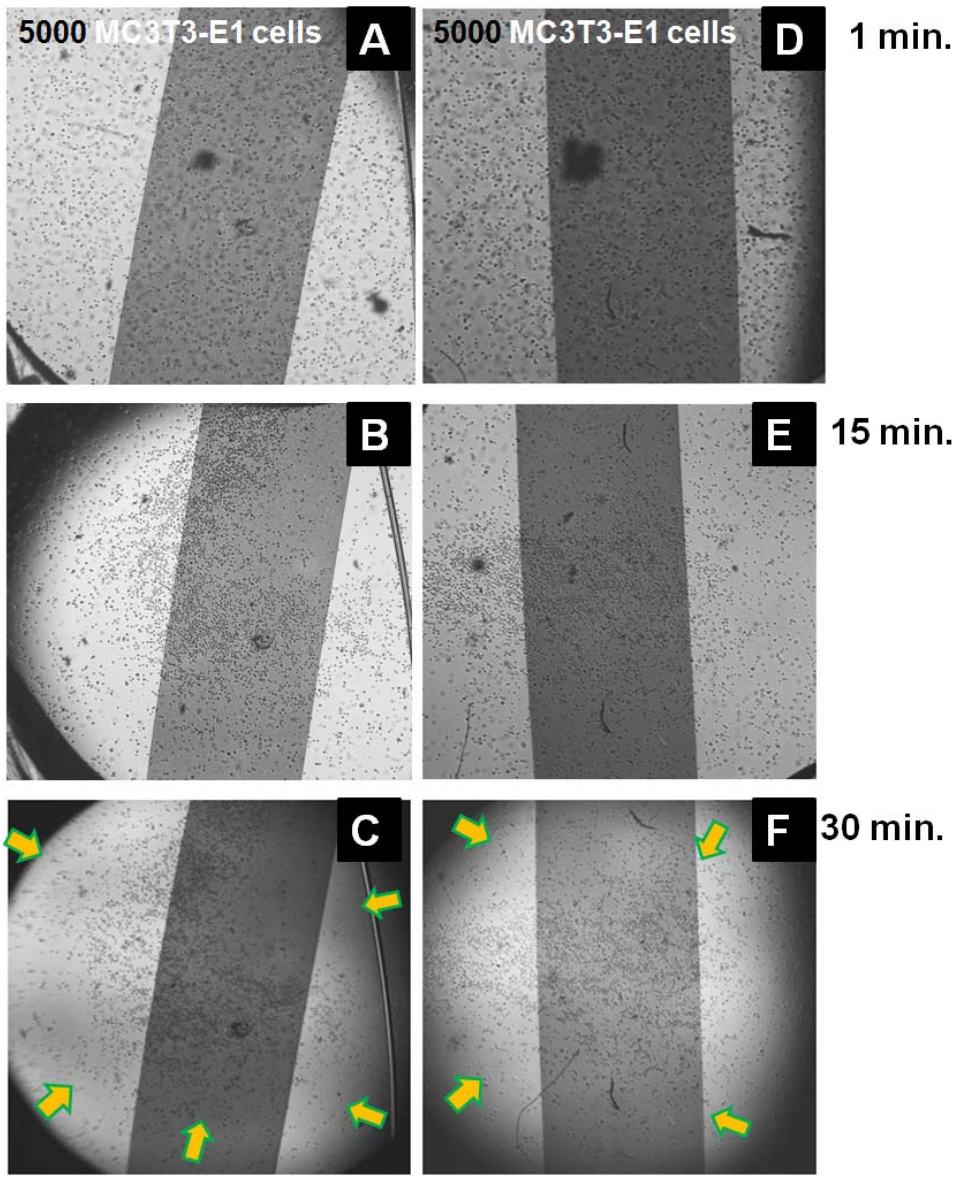

Figure 5.3 Light microscope images of the 5000 MC3T3-E1 cells deposited directly on SWNT networks. (a), Cells are initially well distributed throughout the sample. (b), After 15 minutes, the cells start to move away from the edges. This migration is likely to happen due to the unfavorable geometrical configuration resulting in low surface energies. (c), Cell movement away from the edge is clearly seen after 30 minutes.

Cell cultures were then deposited in different amounts (raging from 500 to 50000) to compare and find the most suitable initial cell number. Below are images with low initial osteoblastic cell number of around 500 (Figures 5.4 a,b) and samples with 100 times

more cells (Figure 5.4 e,f). Optimized carbon nanotube films seemed to attract cells which are present in low numbers. The results are in good agreement with our previous observations. On the other hand, devices with a 50000 cells appeared to be covered densely and uniformly by them (Figure 5.4 e,f).

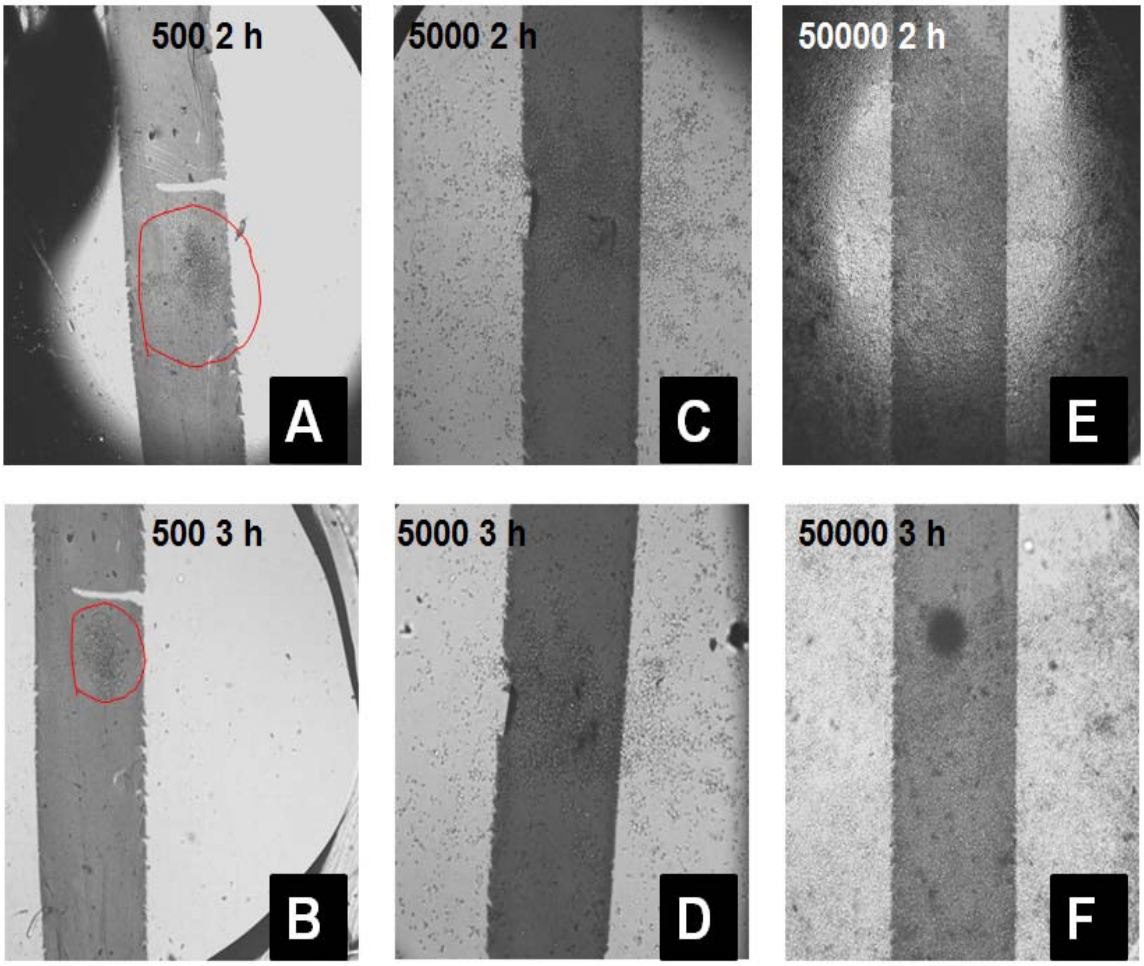

Figure 5.4 Light microscope images of cells at various densities deposited on nanotube films. (a,b) Images corresponding to 500 cells after 2 and 3 hours of culturing, respectively. (c,d) Images of the cells at 5000 and (e,f) at 50000 count.

Our observations insinuate that cells tend to cluster in the middle of the device, without any specific preferences for material (either glass or SWNT films).

In order to further characterize nanotube films responsiveness to biochemical stimuli, pH calibration solutions, were prepared. SWNT networks were tested to define the sensitivity of the matrix to acidic, neutral and basic solutions. Solutions with pH of 4, 7 ,10; corresponding to 1×10^{-4}, 1×10^{-7} and 1×10^{-10} of H^+ molar concentrations respectively were used. The results shown in Figure 5.5 clearly indicate that the networks quickly respond to changes in pH solution. Subsequent SWNT networks were rinsed with DI water to remove physioadsorbed ionic elements. Although the results confirmed that the SWNT networks can sense the change in ionic concentrations, the conductivity changed only by 8% and did not vary linearly with concentration.

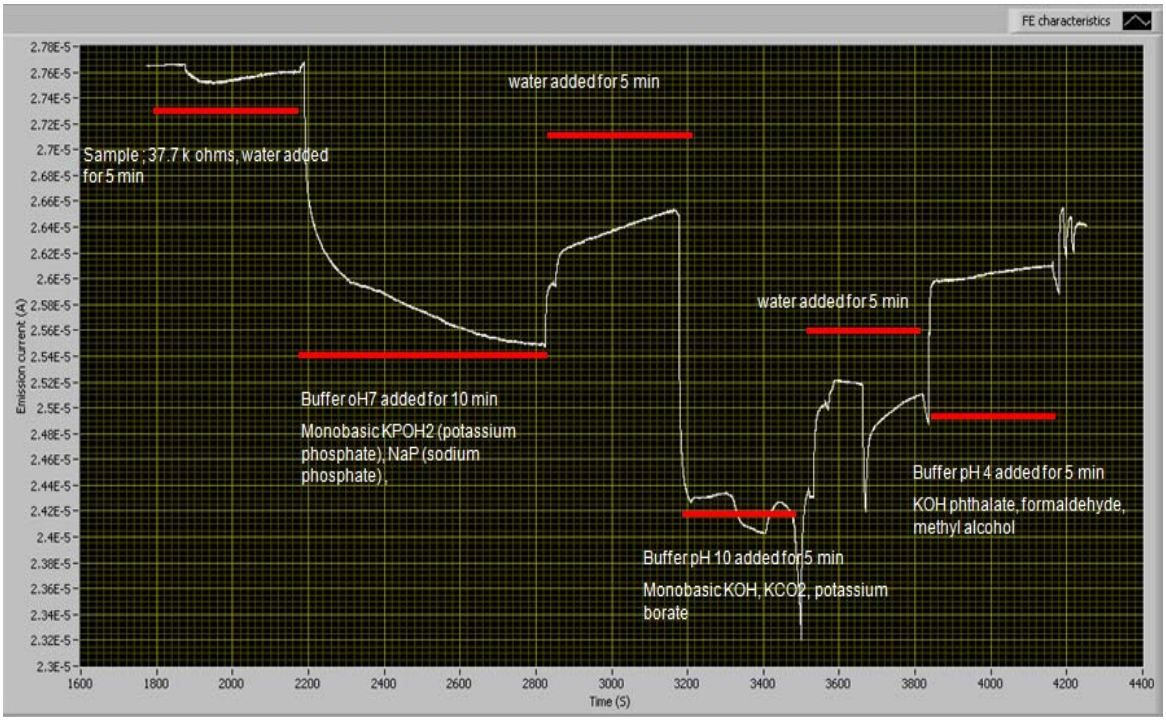

Figure 5.5 SWNT film response to standard pH samples. Network exposure to neutral, water, basic and acidic environments is shown. Strongest response may be seen in SWNT films exposed to high pH but solutions at pH 4 showed more ordered response.

The electrical response of SWNT networks was also calibrated to exposure of medium and cell cultures as well as PBS solution.

Current-time dependent response of such solutions are shown in Figure 5.7. It can be clearly seen that the networks instantaneously respond to the medium and PBS stimuli.

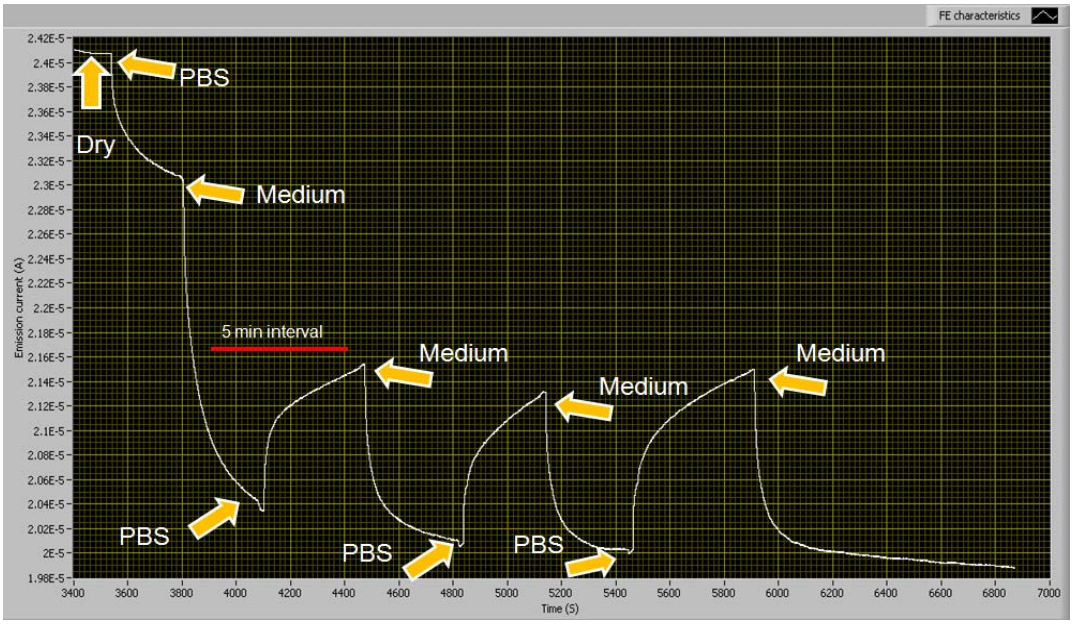

Figure 5.6 The single walled carbon nanotube matrix response to cell culturing medium and buffer saline. The films represent short time response and good nanotube films sensitivity to stimuli.

For comparison, similar devices (physical dimensions) based on gold electrodes (thickness up to 200 nm) were fabricated. The data in Figure 5.7 clearly shows that the devices are insensitive to the various types of solutions.

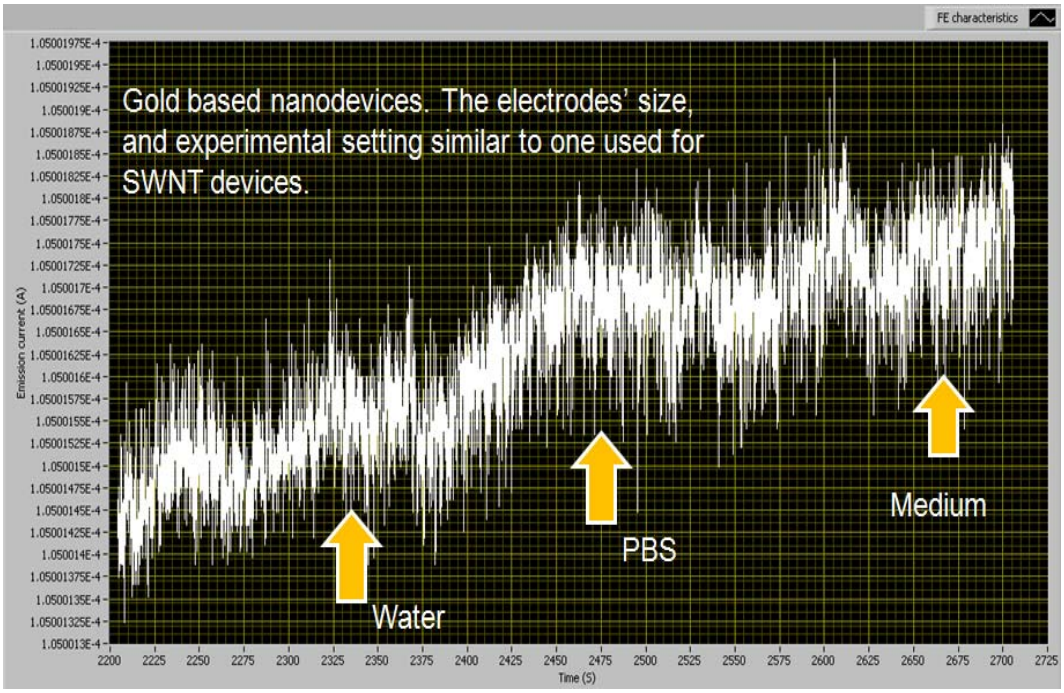

Figure 5.7 Similar devise design based but incorporating gold films was tested. Small relative change in detected current in gold based sensors can be seen.

Finally, the electrical response to SWNT networks exposed to cell culturing medium alone are shown in Figure 5.9 and for comparison the behavior after exposure to MC3T3-E1 cells, under similar conditions are shown in Figure 5.9.

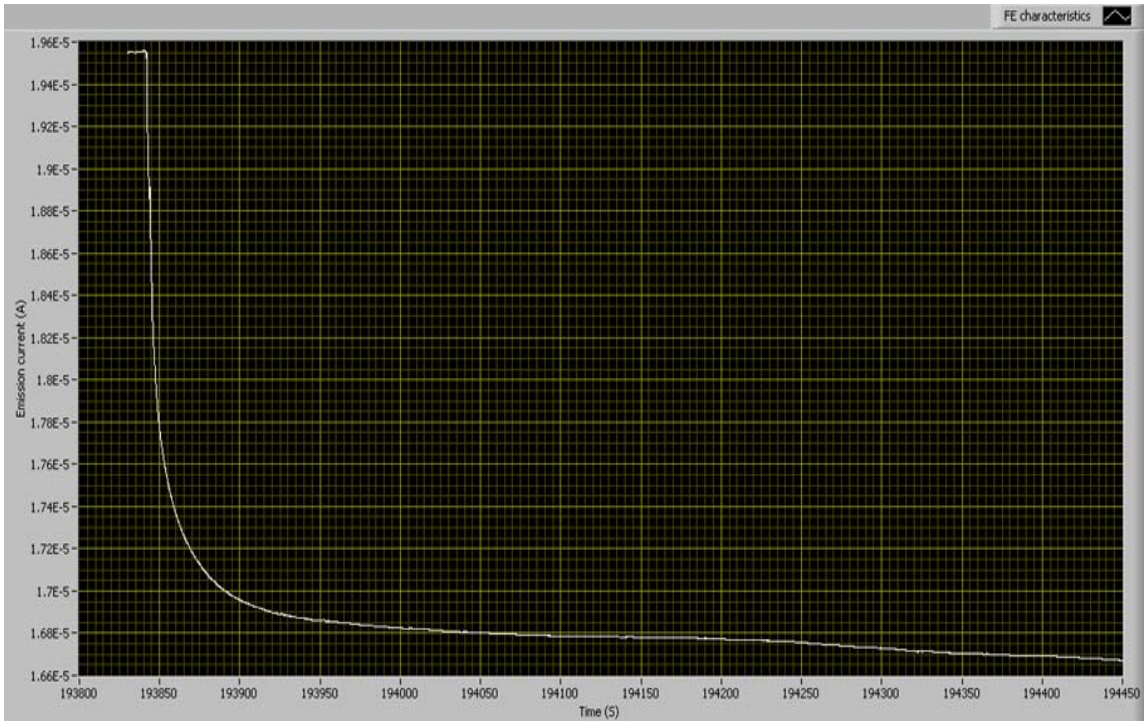

Figure 5.8 Typical diagram corresponding to the SWNT films exposed to cell culture medium alone.

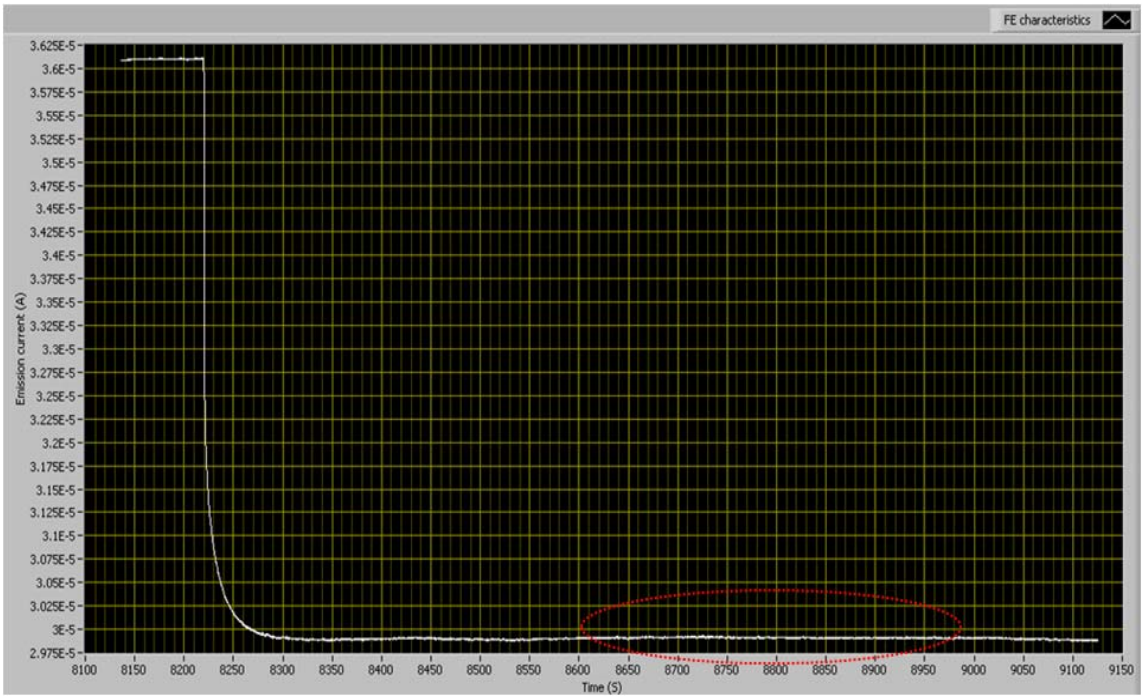

Figure 5.9 Representative image corresponding to a change in electrical current due to 5000 MC3T3-E1 cells deposited on the nanotube film. Small relative increase in film conductivity may be observed (red dotted area).

Qualitative comparison between the two graphs reveals the following features:

1. Short increases in film conductivity occurs soon after cell deposition, see Figure 5.10.

2. Relative rate in drop of electrical current (slope) for control (medium) sample is lower than for cell/medium samples, Figure 5.12 .

The initial cell-materials interactions included a sharp decrease in current initially, with slight decrease in the rate of decline upon exposure to cell interaction with the substrate, as seen in Figure 5.10.

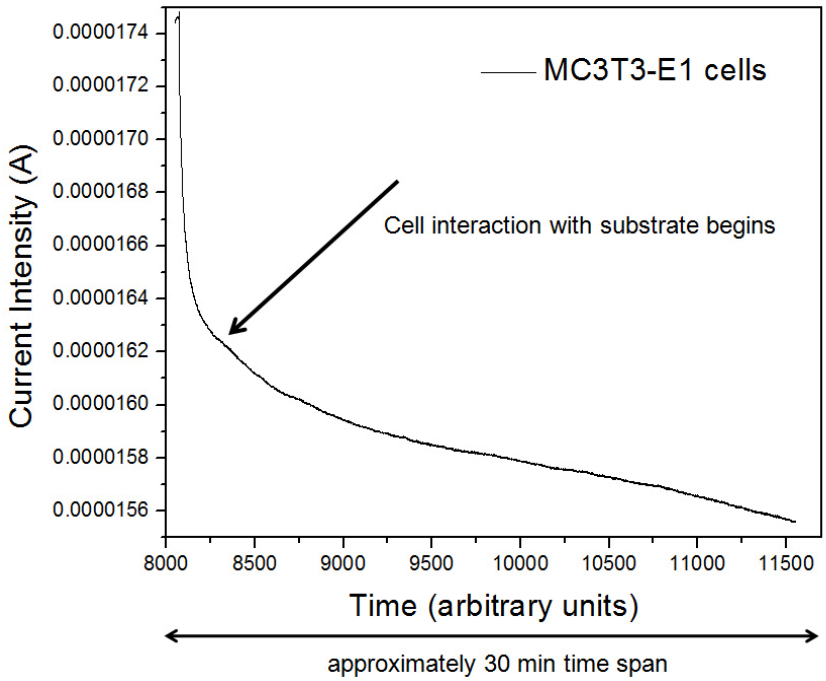

Figure 5.10 Initial cell-material interactions recorded within the first 0.5 h after initial cell exposure. Small increase in recorded film conductivity (approximately 4 minutes after cell deposition) could be assigned to direct cell/matrix interactions.

Second important characteristic of the recorded electrical measurements may be related to a plot angle or "responsiveness rate"(R_r). The rate is defined in equation 5.3

$$R_r = \frac{T_2 - T_1}{A_2 - A_1} \qquad \text{Eq. 5.3}$$

where T_y corresponds to time and A_x electrical current.

The results indicate that these rates may significantly vary depending on stimuli used and could be indicative of initial cell-material interactions. For comparison, a SWNT film response to control PBS solution was recorded and shown in Figure 5.11.

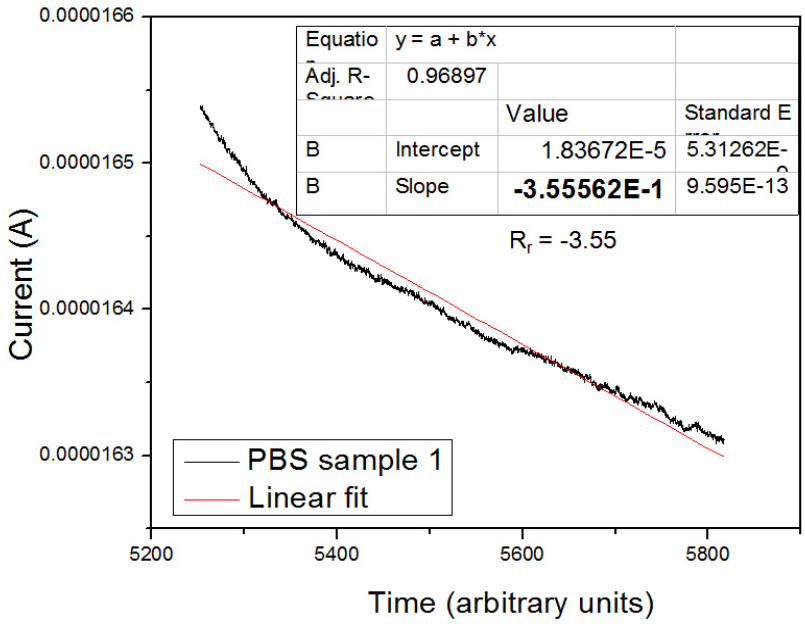

Figure 5.11 Change in nanotube film conductivity when exposed to control PBS solution. Initial current change in film response to the solution is weak, as seen by low slope of fitting line.

However, carbon nanotube networks that were exposed to MC3T3-E1 cultures showed spatially (resistance in time) different behavior that could be indicative of cell interactions, Figures 5.12 .

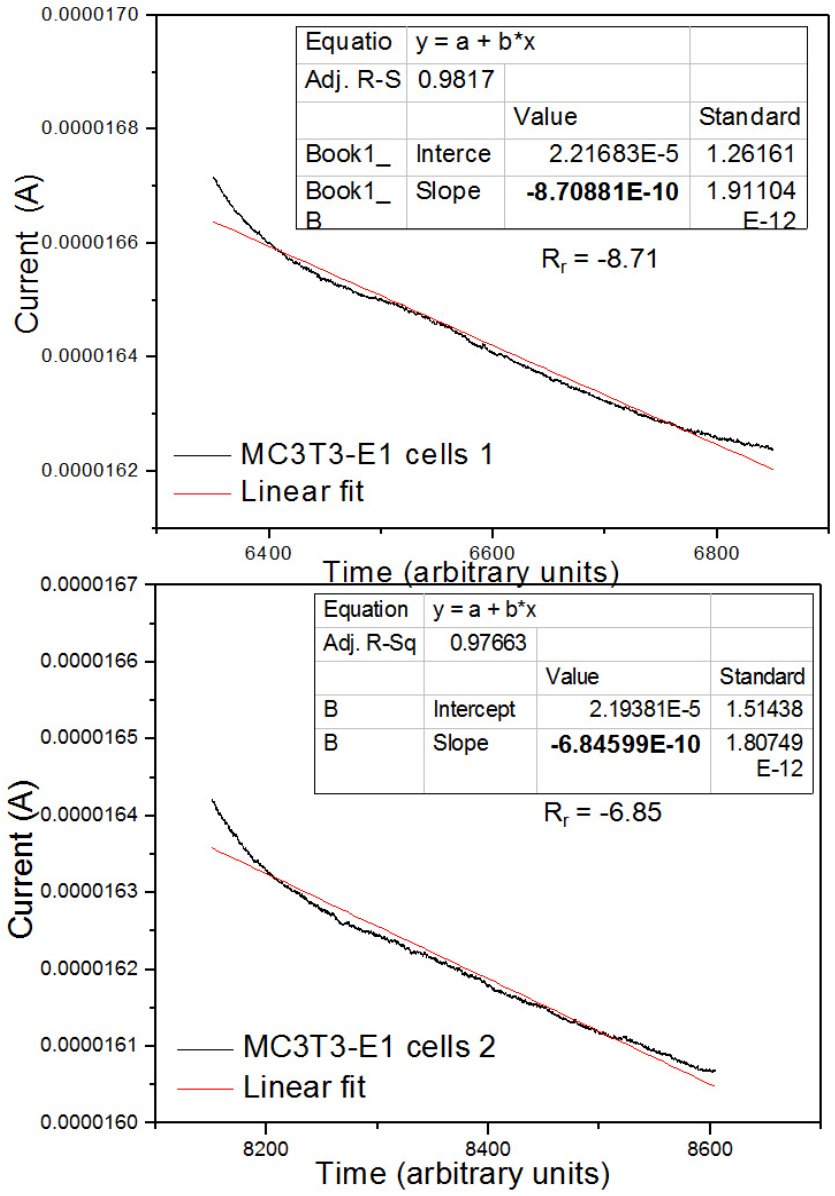

Figure 5.12 MC3T3-E1 cells interacting with carbon nanotube films. Representative graphs of current rate change as a function of time. Cells facilitate greater change in responsiveness rate (R_r), as highlighted by red fitting curve. Below, similar results obtained on another set of samples. Visible change in responsiveness rate is different than one associated with PBS solution.

The above data is consistent with biological behavior of the cells. Cells in cultures are expected to start interacting with a substrate within the first few minutes after initial

deposition [16]. Although, our experiments do not directly confirm the cellular attachment, recorded signals suggest it is a possibility.

The initial cell number was varied to modulate the electric current shift induced by interacting cells. Three samples including control (medium) , 5000 cells and one with 50000 cells were placed in ambient environment and measured simultaneously. For these experiments, presented in Figure 5.14, a hand held multimiter connected to a carbon nanotube strips were used to obtain the film resistance values. The measurements were taken every 5 minutes for up to an hour on MC3T3-E1 cells.

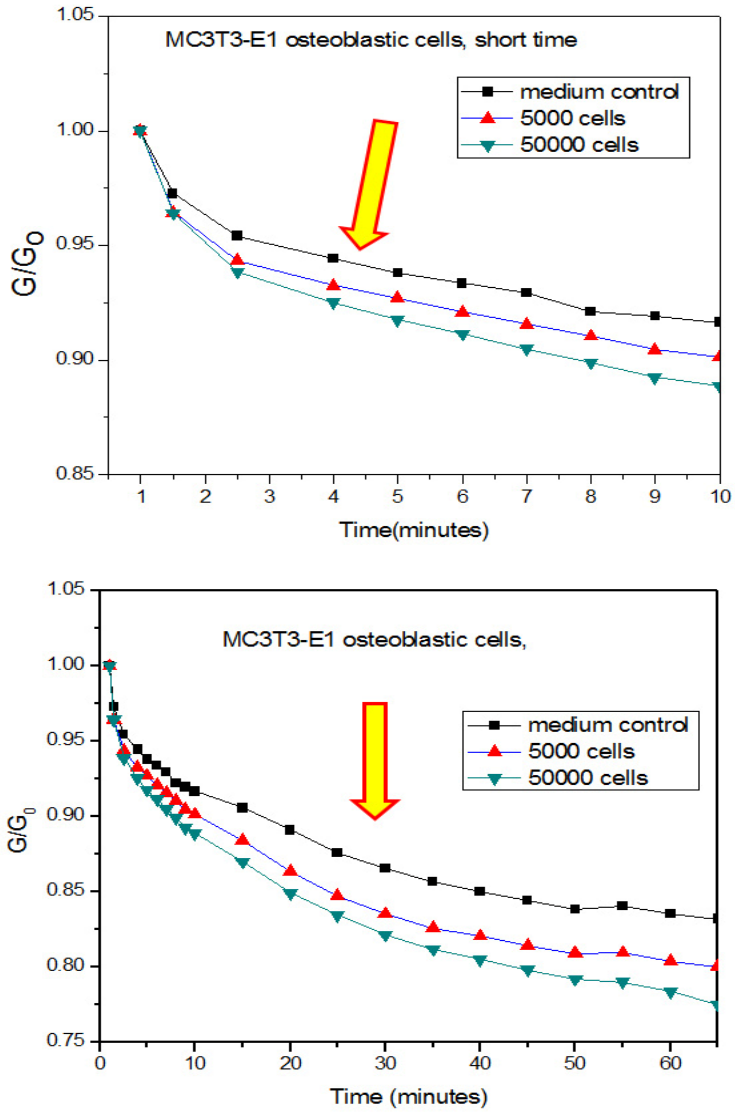

Figure 5.13 Electrical conductance measurements conducted on SWNT networks exposed to cell cultures . Recorded values appear to correlate well with initial cell numbers. Arrows point to a trend in film resistance as function of detected cell number.

It can be seen that the large number of cells decrease the resistance of SWNT networks as a result of medium and cell presence.

Future experiments should aspire to optimize experimental set up and apply multiple electrical characterization techniques to understand and perhaps enhance the network

response to biological stimuli. Providing a controlled environment with the designed atmosphere and temperature would allow for more reliable tests for prolonged time. In addition, measurements of AC impedance under various biological conditions [10] coupled with assembling thin film transistors will help find limits of the networks sensitivity and reveal mechanisms implicated in cell/materials interactions.

5.6 Summary

The data reported in this chapter provide a proof of concept that SWNT films may be used to detect in situ, real time cell-materials interactions. Specifically, our preliminary data shows that the cell attachment on the films contributed to a slight change in the detected electrical current. A slight increase in film conductivity within the first 4 minutes and its subsequent drop is reported. The observed behavior is expected to be caused by cell cultures. Factors like short and long term cell culturing and variation in initial cell number will impact SWNT film conductivity.

5.6 References

[1] Hwang ES, Cao C, Hong S, Jung HJ, Cha CY, Choi JB, et al. The DNA hybridization assay using single-walled carbon nanotubes as ultrasensitive, long-term optical labels. Nanotechnology 2006 Jul 28;17(14):3442-3445.

[2] Notingher I, Hench LL. Raman microspectroscopy: a noninvasive tool for studies of individual living cells in vitro. Expert Rev.Med.Devices 2006 Mar;3(2):215-234.

[3] Heller DA, Jeng ES, Yeung TK, Martinez BM, Moll AE, Gastala JB, et al. Optical detection of DNA conformational polymorphism on single-walled carbon nanotubes. Science 2006 Jan 27;311(5760):508-511.

[4] Hunter RJ. Introduction to colloidal science. 1st ed. New York: Oxford Science Publications; 2003.

[5] Alberts B, Bray D, Johnson A, Lewis J, Raff M, Roberts K, et al. Cytoskeleton. In: Robertson M, editor. Essential Cell Biology. 1st ed. New York & London: Garland Publishing, Inc; 1998. p. 513-546.

[6] Mylvaganam K, Zhang LC. Deformation-promoted reactivity of single-walled carbon nanotubes. Nanotechnology 2006;17:410-414.

[7] Chen RJ, Bangsaruntip S, Drouvalakis KA, Kam NW, Shim M, Li Y, et al. Noncovalent functionalization of carbon nanotubes for highly specific electronic biosensors. Proc.Natl.Acad.Sci.U.S.A. 2003 Apr 29;100(9):4984-4989.

[8] Fanchini G, Unalan HE, Chhowalla M. Modification of transparent and conducting single wall carbon nanotube thin films via bromine functionalization. Appl. Phys. Lett. 2007;90(092114).

[9] Athanassiou G, Deligianni D. Adhesion strength of individual human bone marrow cells to fibronectin. Integrin beta1-mediated adhesion. J.Mater.Sci.Mater.Med. 2001 Oct-Dec;12(10-12):965-970.

[10] Bockrath M, Cobden DH, McEuen PL, Chopra NG, Zettl A, Thess A, et al. Single-Electron Transport in Ropes of Carbon Nanotubes. Science 1997 Mar 28;275(5308):1922-1925.

[11] Tans SJ, Devoret MH, Dai H, Thess A, Smalley RE, Geerligs LJ, et al. Individual single-wall carbon nanotubes as quantum wires. Nature 1997;386(1):474-477.

[12] Reibold M, Paufler P, Levin AA, Kochmann W, Patzke N, Meyer DC. Materials: carbon nanotubes in an ancient Damascus sabre. Nature 2006 Nov 16;444(7117):286.

[13] H. E. Unalan. Single Walled Carbon Nanotube thin films: properties and applications. Rutgers, The State University; 2006.

[14] Cao C, Rogers JA. Ultrathin Films of Single-Walled Carbon Nanotubes for Electronics and Sensors: A Review of Fundamental and Applied Aspects. Adv. Mater. 2008, 20, 1–25 2008;20(4):1-25.

[15] Sahimi M. Applications of Percolation Theory. 2nd ed. London: Taylor and Francis; 1994.

[16] Lee LH editor. Fundamentals of adhesion (New Horizons in Therapeutics). 1st ed. New York: Springer; 1991.

Chapter 6 Conclusions and Future Work

6.1 Summary

Carbon contributes approximately 18 % to the human body mass, and it is a basic building block of all living organisms. Lipids, fatty acids and other biomolecules all contain carbon necessary to form proteins, cells, tissues and organs [1]. From that perspective, carbon based nanodevices provide an interesting oportunity for incorporating functional componenents within living organisms.

Single walled carbon nanotubes are formed by rolling up a graphene sheet. The nanotubes have unique chemical, structural, mechanical and electronic properties. The combination of these characteristics present exceptional opportunity to design and fabricate miniaturized multifunctional nanodevices. Transistors, electrodes or antennas may be assembled using SWNTs to detect, send and receive signals. [2-4]. Due to their size, chemistry and physical properties, nanotubes articulate unique bio-activity but also formidable challenges when applied to biological systems. Available research data show dramatic differences in reported cell response when exposed to SWNT elements. The nanotubes are characterized by high material-cell activity that may be of benefit to cellular activity or cause its toxicity [5-7].

The primary objective of the research described in this dissertation was to investigate the major variables contributing to SWNT films-cell interactions. To enhance our understanding of these factors, we tested numerous samples and applied bio-chemical assays to assess corresponding cellular response.

Experimental carbon nanotube films were assembled using the vacuum filtration technique [8]. The technique allowed for high output, reproducible and uniform film deposition, a crucial step necessary for careful bioresponse assessment. Loose and well adhered carbon nanotube networks were subsequently formed and tested. Observations on cellular response to the networks resulted in defining a new mechanism responsible for increase in collagen I protein expression. The proposed mechanism directly corroborated high protein expression levels with damaged cells and a consequent release of cell cytoplasmic content. Our results also indicated that well adhered SWNT films caused little or no toxicity. Initial cell numbers and growth rates on the films were confirmed to be similar to cells cultured on control substrates. These nanotube matrices were described as bio-inert and used in the next set of experiments surveying cell/material interactions.

Varying the properties of SWNT networks, including surface roughness and chemistry provided means to control matrix surface energy. The surface energy effect on cell response was investigated in detail. Detected short term osteoblastic cell response was most desired on smooth and hydrophilic substrates with high surface energy. Our results revealed that nanotube film surface chemistry is a single important factor modulating short term cell response. The roughness factor appeared to play a secondary role in cell development. An increase in the roughness factor apparently enhanced the effect of surface chemistry. However, in extreme cases presented physical barrier obstructing cell development.

Long term cell response to pristine, low energy films, further revealed implications of nanotube film morphology on the late stage cell development. The results showed that

optimized surface roughness alone is capable of inducing higher cell differentiation levels.

In final part of the dissertation, we investigated in-situ, real time cell interactions with SWNT networks. Our findings showed that the electrical properties of the networks are affected by the presence of biological medium and cells. These electrical characteristics could provide some interesting insight into the initial cell/SWNT interactions. However, significant effort requiring more experiments, data collection, and analysis is needed to understand whether or not such networks can be used as sensors or detectors for cell response.

6.2 Suggestions for Future Research

Although some progress was made during the formulation of this dissertation, the work has also opened up new avenues of research and questions that must be addressed in future studies. The two publications that arose from this work provide new information, which can be used as the foundation for lunching more detailed studies that elucidate the mechanism for cell proliferation and differentiation.

Based on the initial work we suggest the following topics as projects for future research:

1. Cytotoxicity of loose SWNTs has been demonstrated in our first publication but the mechanism at the fundamental biological level of how SWNTs damage cells has not been elucidated. In addition, we showed that the destruction of cells leads to release of cell cytoplasmic biomolecules that enhance collagen I expression. A careful analysis of the biomolecules and mechanism leading to their release is required to understand mechanism of the protein expression. Lastly, detailed compositional and molecular

analysis of the extracellular matrix must be carried out to understand the factors responsible for bone cell histogenesis.

2. In our second paper, we demonstrated that the role of the network surface characteristics affects cell development. A much more detailed study with a range of surface energies and roughness must be planned in order to validate the results. More importantly, the chemistry of the surface must also be studied in detail to monitor how it influences cell development. This can be done by functionalizing the SWNTs with desired molecules or compounds to chemically vary the surface properties of the networks.

3. Finally, continuing on the initial and preliminary work of detecting cell interactions using electrical probing, I suggest the following future work. The data is clearly preliminary, additional measurements at higher frequencies should be carried out to obtain information about the ionic conductivity. This may be useful because it is very likely that the ionic concentrations in biological medium significantly increase when cells release proteins and biomolecules. Thus obtaining information about the ionic conductivity would provide information about specific types of proteins being expressed.

4. Building on such knowledge, future experiments could also investigate the influence of electric current on the cell differentiation and proliferation. That is, electrical pulses could be used to initiate or control cell and tissue development and regeneration.

6.3 References

[1] Henning T, Salama F. Carbon in the Universe. Science 1998;282:2204-2210.

[2] Cao C, Rogers JA. Ultrathin Films of Single-Walled Carbon Nanotubes for Electronics and Sensors: A Review of Fundamental and Applied Aspects. Adv. Mater. 2008, 20, 1–25 2008;20(4):1-25.

[3] Dresselhaus MS, Dresselhaus G, Avouris P. Carbon nanotubes, synthesis, structure, properties and applications. 1st ed. Berlin, Heidelberg,: Springer-Verlag; 2001.

[4] Dresselhaus MS. Applied physics: nanotube antennas. Nature 2004 Dec 23;432(7020):959-960.

[5] Sinha N, Yeow JT. Carbon nanotubes for biomedical applications. IEEE Trans.Nanobioscience 2005 Jun;4(2):180-195.

[6] Saito N, Usui Y, Aoki K, Narita N, Shimizu M, Hara K, et al. Carbon nanotubes: biomaterial applications. Chem.Soc.Rev. 2009 Jul;38(7):1897-1903.

[7] Hussain MA, Kabir MA, Sood AK. On the cytotoxicity of carbon nanotubes. Current Science 2009;96(5):664-673.

[8] Parekh BB, Fanchini F, Eda G, Chhowalla M. Improved conductivity of transparent single-wall carbon nanotube thin films via stable postdeposition functionalization. Applied Physics Letters 2007;90(121913).

Curriculum Vitae

Wojtek Tutak

EDUCATION:

Ph.D., Materials Science and Engineering, Rutgers University, New Brunswick, NJ
Date of graduation: **2010**

B.S., Biomedical Engineering, New Jersey Institute of Technology, Newark NJ
Date of graduation: **2005**

INDUSTRY:

Stryker Orthopedics, Mahwah, NJ 2006
Industry: Biomaterials, implants, design, evaluation
Position held: Researcher/Lab technician in Tribology Laboratory

Colgate-Palmolive, Piscataway, NJ 2005
Industry: Hygiene products, dental products, materials evaluation
Position held: Researcher/ Lab technician in R&D Laboratory

Synergy Microwave Corp, Paterson, NJ 2005
Industry: Electronic devices, signal attenuators, antennas
Position held: Lab technician/Assistant Engineer in Electronic Laboratory

PUBLICATIONS:

Tutak, W., Park, K.H., Vasilov, A., Starovoytov, V., Fanchini, G., Cai, S.Q., Partridge, N.C., Sesti, F. & Chhowalla, M. 2009, "Toxicity induced enhanced extracellular matrix production in osteoblastic cells cultured on single-walled carbon nanotube networks", *Nanotechnology,* vol. 20, 255101.

Tutak, W., Chhowalla M. & Sesti, F. 2010 "The chemical and physical characteristics of single walled carbon nanotube films impact osteoblastic cell response". *Nanotechnology,* vol. 21**,** 315102

Reynolds, S., **Tutak, W**., Yamaguci, H., Sesti, F. & Chhowalla, M. " Single walled carbon nanotube film's slow decomposition in biological environments". In preparation

Sharma, A., Patel, R., **Tutak, W**., Chhowalla, M., Sosnowski, S. & Iqbal, Z. "PECVD growth and characterization of graphene nanowalls". In preparation